Russian Original Vol. 37, No. 1, July, 1974

January, 1975

SATEAZ 37(1) 679–790 (1974)

SOVIET ATOMIC ENERGY

АТОМНАЯ ЭНЕРГИЯ
(ATOMNAYA ÉNERGIYA)

TRANSLATED FROM RUSSIAN

CONSULTANTS BUREAU, NEW YORK

SOVIET ATOMIC ENERGY

Soviet Atomic Energy is a cover-to-cover translation of *Atomnaya Énergiya*, a publication of the Academy of Sciences of the USSR.

An agreement with the Copyright Agency of the USSR (VAAP) makes available both advance copies of the Russian journal and original glossy photographs and artwork. This serves to decrease the necessary time lag between publication of the original and publication of the translation and helps to improve the quality of the latter. The translation began with the first issue of the Russian journal.

Consultants Bureau journals appear about six months after the publication of the original Russian issue. For bibliographic accuracy, the English issue published by Consultants Bureau carries the same number and date as the original Russian from which it was translated. For example, a Russian issue published in December will appear in a Consultants Bureau English translation about the following June, but the translation issue will carry the December date. When ordering any volume or particular issue of a Consultants Bureau journal, please specify the date and, where applicable, the volume and issue numbers of the original Russian. The material you will receive will be a translation of that Russian volume or issue.

Subscription
$87.50 per volume (6 Issues)

Single Issue: $50
Single Article: $15

Prices somewhat higher outside the United States.

CONSULTANTS BUREAU, NEW YORK AND LONDON

227 West 17th Street
New York, New York 10011

4a Lower John Street
London W1R 3PD
England

Published monthly. Second-class postage paid at Jamaica, New York 11431.

Soviet Atomic Energy is abstracted or indexed in *Applied Mechanics Reviews, Chemical Abstracts, Engineering Index, INSPEC—Physics Abstracts and Electrical and Electronics Abstracts, Current Contents,* and *Nuclear Science Abstracts.*

SOVIET ATOMIC ENERGY

A translation of *Atomnaya Énergiya*

January, 1975

Volume 37, Number 1 July, 1974

CONTENTS

	Engl.	Russ.
ARTICLES		
Fast Gas and Thermal Breeder Reactors – S. M. Feinberg	679	3
New Prospects in the Creation of Gas-Cooled Fast Reactors with a Short Doubling Time, using Dissociating N_2O_4 – A. K. Krasin and V. B. Nesterenko	687	11
Radioactive Safety Barriers in Nuclear Power Stations – E. P. Anan'ev and G. N. Kruzhilin	699	22
Low-Temperature Specific Heat and Thermodynamic Functions of Uranium Beryllide – O. P. Samorukov, V. N. Kostryukov, F. A. Kostylev, and V. A. Tumbakov	705	28
Increasing the Efficiency of Separating Isotope-Cascades by Using Steps with More than Two Emergent Flows – N. A. Kolokol'tsov	709	32
Production of Ultracold Neutrons in a Stationary (Steady-State) Reactor of the VVR-K (Water-Cooled, Water-Moderated) Type – E. Z. Akhmetov, D. K. Kaipov, V. A. Konks, V. I. Lushchikov, Yu. N. Pokotilovskii, A. V. Strelkov, and F. L. Shapiro	712	35
Optimizing Resonator-System Power when Accelerating Widely Spaced Bunches – V. L. Serov, Yu. F. Orlov, and A. I. Baryshev	716	39
REVIEWS		
Introduction of the Method of Preplanting Gamma Irradiation of Seeds and the Commercial Kolos Gamma Apparatus into Agricultural Practice – N. M. Berezina, A. M. Kuzin, and D. A. Kaushanskii	721	43
Sputtering of Matter by Fission Fragments – V. A. Bessonov	730	52
ABSTRACTS		
Electrical Conductivity of a Mullite-Corundum Ceramic at Elevated Temperatures during Irradiation – U. G. Gulyamov, N. S. Kostyukov and A. P. Sokolov	735	57
Analytical Calculation of the Range of Ions and the Partial Loss of Energy during Retardation – A. P. Balashov	735	57
Destructive Effect of Hydrogen on the Cladding during Reprocessing of the Fuel Elements of a Water-Cooled/Water-Moderated Power Reactor – A. T. Ageenkov and V. F. Savel'ev	737	58
Linear Perturbation Theory for Fuel Burnup Problems in a Fast Reactor – V. V. Khromov, A. A. Kashutin and V. S. Glebov	738	59
^{40}K Gamma Distribution at the Ocean—Atmosphere Boundary – A. S. Vinogradov, K. G. Vinogradova, and B. A. Nelepo	738	59
The Development of Activity Generators for Industrial Radiation Circuits with Power-Generating Channel-Type Reactors – A. Kh. Breger, S. P. Dobrovol'skii, E. L. Ivanter, V. S. Petrov, N. I. Rybkin, A. M. Sidorov, and Yu. I. Tokarev	739	60
Determination of Fission Product Charge Distribution Parameters – A. B. Koldobskii, V. Yu. Solov'ev, and V. M. Kolobashkin	741	61
Spatial and Spectral Distributions of Gamma Rays Reflected by Shields of Light Materials – D. B. Pozdneev and M. A. Faddeev	741	61

CONTENTS

(continued)

	Engl./Russ.	
LETTERS TO THE EDITOR		
Perturbation Theory of Various Approximations in Steady-State Neutron Transport – V. Ya. Pupko	742	63
Effect of Reactor Irradiation on the Dissociation Pressure of Zirconium Hydride – V. S. Karasev, V. G. Kovyrshin, and V. V. Yakovlev	745	65
Optimal Bringing of Reactor into the Stationary Regime of Fuel Reloading – B. P. Kochurov	747	66
Operational Measurement of Biomedical Proton Beam Intensity – Ya. L. Kleinbok and V. M. Narinskii	751	69
Lead Transmission Curve for 31-GEV Electrons – A. S. Belousov, E. I. Malinovskii, S. V. Rusakov, S. P. Kruglov, and V. D. Savel'ev	754	71
Radiation and Thermal Tests of Electron-Emissive Neutron Detectors and Cables with Magnesial Insulation – I. Ya. Emel'yanov, V. I. Vlasov, Yu. I. Volod'ko, S. G. Karpechko, L. V. Konstantinov, V. V. Postnikov and V. I. Uvarov	756	72
The Problem of Calculating a Polycell in P_3-Approximation – A. D. Galanin, V. V. Smelov and B. Z. Torlin	762	76
Measurement of Certain Characteristics of ^{249}Bk – V. M. Glazov, R. I. Borisova, and A. I. Shafiev	764	78
Use of Radiative Capture of Thermal Neutrons to Determine the Ash Content of Coal – L. P. Starchik and Yu. N. Pak	766	79
INFORMATION		
Black Holes Are Real – N. A. Vlasov	769	81
INFORMATION: CONFERENCES AND MEETINGS		
35th Session of the Academic Council of the Joint Institute of Nuclear Research – V. A. Biryukov	772	82
Conference of the IAEA Group on the Design of Fusion Reactors – G. N. Popkov	777	85
Seminars and Exhibitions of the All-Union "Izotop" Corporation	779	86
INFORMATION: NEW INSTRUMENTS AND FACILITIES		
KTN-2 Tantalum and Niobium Concentration Meter – B. E. Kolesnikov, E. D. Kokhov, Yu. D. Lavrent'ev, and A. P. Khukhyanskii	780	87
Transportation and Reloading Container for Remote-Controlled Gamma Therapy Instruments – V. T. Emel'yanov, V. M. Kondrashov, and M. P. Sinodov	782	89
New Gamma Flaw Detectors for Testing the Welding of Main Pipelines – V. N. Khoroshev, A. I. Murashov, V. N. Polosatov, and N. I. Neustruev	784	90
BOOK REVIEWS		
Yu. M. Dymkov. The Nature of Pitchblende – Reviewed by V. L. Barsukov	787	93
B. I. Spitsyn and B. B. Gromov. Physicochemical Properties of Radioactive Solids – Reviewed by E. V. Sobotovich	789	93
A. Thomas and F. Abbey. Calculation Methods for Interacting Arrays of Fissile Materials – Reviewed by I. A. Stenbok	790	94

The Russian press date (podpisano k pechati) of this issue was 6/27/1974. Publication therefore did not occur prior to this date, but must be assumed to have taken place reasonably soon thereafter.

FAST GAS AND THERMAL BREEDER REACTORS

S. M. Feinberg*

UDC 621.039.524.526

Designs for breeder reactors with molten metal coolants (sodium) have by now been widely disseminated. Several such experimental and experimental-industrial reactors are already working or are being brought into operation in the Soviet Union, the United States, Britain, and France.

However, in addition to the sodium breeder reactors there are also plans for other aspects of breeder development including those of the fast gas and thermal thorium types.

Problem of Uranium Resources

The current phase in the development of nuclear power is characterized by high rates of increase in power. The time for doubling the powers of nuclear installations is estimated as 3-5 years in the 70's and 5-7 years in the 90's. The fast breeders with liquid-metal (sodium) coolants now being built or designed have a doubling time of over 7-10 years and therefore cannot lead to any significant economy in natural uranium until the beginning of next century. Figure 1 shows the natural uranium requirements for nuclear power using thermal reactors of various types and fast breeders with various doubling times (T_2) [1]. The economy of natural uranium depends on changes in the doubling time of fast breeders: only for short doubling times (of the order of three years) can there be a substantial economy in natural uranium before the year 2000. It is true that after the year 2000, with the reduction in the tempo of nuclear-power development, the effectiveness of fast breeders may undergo a relative increase; however, thermonuclear reactors may also enter into the power arena, and even independently of these the conditions and demands relating to the development of power may change so substantially as to make present predictions entirely out of date. We can hardly look into the future further than 2010. Finally it must be emphasized that a moderate saving of natural uranium may from the economic point of view be completely insufficient in order to compensate for the probable increase in capital expenditure associated with the transition to fast breeders. This means that any shortening in the doubling time of fast breeders will also increase their competitiveness.

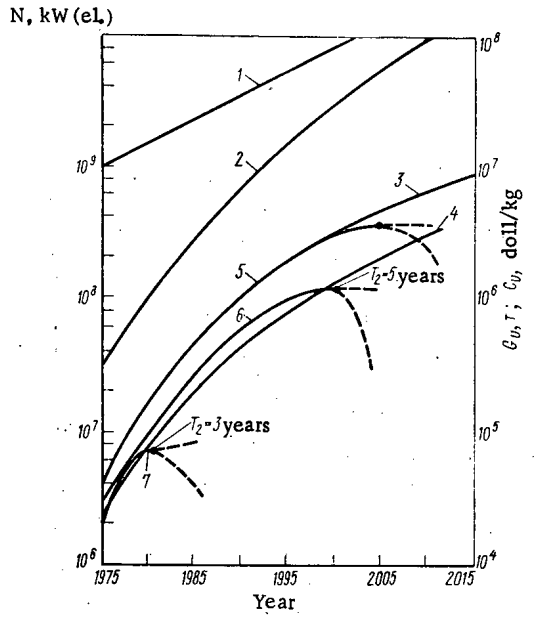

Fig. 1. Demand for natural uranium (G_U) in the development of nuclear power, using various types of reactors (G_U represents the reserves and cost of natural uranium). 1) Total development of electrical power; 2) nuclear power stations of all types; 3) LWR; 4) HWR; 5, 6, 7) breeder reactors with a doubling time of 7, 5, and 3 years respectively.

We should note that the demand for uranium, after reaching a maximum, will rapidly start falling; this means there will be an excessive production of secondary

*Deceased.

Translated from Atomnaya Énergiya, Vol. 37, No. 1, pp. 3-10, July, 1974. Original article submitted September 11, 1973.

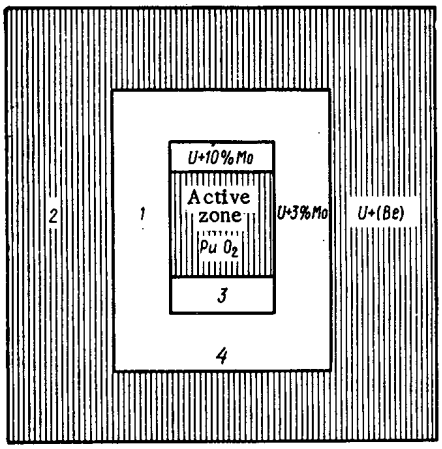

Fig. 2. Arrangement of a reactor with a "plutonium" active zone. 1) First screen; 2) second screen; 3) first end; 4) second end.

fuel in fast breeders. The excess will have to be directed into thermal reactors, particularly "peak" nuclear power stations, which will ensure an economically satisfactory coexistence of breeders and thermal reactors. If 30% of the power is provided by fast gas breeders with a doubling time of 3.2 years, the remaining 70% of the power may be obtained from traditional thermal reactors working in the Th and ^{233}U fuel cycle. The power-doubling time in such a combined nuclear power system will be 10 years.

It is thus clear that in the coming quarter of a century, fast reactors will only be able to become the basis of nuclear power if short doubling times, of the order of 3-years, can be achieved.

Ideology of "Hard" and "Soft" Neutron Spectra in the Active Zone

It is well known that there are two "limiting" solutions of the fast breeder.

1. A physically large active zone with $M^2 \ll R^2$ using plutonium diluted with ^{238}U and other materials so that the macroscopic inelastic slowing-down cross section is much greater than the plutonium fission cross section: $\Sigma^{in}/\Sigma^f \gg 1$. The fission of ^{238}U takes place mainly inside the active zone. The neutron spectrum in the active zone is soft, i.e., the average energy of the neutrons producing fission is of the order of 0.1 MeV [1].

2. A physically small active zone with $M^2 \approx R^2$ in which the plutonium is slightly diluted with oxygen (or graphite), construction materials, and coolant, so that $\Sigma^{in}/\Sigma^f \approx 1$. The fission of ^{238}U then occurs in the reflector zone adjacent to the active zone. The neutron spectrum is hard (mean energy ~1 MeV) [2, 3].

In the first case the conversion ratio is lower and more sensitive to the increment $\alpha = \sigma_c^5/\sigma_f^9$. However, the dilution of the plutonium in the active zone enables the thermal loading of unit plutonium to be increased and an internal "capacity" (for storage space) to be formed for storing a large quantity of fission products, i.e., for increasing the depth of burn-up of the nuclear fuel. It is also possible to choose a composition of the active zone for which K_∞ changes little in the course of burn-up.

The first scheme describing the physical make-up of the active zone we shall subsequently call "dilute" and the second one "plutonium." We emphasize that the "plutonium" scheme in no way limits the size of the active zone or its unit power. In order to increase the size of the active zone (or its power), we must set up several individual plutonium zones inside the large reflector. Depending on the "clearance" (thickness of the reflector), physical interference may arise between the individual modules: for a clearance of the order of 300-500 mm this interference becomes insignificant. We shall call an active zone made up of systems of individual plutonium zones "multiplutonium." A plutonium active zone is shown in Fig. 2, together with the surrounding screens (breeding zones). The latter are situated in a vessel with a diameter of around 2 m. A multiplutonium active zone is illustrated in Fig. 3. The diameter of the vessel increases to 3.5 m and the power by an order of magnitude.

Up to the present time there has really not been any convincing analysis of the relative advantages and disadvantages of the fundamentally different solutions of "dilute," plutonium, and multiplutonium active zones in breeder reactors.

Progress in Breeder Reactors with Gas Coolants

Considerable advances may be achieved by using gas coolants: The possibility of excluding chemical corrosion and so achieving higher temperatures, simplicity of cleaning, and convenience in use, is attracting more and more attention toward gas coolants. We must accordingly regard gas as a coolant offering new prospects for the progress of fast reactors with a short doubling time.

Possible gas coolants include helium, carbon dioxide, and so-called dissociated gases of the N_2O_4 type [4]; the latter possess a great heat capacity at moderate temperatures. Most authors now accept steam coolants as a potentially weaker rival.

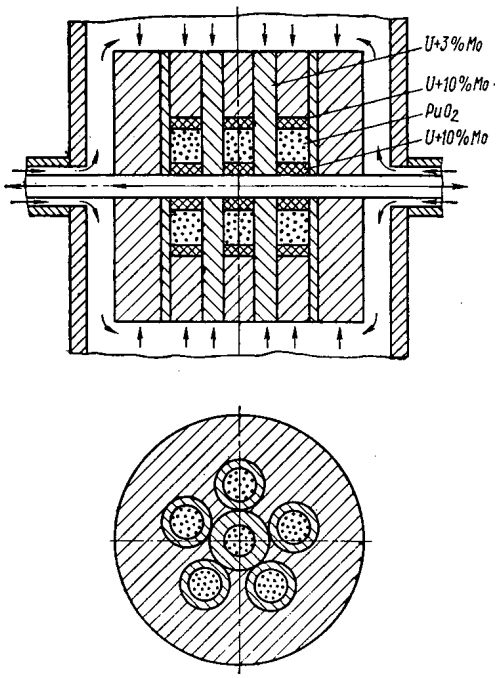

Fig. 3. Scheme of a reactor with a "multiplutonium" active zone.

The fundamental advantage of helium lies in the fact that its interaction with the cores of the fuel elements, their coverings, and other construction materials is minimal. The direct influence of helium on the physics of the reactor is greatly reduced by virtue of the construction materials and diluents introduced into the active zone and the reflector of the reactor so as to ensure a high specific heat take-off from the nuclear fuel.

The introduction of sodium coolant into the active zone slows the neutrons and greatly reduces the conversion ratio, by ~0.15. The conversion ratio is also greatly reduced by the incorporation of construction materials such as iron and iron alloys in the active zone, and also by slowing-down in oxygen, since, in order to achieve a deep burn-up, the nuclear fuel is usually employed in the form of its oxides.

Helium may be used if a large heat take-off is achieved from each unit of nuclear fuel, since without this the doubling time will be greater even for a very high conversion ratio. It is well known that the limiting factor for gas coolants is the consumption of power in circulation and the pressure drop around the circuit. In order to achieve pressure drops and circulation power consumptions acceptable from the engineering point of view, a high pressure of the working gas is essential. On the other hand, it is desirable to minimize the length of the working part of the active zone in order to reduce the pressure drop and also as far as possible to reduce the diameter of the high-pressure vessel, if a metal vessel is in question, so that as far as possible the dimensions of the active zone and the side reflectors should be reduced.

It follows from Table 1 that a gradual, significant progress may be achieved in the parameters of nuclear power stations by raising the temperature and pressure in the system.

If the diameter of the vessel is not very much in excess of 2 m, the creation of such a vessel with a pressure of 300 abs. atm presents no serious technical difficulties. For diameters no greater than 4.5-4.0 m the achievement of pressures up to 55 abs. atm, using multilayer steel vessels, should be perfectly reasonable in the next 15-20 years. Raising the surface temperature of the fuel elements to 800°C is also a reasonable expectation. It is very important to emphasize the relationship between the fuel efficiency of atomic power stations and the doubling time. For example, if T_2 increases from 3.2 to 4.5 years as a

TABLE 1. Effect of Gas Pressure and the Temperature of the Fuel Elements on the Main Parameters of Nuclear Power Stations with Fast Gas Reactors Having a "Plutonium" or "Multiplutonium" Active Zone

Main parameters of the nuclear power stations	Maximum can temperature					
	700			800		
	Working pressure of helium, abs. atm					
	300	400	500	300	400	500
Power used in circulating the helium (6% of the thermal power of the circuit)	2,9	2,9	2,9	2,9	2,9	2,9
Temperature, °C						
at the inlet	210	265	305	250	335	390
at the outlet	420	440	460	440	525	550
Steam pressure before the turbine, abs. atm	30	80	180	65	180	240
Efficiency, %						
gross	30—31	37—39	42—44	35—37	42—44	46—48
net	27—28	32—34	38—40	32—34	38—40	42—44
Conversion ratio	2,05	2,05	2,05	2,05	2,05	2,05
T_2, *years	3,2	3,2	3,2	3,2	3,2	3,2

*For a 30% burn-up of the plutonium in the active zone the time of the campaign is 0.7 of a year; the depth of accumulation of plutonium in the metal reflector is 10 kg/ton and the time of the external fuel cycle is 0.5 of a year.

TABLE 2. Some Characteristics of the MSBR Reactor

Characteristics	Without separation of protactinium	With separation of protactinium
Conversion ratio	1.0538	1.074
Loss of fuel in reprocessing	0.006	0.007
Yield of secondary fuel per atom of fuel passing into the reactor, %	4.96	7.95
Number of secondary neutrons arising per consumed atom	2.221	2.227
Specific loading, MW (thermal)/kg fuel	2.89	3.26
Cost of fuel cycle, *mills/kW·h	0.45	0.33
Doubling time for the system of reactors, years	14	8.7

*Mill = one thousandth part of a dollar.

result of a 40% fall in the thermal loading of the active zone, the helium inlet and outlet temperatures may be raised to 340-500°C, and this will enable the thermal efficiency to be raised to ~40%.

Fuel Element Problems

Metallic uranium and uranium alloys limit the depth of burn-up to ~2%. Hence this solution to this problem is usually sought by employing uranium and plutonium oxides or carbides. Experiments indicate that oxides give a depth of burn-up of ~10%. It is reasonable to expect that in loose fuel elements (uranium or plutonium dioxide poured into a steel can) with a can thickness of 0.1-0.2 mm, a burn-up of ~50% may be achieved if the can is freed from the internal gas pressure of the fission products, and if damage by contact with the coolant is prevented. This latter is achieved by using an inert gas as coolant, and the former by creating an oxide core of low density (~7.5 g/cm^3) and a more or less free outlet for the gaseous fission products from the fuel elements (for example, by incomplete sealing at the ends of the fuel elements). Thus it is essential to allow for the outflow of radioactive gaseous fragments, with a certain time lag, into the coolant circuit. Experience shows that the same applies to reactors with liquid-metal cooling, and also to thermal reactors by virtue of the dehermetization of the fuel-element cans on irradiation.

Estimates show that, on removing the radioactive noble gases and iodine, amounting to 0.5% of the flow of coolant, the radioactivity of the circulation circuit is less than 0.1 Ci/liter (the usual norm for water-cooled water-moderated reactors), which is 2-3 orders of magnitude smaller than in a sodium circuit.

At first glance it might seem that, for a very deep burn-up (30-50%), the fuel-element can will suffer extremely serious radiation damage from the action of the fast neutrons. Calculations show that this damage is not only no greater but (unexpectedly) less than in breeders with a sodium coolant.

In order to reduce the amount of diluents and construction materials as much as possible, metallic uranium should be used in the reflector, while the active-zone fuel elements in the steel cans should be filled with plutonium dioxide only. In this way the amount of oxygen in the reactor is reduced by an order of magnitude. It has been suggested that on slightly alloying the metallic uranium with molybdenum or zirconium the depth of accumulation of fission products may be increased to 0.8-1% without serious swelling of the fuel elements. Fuel elements with very thin cans may then successfully operate in the reflector zones directly bordering the active zone (in layers 10 cm thick). In the case of the end reflectors, if from constructional considerations it is impossible to avoid a simultaneous replacement of the cassettes of the active zone and the end reflector, it may be necessary to use uranium substantially alloyed with molybdenum, having a 2-3% depth of burn-up.

In many designs of gas breeder reactors with a "diluted" active zone it is proposed to use steel tubular fuel elements with a diameter of about 6 mm and an artificially rough surface in order to intensify the heat take-off by the gas coolant. The cores of such fuel elements are either formed from tablets composed of the sintered dioxide of ^{238}U and plutonium or else filled with spheres of the sintered dioxide [5].

The production of a high volumetric energy intensity in reactors of large dimensions, with longitudinal cooling of the rod-type fuel elements, involves large pressure drops and substantial losses of power in pumping of comparatively moderate pressures. It is precisely because of this that, with rod-type fuel

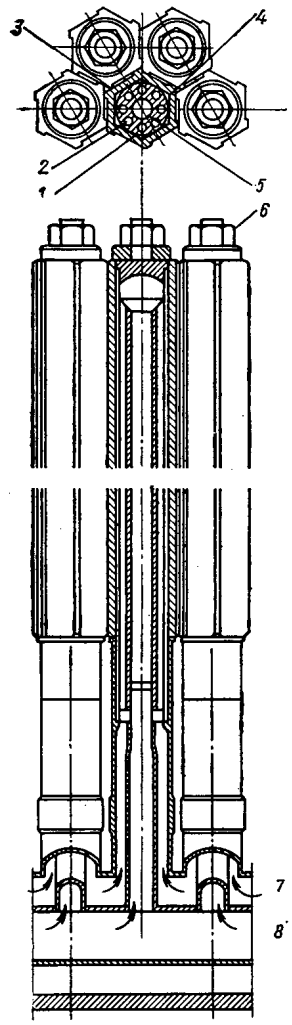

Fig. 4. Schematic section of a cell in the active zone of a salt thermal breeder. 1) Tubes for fuel; 2) upward motion of the fuel; 3) graphite; 4) slot apertures; 5) downward motion of fuel; 6) moderator unit; 7) fuel inlet; 8) fuel outlet.

elements 5-6 mm in diameter, it is impossible to obtain a gas reactor with characteristics much better than those of liquid-metal breeeders. It is essential to find fuel elements with more developed specific surfaces, and more efficient ways of "impelling" the gas through the reactor. The way out may be found by using spherical micro-fuel elements, so creating a longitudinal–transverse motion of the gas in the cassette. A substantial increase in the cooling surface area, an increase in the maximum permissible surface temperature to 1000°C, and the longitudinal and transverse motion of the gas should allow the volumetric loadings to be increased to 1000 kW/liter for a gas pressure of 150 abs. atm. It is considered quite possible to heat the gas to 750-800°C. This opens the attractive prospect of replacing steam turbines by gas turbines and completely eliminating the construction of a second circuit for the circulation of the working substance. Hence the development and adoption of micro-fuel elements is of great interest for the further development of fast gas breeder technology.

Problem of Safety

The problem of the safety of a fast gas breeder working at high pressures and very great specific thermal loadings in the active zone is of vital importance. If leaks occur through gaps of less than 100 cm^2 in the circuit, the shut-down cooling of the active zone may be simply effected by a multiple-loop consideration of the circulatory circuit (at least four loops).* A complicated problem is that of ensuring safety in the improbable emergency of an instantaneous and complete rupture of the pressure vessel, leading to the flying apart of fragments of the latter.

In the overwhelming majority of designs it is proposed that the reactor vessel be made out of prestressed reinforced concrete. The air-tightness of such vessels depends in no small measure on the reliability of the large steel flanges and the covers for the steam generators and gas blowers built into the stressed concrete. Through these covers pass all the many conduits for the water and steam pipes, power cables, and so forth. Thus the weak points of these vessels include the steel covers and flanges with diameters of > 4 m. In order to strengthen these dangerous components for pressures of > 60 abs. atm it is proposed to use a system of double cover plates. The vessel is thus transformed into a cumbersome, complicated, and expensive construction: for a reactor with a power of 1 million kW (el.) and a pressure of 120 abs. atm the diameter reaches ~ 32 m, the height ~ 40 m, and the volume around 30,000 m^3. The cost of such a vessel (together with the thermal insulation) is about 20% of the cost of the whole nuclear power station, i.e., 40 million dollars or over.

In a design proposed for a fast helium breeder with small plutonium active zones, another method of ensuring high strength of the vessels, based on the idea of spreading the stresses, is employed: the high-pressure vessel is placed inside another hermetic vessel of intermediate pressure, designed to accommodate the whole of the working substance if the main vessel ruptures. The low pressure so created (~ 10-30% of the working pressure of the first circuit) is sufficient to ensure proper shut-down cooling of the active zone when the emergency protective system operates. Under normal use the second intermediate-pressure vessel does not carry any pressure, and a low temperature is maintained in this vessel by means of a cooling system and thermal insulation. This vessel is designed solely for short-term operation under emergency conditions.

In order to prevent any serious flying apart of pieces of the high-pressure vessel after its possible instantaneous rupture, strong horizontal bandages and supports for the vessel covers are provided, limiting the flight of pieces of the high-pressure vessel to gaps 1-2 cm wide. These are designed for briefly accepting the pressure of the working substance.

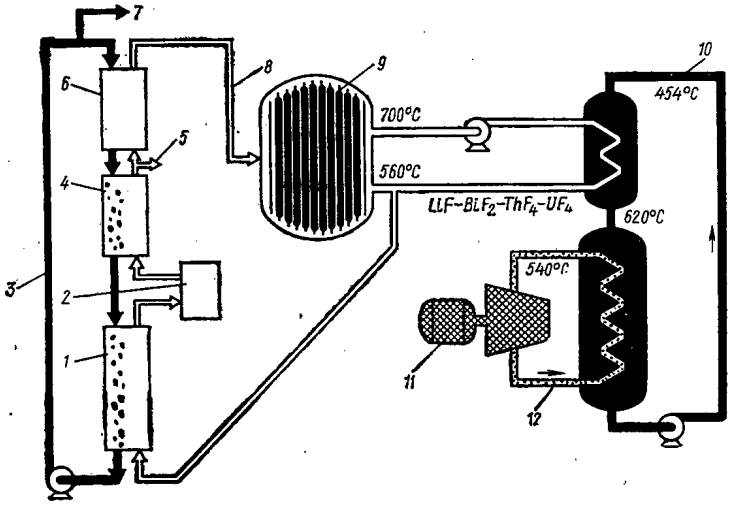

Fig. 5. Arrangement of the circulation loop of a thorium thermal breeder. 1, 4) Salt-liquid mixers; 2) decay of Pa; 3) liquid bismuth; 5) removal of fission products; 6) electrolyzer; 7) bred uranium; 8) purified salt; 9) reactor; 10) cooling liquid salt; 11) turbogenerator; 12) steam.

In our own opinion the provision of bandages to limit the flight of vessel fragments is unnecessary, since no such construction should be required in the presence of a continuous monitoring system, preventing the appearance of dangerous cracks in the high-pressure vessels. This constitutes a reliable guarantee against the sudden rupture of the high-pressure vessel. Methods of nondestructive testing for verifying the state of the pressure vessels are rapidly being perfected and will undoubtedly reach the required level in the near future.

Problem of the Composition of the Reactor

The widely expressed opinion that an increase in the unit power of the reactor is the best way of improving the economy of a nuclear power station is not, in our own opinion, entirely obvious. We consider that it is perfectly possible to conceive powerful nuclear power stations consisting of a large number of individual (module) reactors, relatively small as regards unit power, linked by a single gas circuit and sundry provisions.

What makes us say this?

The conversion ratio of a reactor with a physically small (plutonium) active zone reaches the maximum possible value for fast reactors. In this respect the situation in fast reactors is the opposite of that in thermal reactors, in which an increase in reactor dimensions leads to a rise in the plutonium coefficient and to a fall in the fuel component.

A reactor with a large unit power requires a large (once-only) insertion of plutonium and an assimilation of the technology of large high-pressure vessels, creates difficulties in the reservation of power during reactor shut-downs for recharging, and requires the creation of a very complicated system of recharging while running (one of the reactors of a nuclear power station containing, say, ten reactors may be undergoing recharging at any given time). All this inevitably complicates the design, erection, and development of the primary installations, and makes the creation of the new technology less rapid and more expensive. In our own opinion, it is precisely the expenses and delay involved in mastering the new technology that constitute the chief reason for its retarded introduction. It would therefore appear desirable to seek solutions to the problem in such a way that the unit outlay of plutonium and the unit powers should be comparatively small and not require the development of new technology for the erection of large high-pressure vessels. It does not follow that a reduction in the unit power of the reactor will lead to a considerable increase in the capital outlay for an established 1 kW of electric power. The capital outlay on a nuclear power station is mainly made up of expenditure on the coolant circulation system, on the cassettes, heat exchangers, gas provisions, the equipment of the second circuit, the machine room, the reactor building, the radiation shielding and purification system, the preparation of the site, and so forth. The cost of the

high-pressure steel vessels and the actual reactors amounts to some 10-15%. Hence a nuclear power station composed of several (5-10) smallish module reactors may not be inferior as regards capital outlay to a nuclear power station of equal power consisting of a smaller number of reactors (one or two).

However, the module station will be simpler in its adoption, considerably more reliable in use, and less subject to radiation hazard: ten modules of a total power of 1 million kW (electric) are sited in pockets within a single reinforced concrete unit with a total volume of ~20,000 m^3.

The actual economic efficiency of the "breaking down" of the nuclear power station, i.e., the use of a larger number of individual small reactors, constitutes a problem for future study.

Hence we should at the same time consider versions with a multiplutonium active zone, assuming the use of a high-power reactor, while retaining physically small active zones and all the physical indices associated with these.

At the present time designs for fast gas breeders are being extensively published in the literature of other countries. Common to all these is a scheme based on the reactor having a high-power, diluted active zone of ~10^3 MW (el.). Preferentially proposed is an integrated composition in a large stressed reinforced concrete vessel with a coolant pressure of 60-120 abs. atm. It is proposed to make either ordinary fuel elements in the form of steel tubes with a uranium and plutonium dioxide core or else micro-fuel elements with graphite-based coatings. The reflectors are of the same type, but without plutonium; the conversion ratio is between 1.3 and 1.5.

According to the published economic estimates, the capital outlay is either 10-20% smaller than that of sodium breeders or else approximately the same. The cost of the fuel cycle is 20-30% higher than that of sodium breeders, and differs little from the values obtained for water-cooled, water-moderated reactors. The doubling time is considerable: ten years or over.

A Soviet design based on a similar conception was recently published [2], except that in this case the doubling time was 5-6 years and the helium pressure was rather greater (150 abs. atm). The shortening of the doubling time is here motivated by considerations of the economy of raw materials, i.e., an increase in the cost of mining uranium is envisaged.

Thermal Breeders with a Thorium Fuel Cycle and Circulating Nuclear Fuel

When considering gas breeders, the importance and effectiveness of increasing the conversion ratio is always emphasized; for a reactor consisting of a purely plutonium core surrounded by pure ^{238}U this may theoretically reach 2.5. Under practical conditions the conversion ratio hardly exceeds 2.0; in sodium breeders being constructed or designed it is ~1.5.

In contrast to this, it is possible to make breeders with a conversion factor of little over unity (1.05-1.10) and a comparatively short doubling time. This arises from the fact that the doubling time for the amount of nuclear fuel is mainly determined by two parameters: the conversion ratio and the energy intensity of the nuclear fuel.

In thermal reactors the degree of dilution of the nuclear fuel is several orders of magnitude higher than in fast breeders. Hence there may be tens of times more intensive a heat release in the former as in the latter. Furthermore, there is also the possibility of taking a fundamentally new and important step: that of abandoning solid fuel elements, the use of which is accompanied by a complicated process of radiochemical and metallurgical processing, and organizing the circulation of the nuclear fuel in the form of a salt melt. A number of the reprocessing procedures of the thermal cycle then fall away. Regeneration is considerably simplified, the necessity of ensuring a high degree of purification of the fuel from the fission products is eliminated, and so forth. It is true that every power reactor is thus converted into a radiochemical undertaking, and of course the problem of burying and removing the radioactive waste is much more complicated for radiochemical factories than for reactors.

However, in principle this problem is entirely soluble.

Thus if the (CR-1) of a fast breeder amounts to 0.5-1.0 and the (CR-1) of a thermal breeder to only 0.05-0.10, it is sufficient to increase the energy intensity of the fuel by a factor of 10 in order to achieve the same doubling time.

A reactor with circulating liquid nuclear fuel enables us to reach the required energy intensity.

Fuel Cycle of a Thermal Breeder

Since of all the known fuel cycles of thermal reactors only a composition of ^{233}U and ^{232}Th yields a conversion ratio of greater than unity, it is precisely this fuel cycle which is used in the thermal breeder. Here a new nuclear raw material is introduced into the power system, thorium, and this greatly increases the potential resources of nuclear fuel, since thorium is several times more widespread in the Earth's crust than uranium. In designing fast breeders the possibility of drawing thorium resources into the power system is also envisaged.

A great advance in the development of designs for such thermal breeders was the initiation in 1966 of a small experimental MSBR reactor with a thermal power of 8000 kW in Oak Ridge National Laboratory, USA. This reactor has provided a great deal of working experience, on the basis of which designs of reactors with powers of up to 1 million kW (el.) have been developed.

The active zone of the reactor is formed by a system of vertical graphite tubes (Fig. 4) serving as moderator and construction material. A liquid salt melt containing ^{233}U passes into the graphite tubes from metal collectors placed under the active zone. The melt is carried up through apertures in the graphite and then down through a central graphite tube into the outlet metal collectors. Passing through the active zone, the ^{233}U sustains a chain reaction and heats the salt melt. The usual temperatures are 560°C at the inlet and 700°C at the outlet.

At the reactor outlet the melt passes into metal heat-exchangers in which the heat is transferred to the working substance of the turbine. The active zone is surrounded by a graphite reflector siting the ^{232}Th. The leakage neutrons are absorbed by the ^{232}Th, forming a new nuclear fuel, ^{233}U. The radiochemical system, continuously acting in the bypass of the liquid nuclear-fuel circulation loop, separates the fission products and protactinium, and releases ^{233}U and ^{232}Th to make up the nuclear fuel (Fig. 5).

Table 2 shows the indices of the MSBR.

Thus fast gas breeder reactors may have a somewhat greater conversion ratio than liquid-metal fast breeder reactors, and a coolant technology which is simpler in use. However, these reactors operate at considerably higher pressures and require a great expenditure of energy in circulation. In principle such reactors open the way for a transition to the single-loop system.

These reactors may exceed LMFBR (liquid metal fuel breeder reactor) as regards economic indices, shorten the doubling time, and thus solve the problem of uranium raw material.

Thermal breeders with the circulation of liquid nuclear fuel and with a uranium–thorium fuel cycle have a very small CR-1 factor (~0.05-0.10), but a high specific power, and may therefore also have a short doubling time.

LITERATURE CITED

1. S. Feinberg, Cooled Fast Reactor, Techn. Rep., IAEA-154, Vienna (1973), p. 21.
2. N. Ponomarev-Stepnoi, ibid., p. 191.
3. P. Forteskye, ibid., p. 63.
4. A. Krasin, ibid., p. 89.
5. M. Donne, ibid., p. 267.

NEW PROSPECTS IN THE CREATION OF GAS-COOLED FAST REACTORS WITH A SHORT DOUBLING TIME, USING DISSOCIATING N_2O_4

A. K. Krasin and V. B. Nesterenko

UDC 621.039.534

Future rates of development and economic characteristics of nuclear power will be largely determined by the rate of accumulation of plutonium. It is therefore an extremely urgent matter to solve the problem of ensuring the automatic supply of plutonium for developing nuclear power systems involving fast reactors [1], and also to create fast reactors with physical characteristics such as will advance the construction of nuclear power stations with fast reactors having a doubling time of 4-5 years. This would increase the rate of growth in the powers of nuclear power stations by a factor of two to four as compared with that of thermal power stations.

Allowing for the small part now played by nuclear power in the total power-supply system of the USSR and the need to increase this proportion substantially by the year 2000 (to 30-50% of the total output of all power stations [2, 4]), it was shown in [4, 5] that in 1980-1990 the doubling time for the powers of nuclear power stations should amount to 4-5 years, and in 1990-2000 to 6-7 years.

Further improvements in the physical characteristics of fast reactors may be achieved by raising the specific thermal stress of the active zone and also the specific concentration of the nuclear fuel (for example, by using low-alloy uranium, in which the nuclear concentration is twice as great and the thermal conductivity an order of magnitude higher than in the case of UO_2). However, in such alloys there is a characteristic radiation-induced swelling of the fuel elements and a strict limitation is imposed upon the maximum fuel temperature (no higher than 630-650°C). The heat-takeoff efficiency on the gas side may be raised by increasing the pressure; thus, in order to secure specific thermal stresses competitive with sodium in the case of helium reactors, a pressure of 250-300 abs. atm must be used; for CO_2 the corresponding pressure is 220-250 and for N_2O_4 140-160 abs. atm [6].

Hence in fast gas-cooled reactors with a high specific thermal stress and a large external pressure using UO_2-base fuel it is preferable to prepare the fuel not in the form of pure UO_2 but in matrix form, which has a thermal conductivity two or three times greater, although the maximum temperature of such fuel is lower (1300-1400°C) than in the case of UO_2.

Thus in order to achieve high specific thermal stresses the use of fuel with a greater thermal conductivity than UO_2 requires a reduction in the maximum temperatures of the coolant to 400-500°C for matrix composites and 270-350°C for slightly-alloyed metallic uranium. This leads to a fall in the efficiency of the nuclear power station by comparison with the accepted parameters of sodium breeder reactors. For nuclear power stations with fast reactors the main proportion of the cost of electrical power comes from the capital outlay on equipment. For these stations it is therefore justifiable to seek simpler arrangements for converting the heat, and also ways of reducing the equipment costs.

A most important problem is that of creating a strategy for the development of nuclear power such as will ensure the minimum consumption of natural uranium. These problems may be solved if we make fast reactors with a specific thermal stress of 800-1200 kW/liter, and use thermal parameters of the thermal cycle of the atomic power station such as will allow the use of low-alloy metallic uranium with a maximum fuel temperature of 650°C (allowing for overheating factors). It is therefore necessary to seek new coolants and to develop new systems for heat conversion in atomic power stations working at temperature levels of 250-450°C [7].

Translated from Atomnaya Énergiya, Vol. 37, No. 1, pp. 11-21, July, 1974. Original article submitted April 1, 1974.

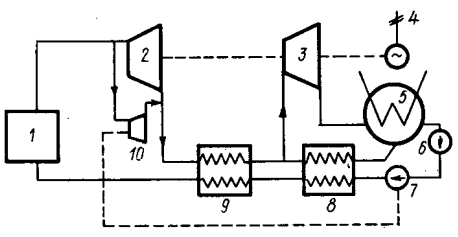

Fig. 1

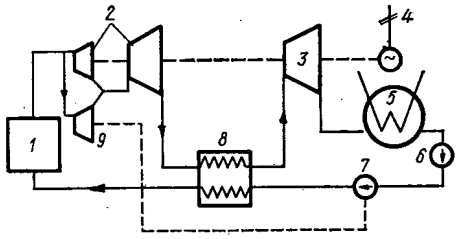

Fig. 2

Fig. 1. Scheme of a liquid-gas cycle with intermediate regeneration and one take-off: 1) Fast reactor; 2) high-pressure turbine (HPT); 3) low-pressure turbine (LPT); 4) electrogenerator; 5) condenser; 6) condensation pump; 7) supply (feeding) pump; 8) regenerative preheater; 9) regenerator; 10) turbine of turbopump.

Fig. 2. Scheme of a gas-liquid cycle with intermediate regeneration: 1-7) see Fig. 1; 8) regenerator; 9) turbine of feeding turbopump.

Thermophysical Characteristics of N_2O_4

One way of solving the problem of choosing a gas coolant for fast reactors may lie in the use of dissociating nitrogen tetroxide ($N_2O_4 \rightleftharpoons 2NO_2$, 149 kcal/kg) in single-loop systems as both coolant and working substance of the nuclear power station [7-12]. A complex study of the thermophysical properties of N_2O_4 has been carried out in the Soviet Union over a wide range of temperatures and pressures: specific heat at 1-170 abs. atm and 30-550°C, p–v–t properties at 50-525°C and 8-150 abs. atm, enthalpy at 50-170 abs. atm and 20-350°C, gas composition at 150-600°C and 1-7.5 abs. atm, viscosity at 30-500°C and 1-140 abs. atm, and thermal conductivity at 30-540°C and 1-150 abs. atm [12]. Heat transfer has been studied during condensation and boiling in a tube and on the flat surface; convective heat transfer has been studied at sub- and supercritical pressures (1-150 abs. atm, 30-550°C) [11-14]. The thermal-radiation resistance has been studied under static conditions for pressures up to 50 abs. atm and temperatures of 300-550°C [11, 12]. The corrosion resistance of construction materials has been studied in N_2O_4 under static conditions at 150 abs. atm and 700°C and under dynamic conditions at velocities of 30-50 m/sec, pressures up to 50 abs. atm, and temperatures up to 550°C [11, 12, 15, 16].

The main factor involved in the favorable thermophysical properties of dissociating gases lies in the existence of large thermal effects in both the first and second stages of the reaction. In experimental investigations into the isobaric specific heat of $N_2O_4 \rightleftharpoons 2NO_2$ at temperatures of 160-300°C and pressures of 115, 130, and 150 abs. atm, large maximum values of the specific heat were obtained: $C_{p115} = 12$ kcal/kg·deg, $C_{p130} = 8$ kcal/kg·deg, $C_{p150} = 5.0$ kcal/kg·deg (Fig. 1 in [11]); the mean specific heat for the range 160-280°C equals 1.95-2.1 kcal/kg·deg. For comparison, we remember that for the same range of temperatures the specific heat of CO_2 is 0.28, that of sodium 0.31, and that of helium 1.243 kcal/kg·deg. Thus the mean specific heat of $N_2O_4 \rightleftharpoons 2NO$ is seven or eight times greater than that of CO_2 and 1.6 times greater than that of helium. In the temperature range 200-500°C the average specific heat of $2NO_2 \rightleftharpoons 2NO + O_2$ is 0.75-0.8 kcal/kg·deg [11]. Owing to chemical reactions taking place in the dissociating gas, in a nonisothermal flow, in addition to the molecular specific heat there is also an additional transfer of a considerable amount of heat in the form of chemical enthalpy by concentration diffusion.

In experimental investigations into the heat transfer associated with the turbulent flow of a dissociating gas $2NO_2 \rightleftharpoons 2NO + O_2$ in a heated tube at supercritical pressures of 115-160 abs. atm, temperatures of 250-530°C, thermal fluxes of 10^6 kcal/m^2·h, and Reynolds numbers of Re $= 2 \cdot 10^5$, heat-transfer coefficients equal to 18,000-38,000 kcal/m^2·h·°C were obtained.

In 1971 experimental work was carried out in relation to the convective heat transfer of a dissociating gas $N_2O_4 \rightleftharpoons 2NO_2$ at temperatures of 165-180°C, pressures of 130-160 abs. atm, Re $= (3\text{-}5) \cdot 10^5$, and thermal fluxes of $(3\text{-}5.5) \cdot 10^6$ kcal/m^2·h in an experimental tube 4 × 1 mm in diameter and 800 mm long (with electric heating), the diameter corresponding to the equivalent diameter in a group of fuel elements ($d_{eq} = 2$ mm). In these experiments, in half the length of the part under consideration a heat-transfer coefficient at 150,000 kcal/m^2·h·°C was attained, the lowest heat-transfer coefficients occurring in the exit section and being about 30,000 kcal/m^2·h·°C. On heating the dissociating gas $N_2O_4 \rightleftharpoons 2NO_2$ from 165 to 280°C the maximum temperature of the can was no greater than 450°C.

Thermophysical calculations carried out for fast gas-cooled reactors at pressures of 120-170 abs. atm and a gas outlet temperature of 250-300°C showed the possibility of achieving a specific thermal stress of 960-1200 kW/liter for specific thermal loadings of the surface of the fuel elements equal to $(3\text{-}5)\cdot 10^6$ kcal/m$^2\cdot$h and a diameter for 6-7 mm. For dissociating gas pressures of 130-160 abs. atm, gas outlet temperatures of 450-500°C, and preheating temperatures of 230-270°C, efficient heat release may be secured from active zone of a fast reactor with a thermal power of 3000-3400 MW for an average energy stress of the active zone equal to 1000-1200 kW/liter and a maximum temperature of the fuel-element cans (allowing for the overheating factor) of 650-680°C.

Experimental work has been carried out on the condensation of recombining gas $2NO_2 + O_2 \rightleftharpoons 2NO_2 \rightleftharpoons N_2O_4$ in vertical and inclined tubes, and on vertical and horizontal surfaces at pressures of 1-9 abs. atm and thermal loads of $0.64\cdot 10^3\text{-}3.1\cdot 10^4$ kcal/m$^2\cdot$h. Average heat-transfer coefficients of 1000-1500 kcal/m$^2\cdot$h$\cdot$°C were obtained for mass velocities of γW = 2-40 kg/m$^2\cdot$sec. A considerable intensification of the heat-transfer processes (by a factor of 2.5-3 times) may be achieved by condensing the chemically reacting gas on finely-undulating ribbed (finned) tubes (horizontal or slightly inclined). In the course of condensation there is a marked intensification of the heat-transfer processes on account of the evolution of the heat of the chemical reactions [12].

Experimental work has also been carried out on the heat transfer associated with boiling both inside a tube and also inside a large vessel with a pressure of up to 90 abs. atm and thermal loadings of $(1\text{-}4)\cdot 10^5$ kcal/m$^2\cdot$h. With such loadings, boiling in a large vessel gave experimental heat-transfer coefficients of 15,000-30,000 kcal/m$^2\cdot$h$\cdot$deg. A characteristic of the boiling of N_2O_4 is the fairly substantial dissociation of $N_2O_4 \rightleftharpoons 2NO_2$, which occurs chiefly at high pressures. Owing to the heat of the chemical reactions, dissociation is accompanied by an intensification of the passage of heat to the vapor bubble as boiling takes place through the boundary film of liquid. In addition to this, on passing from the liquid into the vapor state there is a sudden increase in the degree of dissociation of the N_2O_4 molecules. Corresponding to this process the thermal effect of the chemical reaction is added to the heat of vaporization, and thus intensifies the process of heat transfer while boiling [11-14].

Thermal Schemes of Heat Conversion in Nuclear Power Stations Using N_2O_4

An advantage of the dissociating N_2O_4 system is the possibility of achieving a gas-turbine cycle, so as to be able to use the temperature-varying molecular weight of the gas (specific work of the turbine and compressor) in order to produce a substantial increase in the effective efficiency factor and the specific power of the cycle [17]. Nitrogen tetroxide has a low heat of vaporization, 5.5 times lower than that of water. This simplifies the scheme of heat regeneration in the gas-liquid cycle, since the amount of heat in the gases leaving the turbine is sufficient not only for heating and evaporating the liquid but also for superheating the gas and regenerator by 100-200°C.

At supercritical pressures the use of a regenerator or regenerator and preheater ensures the regenerative heating of the coolant until it passes into the gaseous state, so that a gas-cooled reactor may be used in a condensation cycle with both sub- and supercritical parameters.

The chemical-dissociation reactions occurring on the high-pressure side involve a lower heat of chemical reaction (149 kcal/kg) than those which occur on the low-pressure side in the course of recombination (294 kcal/kg); hence in gas-liquid cycles based on N_2O_4 we have a clear possibility of achieving a higher degree of regeneration of heat in the cycle than in the case of water or CO_2, and hence better thermodynamic indices. As a result of the increased heat-transfer coefficients these processes may be effected in compact heat exchangers.

When studying the mechanism of the chemical reactions and the kinetic constants of the $N_2O_4 \rightleftharpoons 2NO_2 \rightleftharpoons 2NO + O_2$ system it was established that, in any gas-dynamic calculations of the flow parameters of the thermodynamic cycle, the turbines, and the heat-transfer processes taking place in the reactor and heat exchangers, it was essential to allow for the time characteristics of the dissociation and recombination processes. Estimates of the times of chemical relaxation based on existing experimental velocity constants of the chemical reactions showed that in the temperature and pressure ranges of practical importance the first stage of the reaction ($N_2O_4 \rightleftharpoons 2NO_2$) took place in an equilibrium manner ($10^{-6}\text{-}10^{-8}$ sec), while in the second stage of the reaction ($2NO_2 \rightleftharpoons 2NO + O_2$) the chemical relaxation time might vary between $10^{-3}\text{-}10^{-4}$ and 0.1-1 sec, depending on the thermodynamic and geometrical parameters [7]. For intermediate regeneration pressures of 20-25 abs. atm, total regeneration efficiency is achieved, and the

TABLE 1. Results of Radiation Tests on Micro-Fuel Elements

Characteristics	First ampoule	Second ampoule
Thickness of SiC coating, μ	50	90
Burn-ups achieved	11.7	9.2
Limiting temperature, °C	925	925
Number of particles tested	500	500
Number of particles ruptured under irradiation	3	3

effect of the kinetic characteristics of the chemical reactions is almost eliminated; in the high- and low-pressure turbines the flow of gas is almost equilibrium [7, 12].

In the N_2O_4 gas-liquid cycle, the efficiency of the nuclear power station in the temperature range 450-550°C and the pressure range 80-240 abs. atm is 4-6 abs. % higher than that of the water-vapor cycle [7]. For systems with intermediate regeneration we may find an additional increase in the thermodynamic efficiency on account of the introduction of the regenerative take-off processes. However, for nuclear power-station schemes involving fast reactors the greatest interest will lie in arrangements involving intermediate regeneration and one take-off (Fig. 1), and also a simple scheme with intermediate regeneration (Fig. 2).

The pressure of the gas-liquid N_2O_4 cycle after the turbine is equal to 1.5-2 abs. atm, while the specific volume of the N_2O_4 is 34-40 times less than that of water vapor at the same condensation temperature (p_s = 0.04 abs. atm). This enables us to increase the power of a single stroke of the gas turbine very substantially, bringing it up to 500-1000 MW. In addition to this, when using N_2O_4 the flow section of the gas turbine may be made with a small number of steps, since the heat differentials in N_2O_4 turbines are 2.2-2.5 times smaller than in water vapor [12]. Gas-dynamic calculations and design developments for an N_2O_4 gas turbine with a power of 500 MW at 280°C and 150 abs. atm revealed the possibility of making single-shaft two-flow turbines with a total weight of 250-270 tons and a length of 16-18 m [6].

The results of experimental investigations carried out at 25-550°C under thermal conditions at 1-150 abs. atm and radiation-thermal conditions at 10-60 abs. atm showed that the N_2O_4 system had thermal and radiation resistance sufficient to allow its practical use in nuclear power production. The thermal/radiation resistance of N_2O_4 was studied experimentally in the field of n, γ radiation produced by a thermal-neutron reactor in a flow-type loop installation operating at 30 abs. atm and 550°C, and the radiolysis of this coolant in the n, γ radiation field of a fast reactor was calculated. In the dissociating system $N_2O_4 \rightleftharpoons 2NO_2 \rightleftharpoons 2NO + O_2$, by virtue of the specific characteristics of fast reactors, radiochemical effects arise from the action of radiation at a high dose rate ($\sim 10^{19}$ eV/cm^3·sec) after contact times of $\sim 10^{-2}$ in the active zone, the temperature varying over the range 160-280 or 200-450 (500)°C and the pressure over the range 150-170 abs. atm. The radiolysis products of NO_2 are N_2O, N_2, and O_2. The proportion of decomposing coolant in a fast reactor is about 10^{-6} [11].

A great deal of attention has been paid to verifying the chemical stability of an N_2O_4 gas-liquid cycle. Experiments have been carried out in a test-bed with a closed N_2O_4 gas-liquid cycle at 504°C and 5 abs. atm (360 kg of N_2O_4 in the circuit) at a power of 1070 kW with a gas flow of 1400 kg/h for 372 h. In a continuous experiment lasting 170 h, more than 1000 cycles involving the return of the dissociating N_2O_4 coolant along the circuit were achieved on the principle of the sequence liquid-evaporation-heating-dissociation-cooling-recombination-condensation-liquid, and so forth. In these experiments a high thermal stability of the gas parameters was achieved, no irreversibility of the coolant being apparent [12]. In experiments carried out over the period 1966-1971 in a closed gas-liquid loop for 600 h, using 80 kg of N_2O_4, with parameters of 30-550°C and 10-60 abs. atm, complete reversibility of the gas-liquid cycle was also achieved. Altogether the test-bed operated for more than 1500 h under working conditions, including 1000 h without any change of coolant. Chemical analysis of samples taken off revealed no marked change in the composition of the coolant (impurities in the circuit amounted to no more than 0.8%) [12].

In a loop installation working for 600 h under radiation-thermal conditions at 10-30 abs. atm and 500°C; the stability of the gas-liquid cycle was further confirmed [11].

These experiments indicated the complete reversibility of the gas-liquid cycle and the practicable applicability of N_2O_4 as a working substance and coolant for nuclear power installations.

TABLE 2. Characteristics of the Thermodynamic Cycle of an N_2O_4 Atomic Power Station

Characteristic	t, °C	
	280	450
Gas temperature at the reactor inlet/outlet, °C	166/280	200/450
Gas pressure at the reactor inlet/outlet, abs. atm	169/154	169/154
Thermal power of the reactor, MW	4190	3253
Power of the gas turbines, MW	1200	1148
Flow of gas through the reactor, kg/sec	5930	3853
Efficiency of turbine installation, %	28.6	35.3
Efficiency of nuclear power station (gross), %	27	34.5
Power of the turbine drive pumps, MW	80.7	—
Efficiency of the high-pressure turbine, %	88	88
Efficiency of the low-pressure turbine, %	87	87
Efficiency of the turbine pumps, %	80	80
Minimum head in the regenerator, °C	12	15
Minimum pressure in the condenser, abs. atm	2.06	2.06
Minimum temperature, °C	35	35
Pressure of N_2O_4 beyond the pump, abs. atm	173	173
Proportion of coolant take-off to the preheater, %	20	—
Proportion of gas take-off to turbopump drive, %	15	—
Gas pressure beyond the HPT, abs. atm	32	22
Gas temperature beyond the HPT, °C	190	327.5
Temperature at the condenser inlet, °C	65	65
Pressure at the condenser inlet, abs. atm	2.36	2.36

Corrosion Resistance of Construction Materials in N_2O_4

Many years of corrosion tests applied to the construction materials (including tests under stress and thermal loading) revealed no specific forms of corrosion. The construction materials employed were mostly highly resistant to N_2O_4: For those with chromium contents of over 10-13% (Kh18N10T and Kh16N15-M3B steels, etc.) a loss of 0.001-0.005 mm/year was typical at pressures of 1-150 abs. atm and temperatures of 25-700°C, while at lower temperatures good results were obtained for aluminum and titanium alloys, high-chromium cast iron, graphite, silicized graphite, Teflon, and so on. When studying the Kh18N10T and Kh16N15M3B steels used for the cans of the fuel elements, a high resistance to corrosion was obtained at temperatures up to 750°C and pressures of 150 abs. atm under static conditions for tests lasting 1000-12,500 h, and under flow conditions at temperatures up to 550°C and pressures of 50 abs. atm for 4000-5000 h [12, 15, 16].

Using a PGZh-1 loop installation and an ampoule system, the effect of the n, γ radiation of a nuclear reactor and dissociating N_2O_4 on the corrosion resistance of such stainless steels as Kh18N10T, Kh16N15-M3B, etc. was studied at 20-50 abs. atm and 500-550°C. Under these conditions, no difference appeared in the corrosion rate of irradiated samples as compared with those working under simple thermal conditions [11].

The surface of the construction materials exhibits a compact protective oxide film, firmly adhering to the surface of the steel. The preliminary formation of an oxide film by using special solutions or heating in an oxidizing atmosphere at 300-400°C greatly reduces the corrosion rate. Prolonged tests (up to 11,000 h) at 500 and 700°C and a pressure of 50 abs. atm showed that the protective properties of the film were not only preserved but also enhanced. This leads to a further reduction in corrosion rate [12].

Tests were carried out on samples of Kh18N10T steel under loads of 0.9 $\sigma_{0.2}$ at 500-550°C and 50 abs. atm for 1000 h and also on Kh18N10T bellows in a stressed state with a stress factor of 3.25 kg/mm^2. Metallographic analyses of welded and nonwelded heat-treated samples after tests in the stressed state revealed no structural changes. No intercrystallite corrosion was observed; the mechanical characteristics remained unaltered.

TABLE 3. Thermophysical and Gas-Dynamical Characteristics of a 1000 MW (El.) Gas-Cooled Fast Reactor Working with N_2O_4

Characteristic	VBRGD-1000	NBRGD-1000
Thermal power of reactor, MW	3250	3980
Flow of coolant, kg/sec	3850	5900
Gas temperature at reactor inlet/outlet, °C	200/451	166/281
Gas pressure at reactor inlet/outlet, abs. atm	169/154	169/154
Specific thermal stress of active zone, kW/liter	727	960
Volume of active zone, liters	4220	3840
Diameter of active zone (equivalent), m	2.32	2.168
Height of active zone, m	1.0	1.04
Flattening of active zone (D/H)	2.32	2.08
Diameter of fuel-element cans, mm	6.2 × 0.3	7.0 × 0.4
Number of fuel elements in cassette	397	397
Size of cassette under the "key" and can thickness, mm	145 × 2	161 × 2
Thickness of the side breeding zone SBZ, mm	300	330
Thickness of the end breeding zone EBZ, mm	400	400
Thermal loading of fuel-element surface, kcal/m^2 · h		
average	$1.93 \cdot 10^6$	$2.90 \cdot 10^6$
maximum	$2.53 \cdot 10^6$	$3.77 \cdot 10^6$
Maximum temperature of fuel-element cans (outer/inner), °C	549/578	341/412
The same allowing for superheating factor, °C	625/657	—/453
Maximum fuel temperature (nominal/allowing for superheating), °C	1134/1314	568/635
Mean gas velocity in cassette, m/sec	25.3	30
Mean heat-transfer coefficient in the most-stressed set of fuel elements, kcal/m^2 · h · °C	22730	68000

Fuel Compositions of Fast N_2O_4 Reactors

As regards the one-circuit arrangement for converting the heat of nuclear power stations with fast N_2O_4 reactors into energy, stringent demands are made upon the air-tightness of the fuel elements for a burn-up of up to 10 at.% in UO_2 and 5 at.% in metallic fuel in order to preserve access to the working circuits of the nuclear power station.

For gas-cooled fast reactors with a high specific thermal stress of 1000-1200 kW/liter and a high external pressure, fuel composites of the matrix type (which have higher thermal conductivities [19, 20]) are preferable to those in the form of pure UO_2 [10] or uranium carbide. At the present time fuel composites of UO_2 + 30% Cr–Ni in fuel-element cans developed in the Federal German Republic are undergoing reactor tests in Belgium, using a BR-2 reactor operating at up to 5-6 at.% burn-up, with fuel-element diameters of 5.5-7.5 mm, fuel-element can thicknesses of 0.4 mm, a linear thermal loading of the fuel element equal to 500-600 W/cm, a fuel-element can temperature of 600-700°C, and a fuel temperature of 650-1300°C. No radiation swelling of the fuel elements has been detected [17].

Good prospects for use in fast reactors and excellent compatibility with N_2O_4 are offered by a fuel composite made of UC + SiC in the form of microparticles 0.6-2.5 mm in size. Tests were carried out in [20] on fuel particles 850 ± 50 μ in diameter made from $(U_{0.75}, Pu_{0.25})O_{2-x}$ using the gel method; these are being used in producing UO_2–PuO_2 spheres for the VIPAK reactor (a sodium-cooled fast reactor). The particles are coated with a porous buffer layer of pyrocarbon 45-55 μ thick with a compact layer of pyrocarbon 10 ± 5 μ thick on top of it, followed by a layer of SiC 45-90 μ thick. Then the particles were roasted and the fuel core sintered to a high density, forming fuel of the "peas in a pod" type.

Tests were also carried out on two forms of particles under irradiation at 900-950°C in a medium of CO_2. We see from Table 1 that the problem of obtaining fuel for fast reactors is being solved positively, and even at the present time we have fuel yielding average burn-ups of 5-8 at.%.

On the basis of experience gained in the use of fast reactors in the Soviet Union and elsewhere, we may conclude that the most suitable material for the cans of fuel elements in the next decade will be Kh16-N15M3B austenitic stainless steel, which exhibits a high corrosion resistance in N_2O_4 up to 150 abs. atm and 700°C [8].

TABLE 4. Physical Characteristics of a Gas-Cooled 1000 MW (El.) Fast Reactor Working with N_2O_4

Characteristic	t = 450°C		t = 280°C	
	breeder	refabricator	breeder	refabricator
Thermal power of reactor, MW	3250	3250	3980	3980
Gas temperature at reactor inlet/outlet, °C	200/452	200/452	160/281	160/281
Gas pressure at reactor inlet/outlet, abs. atm	169/154	169/154	169/154	169/154
Specific thermal stress, kW/liter	1167	1167	960	960
Form of fuel	Matrix	Matrix	Metal	Metal
Critical mass, kg	1555	2040	1985	2960
Enrichment of fuel with respect to profiling zones, %	9.6/13	14.5/20.8	5.4/7.7	8.1/11.6
Average enrichment of fuel, %	11.5	17.5	6.5	9.8
Maximum burn-up, at. %	10	10	5	5
Plutonium conversion ratio	1.55	1.15	1.95	1.45
Doubling time for a single recharging in closed cycle				
$T_{e.c.}$ = 1 year	7.2	4*	5	3.1*
$T_{e.c.}$ = 0.5 year	5	–	3	–
Off-loading of excess plutonium from the reactor in the continuous off-loading mode	618	931	944	1512
Annual consumption of natural uranium per ton of excess plutonium, tons		261		153
Nuclear power campaign (φ = 0.8), years	0.81	0.875	0.83	0.82
Time required to find fuel in side screens, years	0.97	1.14	2.1	2.4
Characteristics of fission-neutron spectrum:				
average number of neutrons per capture η	2.36	1.90	2.59	2.04
average ratio of fission to radiative capture cross section α	0.237	0.291	0.134	0.213

*In open cycle.

Choice of Parameters for the Equipment of a Single-Circuit Nuclear Power Station with a Fast N_2O_4 Gas-Cooled Reactor

The characteristic features governing the cost of electrical power in nuclear power stations with fast reactors (capital component 60-70%) suggest that the optimum top temperature of the cycle will be considerably lower than in thermal power stations. In view of this, calculations were carried out for the gas-cooled reactors, regenerators, condensers, preheaters, and turbines of N_2O_4 nuclear power stations on a thermophysical, gas-dynamical, and physical basis, with a view to optimizing the parameters, due allowance being made for the kinetics of the chemical reactions. The remaining components of the net cost, such as the technological water supply, the fittings, pipelines, auxiliary systems, and the cost of erection and structural work were taken into account by analogy with data relating to nuclear power stations of other types.

These calculations revealed the maximum gas pressure in front of the turbine (150-170 abs. atm), the minimum temperature heads in the heat exchangers (15-30°C), and the bottom pressure of the cycle (1.9-2.1 abs. atm) giving the best economic indices. These calculations also showed that, owing to certain special characteristics of the properties of N_2O_4 within the hypercritical range of parameters ($p > 103$ abs. atm), there were two economically-equivalent optimum regions as regards specific computed expenditure for the maximum temperatures of the gas beyond the reactor: 430-480 and 250-300°C.

The thermal system of the nuclear power station provides for two parallel-connected gas turbines of 2×500 MW for each 1000 MW (el.) reactor. The characteristics of the thermodynamic cycle for these versions are given in Table 2 [11].

It is very hard to analyze the emergency conditions applicable to gas-cooled fast reactors and to ensure the reliable emergency shut-down cooling of a fast reactor in the case of a rupture in the pipeline of the main circuit. The system of emergency shut-down cooling for a gas-cooled fast N_2O_4 reactor constitutes a closed gas-liquid circuit connected to the reactor in parallel with the loops of the main circuit, and consists of an evaporator-regenerator, a condenser, a pump, and a liquid store (30-50 m^3) containing liquid N_2O_4. In the case of emergency involving a loss of pressure in the reactor vessel, superheated liquid is emitted from the pressure store and ejected into the active zone (even passing out into the reactor

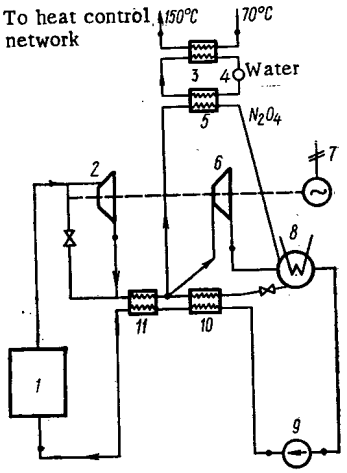

Fig. 3. Basic thermal scheme of the BRIG-50: 1) First reactor; 2) HPT; 3) mains water heater; 4) water pump; 5) water heater; 6) LPT; 7) electrogenerator; 8) condenser; 9) pumps; 10) regenerative preheater; 11) regenerator.

room itself). In order to neutralize the emergency ejections of coolant, a water spray is provided, with subsequent neutralization by means of an alkaline solution.

Thermophysical and Physical Characteristics of Gas-Cooled N_2O_4 Fast Reactors

Thermophysical calculations of a gas-cooled fast reactor were carried out for an active zone corresponding to the dimensions of a steel vessel of the VVÉR-1000 type with working pressures of 170 abs. atm, a maximum diameter of 4.2-4.3 m, and a height of 10-12 m. Engineering design showed that vessels of this kind might house the active zone of a fast reactor with dimensions of 2.2-2.4 m and a diameter/height ratio of 1.8-2.2, with end and side breeding zones 400-500 mm thick, and also radiation and thermal screens for protecting the reactor vessel from fast neutrons. The favorable thermophysical properties of N_2O_4 facilitate the efficient take-off of heat from the active zone of the gas-cooled fast reactor.

Thermophysical and gas-dynamical calculations of gas-cooled fast reactors were undertaken on the basis of experimental data relating to heat-transfer coefficients for the two ranges 160-280 and 200-450°C. The calculations showed that dissociating N_2O_4 gave an efficient heat take-off from the active zone of a fast reactor with a mean thermal stress of 1000-1200 kW/liter, a maximum fuel-element can temperature (allowing for overheating factors) of 650-680°C, a gas temperature at the reactor outlet of 450-480°C, a pressure of 140-170 abs. atm, and a gas preheating of 230-270°C (Table 3).

As fuel for a fast reactor with parameters of this order a matrix-type fuel composition was considered. The maximum temperature of the matrix fuel equalled 1300-1400°C. The effective density of the fuel was taken as 7 g/cm^3. In calculating the doubling time, it was assumed that the time of the external fuel cycle was either 1 or 0.5 of a year; the maximum depth of burn-up was 10 at.%. In these calculations it was found that T_2 = 6-7.2 years ($T_{e.c.}$ = 1 year) or T_2 = 4.5-5 years ($T_{e.c.}$ = 0.5 year), and the conversion ratio CR = 1.55. Analysis of the results of the calculations shows that the reduction in the doubling time relative to the sodium reactors is a consequence of the harder neutron spectrum and the much greater energy stress in an N_2O_4 gas reactor. The gas reactor also has more favorable characteristics from the point of view of safety (the reactivity effect arising from the removal of coolant is 2-3 times smaller than in a sodium reactor).

Thermophysical and physical calculations of a gas-cooled fast reactor with maximum temperatures of 200-300°C were also carried out for a fuel composite based on metallic uranium. The fuel composite was taken in the form of a uranium alloy. Table 4 shows the results of the physical calculation for fast N_2O_4 reactors.

Thermophysical calculations carried out on the basis of experimental data for thermal fluxes of (3-4) $\cdot 10^6$ kcal/m$^2\cdot$h and a temperature range of the gas in the reactor equal to 165-281°C at pressures of 150-170 abs. atm indicated the practical possibility of reaching specific thermal stresses of 950-1200 kW/liter for a maximum fuel-element can temperature of no greater than 500°C and a fuel temperature (allowing for overheating) no higher than 635°C. Such thermophysical characteristics of fast reactors (using low-alloy metallic fuel) yield a considerably harder neutron spectrum and a CR of 1.95, with T_2 = 5 years, and an annual off-loading of excess plutonium equal to 944 kg/year. The use of such a reactor in the guise of a refabricator yields high conversion ratios, amounting to 1.45 and a T_2 of 4 years on supplying ^{235}U (10% enrichment). Working in the guise of reactor-refabricator with $U^5 + U^8$, the annual development of plutonium amounts to 1700 kg/year.

TABLE 5. Technical Characteristics of the BRIG-50 Nuclear Power Station

Technical data	NBRIG Low Temp	VBRIG High Temp
Coolant	N_2O_4	N_2O_4
Number of circuits in the nuclear power station mode	1	1
Number of circuits in the power-and-heat and power-or-heat modes, including the external thermal newtorks	3	3
Number of loops of the nuclear power station from safety considerations	2 × 25 MW (el.)	2 × 25 MW (el.)
Number of systems of emergency shut-down cooling	2	2
Electrical power (net), MW	50 (25 × 2)	50 (25 × 2)
Thermal power of the reactor, MW	227	168
Basic parameters of the coolant in front of the turbine;		
temperature, °C	320	450
pressure, abs. atm	150	150
Power required for internal use, MW	6	5.2
Maximum heat production in the power-or-heat mode, kcal/h	147	123.5
Parameters of the hot water of the external network:		
temperature at outlet from power-or-heat and power-and-heat stations, °C	150/130	150/130
temperature at inlet into power-or-heat and power-and-heat stations, °C	70	70
Parameters of the water in the intermediate circuit		
temperature (inlet/outlet), °C	80/160	80/160
pressure, abs. atm	15	15
Net efficiency of the installation in the nuclear-power-station mode (t_f^m = 150°C/130°C), %	22/28.9	29.8/32.3
Net efficiency of the installation in the power-or-heat mode t_f^m = 150°C/130°C), %	84/82.6	83.5/82.6
Net efficiency of the installation in the power-and-heat mode (t_f^m=150°C/130°C), %	85.0/84	87.0/84
Flow of cooling water in the condenser in the case of a cooling agent, tons/h		
reservoir	$1.28 \cdot 10^4$	$1.06 \cdot 10^4$
cooling tower	$2.12 \cdot 10^4$	$1.41 \cdot 10^4$
Supply of cooling water in the case of a cooling agent, m^3/sec		
reservoir	0.028	0.024
cooling tower	0.075	0.05
Total period of service, years	30	30
Campaign of reactor, years	0.63	0.4
Maximum possible fast neutron flux operating as nuclear power station, power-and-heat and power-or-heat station, neutrons/$cm^2 \cdot$ sec	$3.56 \cdot 10^{15}$	$4.5 \cdot 10^{15}$
Maximum possible fast neutron flux with the active zone working as a research reactor (fuel-element diameter 3 mm), neutrons/$cm^2 \cdot$ sec	$6.16 \cdot 10^{15}$	$6.3 \cdot 10^{15}$
Initial charging of ^{235}U, kg	414	200
Enrichment of nuclear fuel with ^{235}U, %	34.7	75.6
Doubling time ($T_{e.c}$ = 0.5 year)	4.1	4.4

Technical Proposals for an Experimental-Industrial Nuclear Power Station with a Fast-Neutron Gas-Cooled Reactor Having an Electrical Power of 50 MW

In developing ideas for an experimental-industrial nuclear power station with a BRIG-50 reactor (a fast reactor based on N_2O_4), the following aims were envisaged: the achievement of nominal fast neutron fluxes of $(6.7\text{-}7.0) \cdot 10^{15}$ neutrons/$cm^2 \cdot$ sec and specific thermal stresses of 900-1200 kW/liter for gas parameters of 130-150 abs. atm and 280-450°C, as characteristic of 1000-1200 MW nuclear power stations. For such values of the thermal stress it is possible to achieve a short doubling time for the nuclear fuel (4-5 years). It was also naturally wished to select the minimum thermal power of the experimental reactor in order to reduce the cost of constructing the experimental-industrial nuclear power station. Furthermore it was extremely important to ensure the possibility of testing the fuel composites, fuel elements,

TABLE 6. Characteristics of the Reactors of the Experimental-Industrial Installation BRIG-50

Characteristics	NBRIG-50 Low T.		VBRIG-50 High T.	
	producer	test (research)	producer	test (research)
Thermal power of reactor, MW	227	227	168	242
Flow of coolant, kg/sec	295	295	246	238
Gas temperature at reactor inlet/outlet, °C	171/321	171/321	208/451	175/451
Gas pressure at reactor inlet/outlet, abs. atm	169/154	169/154	169/154	169/154
Average energy stress of active zone, kW/liter	843	1880	1300	2560
Equivalent diameter of active zone, m	0,654	0,528	0,586	0,492
Height of active zone, m	0,763	0,524	0,455	0,472
Flattening of active zone (D/N)	0,857	1,01	1,29	1,04
Volume of active zone, liters	256	114,7	122,8	89,8
Thickness of end screen, m	0,6	0,6+0,2 st.	0,6	0,4
Thickness of side screen, m	0,6	0,6+0,2 st.	0.6	0,4
Size of fuel-element array under the key, mm	39	39,5	39	39,5
Step of fuel-element array in a triangular lattice, mm	40	40,5	40	40,5
Number of cassettes in the active zone	242	154	195	134
Thickness of cassette can, mm	1,0	1,0	1,0	1,0
Number of fuel elements in a cassette	37	91	37	91
Diameter of fuel element, mm	5,0	3,0	5,0	3.0
Form of fuel	Metal	Metal	Matrix	Matrix
Effective density of fuel composite in the core, g/cm^3	14,1	14,1	7	7
Total thickness of fuel-element can, mm	0,3	0,16	0,3	0,16
Step of fuel element (triangular lattice), mm	5,8	3,8	5,8	3,8
Maximum temperature of fuel-element can (external/internal), °C	410/437	442/467	570/629	591/624
Maximum temperature of inner can, allowing for superheating factors, °C	492	530	720	720
Maximum temperature at the center of the fuel tablet, allowing for superheating factors, °C	635	635	1203	989
Enrichment of fuel with the fissile isotope ^{235}U	28,25	46,8	73	90
Maximum fuel burn-up, at. %	5	5	10	10
Reactor campaign, years	0,6	0,21	0,38	0,20
Coefficient of nonuniformity of heat evolution K_r/K_z	1,37/1,2	1,2/1,1	1,37/1,2	1,15/1,1
Volumetric proportions of materials in the active zone, %				
fuel	25,65	21,46	27,8	24
coolant	33,16	40,48	39,5	48
metal structures	27,01	25,46	32,7	28
others	14,68	13,6	—	—
Volumetric proportions of materials in the side screen, %				
fuel ^{238}U	56,61	—	56,61	—
steel	19,65	80	19,65	80
coolant	21,08	20	21,08	20
Charging of fuel per campaign, kg	316	215	219	177
Maximum flux, neutrons/cm^2 · sec	$7,74 \cdot 10^{15}$	$11,7 \cdot 10^{15}$	$9,9 \cdot 10^{15}$	$14 \cdot 10^{15}$
Maximum neutron flux integrated with respect to time, neutrons/cm^2	$11,2 \cdot 10^{22}$	$6,26 \cdot 10^{22}$	$11,8 \cdot 10^{22}$	$8,8 \cdot 10^{22}$
Maximum neutron flux with $E \geq 0,4$ MeV, neutrons/cm^2 · sec	$3,56 \cdot 10^{15}$	$6,16 \cdot 10^{15}$	$4,5 \cdot 10^{15}$	$6,3 \cdot 10^{15}$
Maximum neutron flux with $E \geq 0,4$ MeV, integrated with respect to time, neutrons/cm^2	$5,17 \cdot 10^{22}$	$4,1 \cdot 10^{22}$	$5,4 \cdot 10^{22}$	$4 \cdot 10^{22}$
Total conversion ratio	1,45		1,28	

and construction materials developed in nuclear power stations of the BRGD-1000 type under conditions involving the use of an experimental fast-neutron reactor with a neutron flux characteristic of high-power nuclear power stations.

These aims may be achieved in a nuclear reactor with a thermal power of 150-200 MW using the proposed parameters of the coolant and high specific thermal stresses. The nominal neutron flux characteristic of the BRGD-1000, $(6-7) \cdot 10^{15}$ neutrons/cm^2 · sec, may be achieved in the experimental BRIG-50 reactor by increasing the specific thermal stress to 1800-2500 kW/liter on converting it to the research mode of operation (Tables 5 and 6).

The experimental-industrial nuclear power station with the BRIG-50 reactor is intended for solving the principal technological and constructional problems involved in making a fast-neutron reactor of the gas-cooled type using the dissociating coolant N_2O_4. It is intended to carry out the following work with the experimental-industrial nuclear power station:

1) Mass resource tests on fuel elements under conditions corresponding to the working parameters (with respect to fast-neutron flux and thermal and energy stress) of BRGD-1000 industrial reactors; the experimental-industrial development of a fast gas-cooled BRIG-type reactor as the prototype of a reactor /secondary-nuclear-fuel producer as recommended for power-or-heat and power-and-heat stations. For these purposes an electrical power of the atomic power station of around 50 MW is assumed (Fig. 3);

2) the experimental-industrial development of an efficient closed gas-liquid cycle, equipment for the technological circuit, and a complex of technological problems associated with the use of N_2O_4 as a coolant and working substance for high-powered nuclear power stations;

3) the development of standards for the main equipment of nuclear power stations and the carrying out of the necessary material-science tests in order to verify the validity of the choice of construction materials.

The design of a fast gas reactor should ensure the accommodation of two active zones in the reactor vessel, corresponding to low-temperature (NBRIG) and high-temperature (VBRIG) versions of the nuclear power station. The technological scheme, the equipment, and the composition of the nuclear power station should have a single technological embodiment, allowing the practical use of the experimental-industrial nuclear power station with NBRIG or VBRIG reactors, and also in the modes of combined and separate production of heat and electrical power, i.e., the nuclear-power-station, "ATÉTs," and "AK" modes.

Nuclear and Chemical Safety of the BRIG-50 Installation

In view of the absence of experience in the use of nuclear power installations involving fast reactors cooled by means of a dissociating coolant, a particularly meticulous approach must be made to the solution of these problems.

Emergency situations to be foreseen, as far as possible prevented, and ameliorated as regards their harmful consequences, include the unsealing or rupture of the circuit at any point in the technological system, deenergizing of the whole nuclear-power installation, and also processes in the reactor or reactor control and monitoring systems leading to a dangerous change in reactivity or radioactive contamination of the circuit.

Under certain emergencies such as the stopping of the pumps as a result of power failure or jamming, the use of N_2O_4 as coolant in the gas-liquid cycle may play a decisive part in preventing the melting of the active zone. In this case there are two favorable circumstances: the large amount of coolant in the circuit as compared with its rate of flow, and the considerable pressure differences in the circuit, which may provide for an initial natural shut-down cooling of the active zone within 20-60 sec.

In order to ensure safe use of the BRIG-50 nuclear-power installation, the following measures of radiation and chemical safety are proposed.

1. To use a two- or three-loop system of reactor cooling and two independent loops of emergency shut-down cooling, based on different principles. Simple operation of the installation with a single loop is not to be allowed.

2. To eliminate the possibility of rupture in the reactor vessel and the cooling pipes in front of the cut-off valves by suitable constructional measures (by taking large reserves of strength in the design calculations and ensuring quality control of the manufacture and erection). In the case of rupture of the vessel, to ensure cooling of the active zone with liquid coolant.

3. To provide reserves for the pumps of the main circuit and the coolant circulating system, and to provide inertial masses on the rotors for emergency running-down purposes.

4. To provide the BRIG-50 nuclear-power installation with autonomous emergency electrical supply systems.

5. To enclose the whole equipment of the installation (including any parts which might lead to radiation or chemical hazard in the event of damage or partial failure) in a hermetic concrete sheath; personnel and equipment should only pass into this region through special locks.

LITERATURE CITED

1. A. P. Aleksandrov, Izvestiya, December 25 (1971).
2. G. B. Levental' et al., At. Énerg., 32, No. 3, 187 (1972).
3. A. M. Petros'yants et al., At. Énerg., 31, No. 4, 315 (1971).
4. V. V. Orlov, ibid., 295.
5. V. V. Orlov, M. F. Troyanov, and V. B. Lytkin, At. Énerg., 30, No. 2, 170 (1971).
6. A. K. Krasin et al., Fourth Geneva Conf., R-431 (1971).
7. V. B. Nesterenko, Physico-Technical Bases of the Use of Dissociating Gases as Coolants and Working Substances in Nuclear Power Stations [in Russian], Nauka i Tekhnik, Minsk (1971).

8. A. K. Krasin and V. B. Nesterenko, Thermodynamic and Transfer Properties of Chemically Reacting Gas Systems [in Russian], Nauka i Tekhnika, Minsk Pt. I (1967); Pt. II (1971).
9. A. K. Krasin et al., Heat Transfer in Chemically Reacting Gas Coolants [in Russian], Nauka i Tekhnika, Minsk (1971).
10. A. P. Leipunskii et al., see [3], p. 383.
11. "Dissociating gases as coolants and working substances of power installations," Trans. of the Third All-Union Conference on Dissociating Gases, Nauka i Tekhnika, Minsk (1972).
12. "Dissociating gases as coolants and working substances of power installations," Trans. of the Second All-Union Conference on Dissociating Gases, Nauka i Tekhnika, Minsk (1971).
13. L. I. Kolykhan, V. F. Pulyaev, and V. T. Derov, Izv. Akad. Nauk Belorussian SSR, Ser. Fiz.-Énerg., Nauk, No. 2 (1971).
14. B. S. Petukhov, A. S. Komendantov, and S. A. Kovalev, Teplofiz. Vys. Temp., No. 6 (1969).
15. A. M. Sukhotin and L. N. Lantratova, Izv. Akad. Nauk Beloruss. SSR, Ser. Fiz.-Énerg. Nauk, No. 2 (1968).
16. A. M. Sukhotin and L. N. Lantratova, Handbook of Chemistry, Corrosion and Protection of Chemical Apparatus, Vol. 3 [in Russian], Khimiya, Leningrad (1970).
17. M. A. Bazhin et al., Optimization of the Parameters of Power Installations Using Dissociating Working Substances [in Russian], Nauka i Tekhnika, Minsk (1970).
18. J. Yellowflies et al., Atomnaya Tekhnika za Rubezhom, No. 3, 14 (1973).
19. H. Bumm et al., Proc. Inernat. Meeting on Fast Reactor Fuel and Fuel Elements, Karlsruhe, September (1970).
20. I. Sayer, The U. K. Support of the Coated-Particle-Fuelled Gas-Cooled Fast Reactors, Minsk (1972).

RADIOACTIVE SAFETY BARRIERS IN NUCLEAR POWER STATIONS

E. P. Anan'ev and G. N. Kruzhilin

UDC 614.876

The problem of radioactive safety in the operation of nuclear power stations is quite multilateral and widespread. Nevertheless, it may be mentioned, bearing in mind the previous period, that its tenor has been well-known to specialist physicists from the very beginning of the construction of nuclear installations. Undoubtedly, it may be assumed also that at that time, just as now, it was important to preserve the active zone from burn-out of the fuel elements in all possible situations at nuclear power stations. This problem is imposed, first of all, on the automatic emergency protection system and signalization of the reactor, and secondly on the active zone cooling system during normal operation of the reactor and during shutdown, and also in the various possible emergency states of a nuclear power station.

However, in water-cooled reactors, there is a quite substantial radioactivity even under "normal" operating conditions. It comprises the "oxygen" radioactivity of the water, the radioactivity of the circulation loop corrosion products present in the water and the radioactivity of fission fragments which enter the coolant flow from individual leaky fuel elements. The first two components are inherent in the very process taking place in the reactor, i.e., they are technological. The latter component, i.e., the radioactivity of the water, due to leakage from the fuel elements of fission fragments, is essentially of a probability nature. Despite the great improvements achieved in the design development of fuel elements for power reactors and in the technology for their mass production, nevertheless, during operation of nuclear power stations some of the fuel elements become leaky, and the consequence of this is that highly radioactive fission fragments start to discharge into the coolant flow. In general, this is not difficult to understand, because on the one hand the fuel elements are quite "delicate" in their construction, and correspondingly complex in relation to ensuring their reliability under operating conditions and, on the other hand, their total number in power reactors is enormous. Thus, in the Novovoronezh nuclear power station there are about $31 \cdot 10^3$ fuel elements in the VVÉR-210 reactor, about $43 \cdot 10^3$ in the VVÉR-365 reactor and about $43.9 \cdot 10^3$ in the VVÉR-440 reactor.

It is well-known that in the core of a uranium metal fuel element, the water which is passing through its leak-tight cladding interacts chemically with the uranium. As a result of this, uranium hydride is formed in particular with a friable structure and with a considerably greater specific volume than uranium, which leads to total destruction of the cladding and leaching-out of the core material. In consequence of this, the radioactivity of the circulating water becomes extremely high even in the case of damage to only a single fuel element. As a result of this, the inside surfaces of the circulatory loop also are strongly contaminated and become highly radioactive; these contaminants are leached-out only poorly and maintain a high radioactivity over a long period. Operation of power reactors under these conditions would be marginally difficult. On account of this, the cores of power reactor fuel elements are made from UO_2 and not uranium metal, although in this case the fuel requirement is increased somewhat.

Uranium dioxide does not react with water and it is not leached-out. Because of this, a leaky fuel element – if it appears under operating conditions – does not rupture in the flow of water. In this case, mainly the fission products xenon and krypton pass through the crack of a leaky fuel element. They diffuse preliminarily from the body of the fuel to the surface of the core, which amounts to 0.1 of their total amount. Then they diffuse through the gas space to the crack which has formed; the quantity here can be estimated at 0.01. Thus, the release of gaseous fission products from the fuel element can be estimated at 10^{-3} of the total amount of fission products. As a result of this, it can be assumed that the radioactivity of these

Translated from Atomnaya Énergiya, Vol. 37, No. 1, pp. 22-27, July, 1974. Original article submitted September 7, 1973.

fission products is less, approximately by a factor 10^{-5}, than the radioactivity which would enter the flow in the case of rupture of a single fuel element of uranium metal. Thus, the practical value of converting to the use of UO_2 in reactors with water cooling is extremely significant. Research work resulting from this conversion was carried out at one time in the I. V. Kurchatov Institute of Atomic Energy by V. V. Goncharov and other coworkers, under the direction of Academician A. P. Aleksandrov.

The widespread practice of operating power reactors with UO_2 fuel elements has shown that their operating conditions are completely acceptable in relation to the radioactivity of the environment. At the same time, it is obvious that certain improvements in this respect must be carried out. Obviously, the most important of these improvements must be special technological measures for increasing the reliability of the fuel elements. As shown in practice, decontamination of the flow of circulating water in ion-exchange filters is also of great importance; here, the radioactive particles are trapped in ionic form and thus the amount of corrosion products in the circuit is maintained at a low level, which leads to a significant effect in relation to the radioactivity of both the cooling water and of the surfaces of the cooling circuit. As applicable to a power generating unit with a boiling reactor, methods of handling the radioactive gases from the turbine condenser and the conditions for operation and maintenance of the turbine also are important. There are problems associated with this, which are narrowly specialized in their tenor; they are being solved in the proper manner with the assurance of the existing standards of radioactivity both at nuclear power station sites and beyond their boundaries.

We note additionally that fuel elements of UO_2 have a special future: if a fuel element becomes leaky in the water flow, its shape remains unchanged and therefore it is not amenable to visual detection. Definition of a cassette with leaky fuel elements is quite difficult in this case. In case of necessity, this is undertaken after removing the cassette from the reactor; according to the presence in the fuel element of specific radioactive isotopes [1]. This operation is complex and requires a long time to carry it out. Because of this, and also owing to the generally insignificant escape of fission products (mainly gaseous) through leakage, as mentioned, a search for the damaged fuel elements as a rule is not undertaken in the period between fuel rechargings into the reactor. According to current estimates, it is considered "permissible" if the number of leaky fuel elements does not exceed 1% of the total number in the active zone. However, according to operating data, the relative number of damaged fuel elements is considerably less. Undoubtedly the damage probability will be reduced further by improvements in design and production technology. Therefore, the special features of UO_2 fuel elements mentioned are recalled here only as a statement of fact and not for the purpose of any justification or protection whatsoever of the "admissibility" of damage to fuel element claddings occurring during operation of the reactors.

Thus, in the light of performance and accumulated experience, the first and principal barrier against radioactivity in a nuclear plant has always been assumed to be the fuel element claddings which, in their turn, are protected from dangerous burn-out by a system of automatic equipment and by the appropriate systems for cooling the active zone in normal, shutdown and emergency situations.

Among the possible emergencies in nuclear power stations, the case of coolant leakage must be counted as particularly valid. Such cases are inevitable during prolonged operation. In organic-fuelled steam powered plants, very small leakages through looseness of the individual parts of the shut-off equipment or its packing gland present no hazard and therefore they do not cause any special worry. But with the appearance of a leak through breaks in the flange gaskets or through direct damage to one or another small-diameter tube, a more or less urgent shutdown is necessary for repair, in order to avoid the possibility of this type of damage developing with increased leakage, leading to more dangerous consequences. However, in these cases shutdowns do not usually take place immediately, but they are effected during certain hours in order to take into account the operating requirements of the users. Thus, on power stations feeding into the grid system, shutdowns for maintenance in such cases are coordinated provisionally with a grid system dispatcher and account is taken of the grid load, for the possibility of shifting beyond the peak loading period. It may be mentioned for correctness that, during the operation of modern power generating units with a capacity of 300 MW, such delays in a shutdown occur with a leakage through a damaged tube of up to 20 t/h.

It is obvious that in nuclear power stations there is the same attitude toward similar leakages. For the closed circulatory loop of a water-cooled/water-moderated reactor, only leakages are classified as "small" which do not lead to a reduction of pressure in the circuit; in the contrary case, the emergency protection system operates, with shutdown of the reactor. However, in this case of reactor shutdown, safety is not completely guaranteed because when the pressure in the circuit is reduced to the saturation

pressure corresponding to the temperature of the circulating water, steam generation will take place in the reactor vessel and, as a result of this, the danger will arise of steaming of the active zones with heating up or even burn-out of the fuel elements. Therefore, when the pressure in the circuit is reduced to a specified limit, an emergency reactor cooling system is switched on automatically. For this, the required quantity of water containing boric acid (in order to exclude nuclear reactions in the active zone [2]) is supplied to the reactor vessel from special reservoirs by means of emergency electric pumps.

With the appearance of hot water leakage from the loop, steaming occurs and, at the same time, radioactive contamination of the corresponding location occurs. In order to localize this hazard, the places through which the conduits carrying the hot radioactive water pass are made hermetically tight. Moreover, they are provided with sprinkler devices for spraying cold water for the purpose of condensing any steam which is released by the leak.

The emergency cooling and hazard localization systems mentioned are designed to operate on the appearance of a significant leakage of hot water from the reactor circuit, including damage or fracture of any small-diameter pipe and, in our opinion can be regarded as the second radioactive safety barrier.

It should be emphasized that the efficiency or, more precisely, the effectiveness of this barrier is determined, as in the case of the first barrier mentioned above, also by the reliability of the electric power section, including the power supply to the electric motors of the emergency pumps. In order to avoid interruption of the power supply to a number of important consumers, an emergency electric power supply is provided for reactor shutdown in these circumstances, in the form of a large battery of accumulators, calculated to operate for approximately one hour, and Diesel generators designed for continuous operation over several hours or even several days. It is obvious that the importance of this plant is enormous, just like the electrically powered safety control, as a whole, in the radioactive system in nuclear power stations. The main specific difficultly consists in that the emergency equipment mentioned is located in a deep emergency system. At the same time, in accordance with its purpose, it must always be in complete readiness. Therefore, a systematic check of the readiness of this equipment, in particular, is exceptionally important under normal operating conditions of the nuclear power station.

The concept discussed is completely logical and conclusive. It can be assumed that it has found wide recognition among specialists and that it is used in practice. Nevertheless, in designing nuclear power stations with pressure-vessel reactors in the USA, one further safety barrier has received widespread recognition – protective envelopes (the so-called containment vessels), intended to retain the steam released from the entire bulk of hot water contained in the hot water loop. As reported in primary sources, for this, one must bear in mind the case of total transverse rupture of the main duct of the circulatory loop, with the discharge of vaporizing water from both ends of it.

The majority of experimental reactors, and also plutonium production reactors have been constructed without containment vessels. Gas-cooled power reactors without containment vessels have been constructed in England and France. Containment vessels appeared for the first time at the Shippingport (USA) reactor, where three were installed – one above the reactor and two correspondingly above each of the two steam generators. In connection with this, one of the Westinghouse technical directors, I. Simpson, said at the time [3]: "It is obvious that containment vessels are expensive and will be phased out with time. We consider it to be extremely improbable that these devices would ever function. But in order to double the safety in this first commercial nuclear power station, we consider it necessary to construct these expensive facilities."

Since that time, American firms have continued to construct and improve containment vessels. For example, in the latest design of a containment vessel built by the firm of Westinghouse [4], ice condensers are being installed (around the perimeter), intended for rapid condensation of steam escaping as a result of bursting of the primary loop duct. The total weight of ice amounts to 1000 t. It is contained in the form of fine pieces in wire baskets at a temperature of $-10°C$ approximately, which is achieved by means of continuous blowing with cooled air and also by suitable thermal insulation structures. At the Sequoia (USA) nuclear power station, the ice condenser for the 1125 MW unit with a water-cooled/water-moderated reactor consists of 24 moduli, each having cross-sectional dimensions of 4×4 m approximately and a height of 24 m. Thus, I. Simpson's forecast relating to the rejection of containment vessels has not come true in American practice.

Let us consider now the question of containment intrinsically. As already mentioned, the advisability of this problem is motivated by the assumption of total rupture of the primary duct of the circulatory loop.

Because of this, we recall that in the Novovoronezh nuclear power station the primary circulatory duct of the VVÉR-440 reactor has an external diameter of 560 mm and a wall thickness of 32 mm. For the VVÉR-1000 project, the primary pipeline will operate at a pressure in the first loop of 150 atm, its internal diameter will be 850 mm and the wall thickness 55 mm. The circulatory pipeline in the Sequoia nuclear power station operates at a pressure of 175 atm and its diameter is 740 mm. Thus, it is obvious that the primary ducts of power-generating reactors are related, in their dimensions, to a class of pressure vessels. The reactor vessel is also related to this class, rupture of which is excluded according to present day concepts.

In view of this, on the basis of the existing formal logic, the obvious scientific intension would appear to be that rupture of these ducts should also be assumed to be excluded.

But, of course, experience here is decisive. According to verbal information from the Deputy Head of the Division of Boiler Inspection (Kotlonadzor), L. B. Segalov, during at least 13 years in steam boilers there has been no first category emergency (according to after effects). Accidents from rupturing of drums have occurred earlier, on fire-tube horizontal boilers and also on vertical boilers of the Shukhov type. The cause of these accidents were oversights of the water level, the formation of a layer of scale and caustic embrittlement in riveted seams. As a consequence, production of these boilers was discontinued in the USSR and they were replaced by DKV low-capacity tubular steam boilers of the Biisk boiler factory, which are safer in these respects.

The degree of reliability of operation in industry of tubular steam boilers can be defined in that of 50,000 twin-drum tubular DKV boilers, manufactured by the Biisk boiler factory since 1950, not a single boiler has had an accident of first category nor has a single drum ruptured. The drums of these boilers are rolled from a sheet of boiler steel, they have longitudinal and transverse welded seams and welded spherical bottoms. The drum diameter is 1000 mm and the wall thickness is 13 mm. The boiler tubes, with a diameter of 51 mm, are secured in openings of the drum with expansion, so that the calculated attenuation factor (weakening factor) from the openings is 0.5. The boilers operate up to a pressure of 13 atm. The overall length of the 50,000 DKV boilers amounts to about 400,000 linear meters.

It is more convenient, according to wall thickness, to compare as containers the circulating ducts of nuclear power stations with the drums of high-pressure steam boilers. In the USSR, these drums are manufactured from carbon steel 22K at a pressure of 115 atm, with internal diameter 1300-1600 mm and wall thickness 70-90 mm. The drums of boilers at a pressure of 155 atm with internal diameter 1300-1800 mm and wall thickness 90-115 mm are made of 16 GNM steel. A large number of these drums have been operating in our electric generating stations during approximately 20 years without accidents caused by rupture of the welded seams or of the walls. Nevertheless, with drums of 16 GNM steel, considerable difficulties were experienced at first (this steel is a new one, developed by the Central Scientific Institute of Technical Information for Machinery Manufacture (TsNIITMASHem). Longitudinal surface cracks appeared on the inside wall of drums made from this steel, sometimes several mm in depth. In order to prevent possible complications or accidents, these cracks which were revealed by inspection during installation of the boiler, were removed by grinding with an abrasive wheel down to intact metal and without subsequent filling. Further, in order to increase reliability, the wall thickness of these drums was increased by 13 mm. Moreover, this steel was produced for them by only one factory.

Accidents in steam boilers in industrial plants and in the Minénerge system of the USSR, with rare exceptions belong to the second category according to consequences. Mostly they are expressed in overheating of the DKV boiler tubes because of oversight of the water level through noninspection by the operating personnel. There have also been accidents from damage to the welded seams in steam tubes. The appearance of a through transverse crack in the vicinity of the seam is typical of this, as a consequence of unsatisfactory heat treatment of the regions of the conduit adjoining a welded seam under assembly conditions. These cracks are revealed by leakage and they sometimes reach 1/3 of the circumference in size.

In addition, numerous cases are known of damage of a different nature to small diameter pipes under operating conditions of steam power plants. After a long period of service, the thin-walled pulse tubes which lead to the flowmeters and manometers, corrode. The elbows of the bypass and drainage pipes undergo internal erosion due to the movement in them of the steam-water mixture at a high flow rate. Fatigue cracks appear at the transverse seams of fine pipes because of normally imperceptible vibration. Damage to these pipes occurs as a consequence of unsatisfactory compensation of their thermal expansions.

Under operating conditions, damage is encountered which arises from factory defects: for example, the use of fine tubes and accessories with imperceptible internal defects; imperceptible "undercuttings" during working of the connecting pipes of accessories, which become concentrators of mechanical stresses; low-grade bends of tubes in the cold state, which may lead to considerable thinning of the wall and, at the same time, to a decrease of its elasticity; this is especially dangerous in the presence of bending stresses. It is well-known, in particular, that as a result of the latter cause, cases have occurred in our "old" high-pressure steam generators of fractures at the bends of unheated tubes with external diameter of 133 mm and with a wall thickness of 10 mm, made from boiler steel 20.

For even larger ducts (such as the main circulation ducts of power generating nuclear reactors with water cooling), the most probable cause of their damage with the appearance of cracks are only thermal stresses, associated with their thermal compensation. From this point of view, there is a definite value for the freedom of box-grouping of the pipes and which is characteristic for our nuclear power stations. In the case of construction of a containment, constrained grouping of pipelines is inevitable, in consequence of which their operating reliability, at least according to this assessment, is correspondingly reduced. At the same time, constrained grouping of plant under containment and especially under structures which are dependent on the conditions of their leak-tightness, considerably complicates the operation of nuclear power stations. This concerns monitoring the state of the plant, which is carried out periodically in some or other established order, including work due to maladjustments, and also during startup of the plant after temporary shutdown or after repair, when personnel inspection by specialists is necessary. This relates also to various maintenance operations. In carrying out the latter on radioactive plant, the most important factor is the total expenditure of time, as the radiation dosage for maintenance personnel is approximately proportional to this time. It is well-known from experience, that in order to shorten the time of maintenance, suitability of procedure and access to the plant are of first degree importance and, especially, freedom for carrying out work on the disassembly and removal of one or other damaged unit, and also the delivery and installation of a new unit. Because of this, it is relevant to assume that with respect to maintenance conditions for radioactive plant at nuclear power stations, it is essential to have convenient and maximum possible freedom of grouping of the facilities.

Thus, the installation of a containment, together with an increase of radioactive safety of nuclear power stations, involves a number of negative instants which cannot possibly be taken into account. Costs, even on the design of the containment and its system, on the whole are considerable in absolute magnitude. Therefore, the advantage of installing a protective envelope is not only not obvious but, to a certain extent, it is even doubtful.

The practice of constructing protective envelopes in the USA is associated, first of all, as already mentioned, with the history of the problem or, more precisely, with the start of construction of nuclear power stations, when "double safety" also was important for social opinion in the USA. In connection with this, reference should be made again to Simpson, who from the very beginning drew attention to the fact that in essence protective envelopes for nuclear power stations are not necessary. But, up to the present time, American specialists have emphasized invariably that protective envelopes in nuclear power stations are to be constructed in case of: "the improbable fracture of the circulatory duct of the reactor" [5], or in case of "hypothetical fracture of the reactor duct" [6]. Obviously, it may be supposed that the continued construction of protective envelopes is also associated with the caution which naturally exists with the doctrine of safety on the one hand, and with the technology of heavy machine construction on the other hand.

In pressurized installations (especially thermal), relative to conditions of strength, an excessive increase of pressure is the most dangerous. According to statistical data of Kotlonadzor, accidents from this cause with fracture of one or other unit of the plant are still occurring. The majority of cases are due to the fact that with controlled hydrostatic molding, wedging of safety valves is practised and after molding in haste, it is forgotten to unwedge them.

Of course, such cases are possible only on subsidiary industrial plants with a correspondingly low level of operation. As far as we know, such cases have never occurred in domestic thermal generating stations. It is obvious, that nuclear power stations in relation to operating level, should be at least no less than the State Regional Electric Power Stations. Nevertheless, as applied to nuclear power stations, this situation is worthy of specific attention. It should be noted that the dangers associated with it can be eliminated by the installation in the reactor circuit of two groups of valves – dump valves and emergency valves – designed so that the latter operate at a somewhat higher pressure than the former. In this case, the

limiting pressure for the dump valves is set at the normal level. In case of nonfunctioning for any reason whatsoever in an emergency situation, the emergency valves will operate at a somewhat higher pressure. We recall that in the circulatory loop of the reactor at the Sequoia nuclear power station, both these groups of valves are present.

In relation to mechanical strength, the most important and decisive factors are the choice of materials, the technology of manufacture of the plant components, and also the methods for their assessment. As applicable to nuclear reactors, the latter have been extended recently with the introduction of a computation on the limiting state, developed by N. P. Mel'nikov [7], which will provide an additional guarantee of the operating reliability of the reactor circulatory loop.

Only a part of the problem being considered here has been touched on. Actually, the urgency remains for further improvement to some or other degree of all systems as a whole, which will ensure in our nuclear power stations in emergency situations, the necessary cooling of the active zone and also will prevent the escape of radioactivity beyond the bounds of the nuclear power station itself. In this respect, it can be assumed that the system of box-grouping of reactor plant has been successfully and completely accepted in the USSR. A logical extension of this may be an additional system for steam condensation in emergency conditions by means of a water bubbler, located in an annex. It is important, that in the counterpoise to the protective envelope of this type of system, it does not affect at all the grouping conditions of the main ducts. Nevertheless, by choosing the dimensions of the water bubbler and taking account of the possibility of rupture of the main duct, the "double safety" which has been mentioned is ensured with this type of system.

Thus, the advisability of double safety is motivated by universal practice in the design of nuclear power stations and is intended for their widespread construction. It should be noted that any discussions whatsoever in this connection have almost no significance at the present time. But in spite of our confidence in the fact, that with the present-day level of technology, the possibility of rupture of the main duct is improbable, they, undoubtedly, remain valid.

LITERATURE CITED

1. F. Ya. Ovchinnikov et al, Operation of the Reactor Facilities of the Novovoronezh Nuclear Power Station [in Russian], Atomizdat, Moscow (1972), p. 102.
2. F. Ya. Ovchinnikov et al, Operation of the Reactor Facilities of the Novovoronezh Nuclear Power Station [in Russian], Atomizdat, Moscow (1972), p. 123.
3. I. Simpson, The Pressurized Water Reactor Forum, Mellon Institute, Pittsburg, December 2, 1955, p. 29.
4. A. Tredale and N. Grimm, Nucl. Eng. Internat., 16, 185, 47 (1971).
5. S. Weems, Nucl. Eng. Internat., 15, 164, 47 (1970).
6. A. Tredale and N. Grimm, Nucl. Eng. Internat., 16, 185, 864 (1971).
7. N. P. Mel'nikov, Structural Shapes and Methods of Calculating Nuclear Reactors, [in Russian], Atomizdat, Moscow (1973).

LOW-TEMPERATURE SPECIFIC HEAT AND THERMODYNAMIC FUNCTIONS OF URANIUM BERYLLIDE

O. P. Samorukov, V. N. Kostryukov, F. A. Kostylev, and V. A. Tumbakov

UDC 669.2/85:669.822:536.63.7(083)

Of the fundamental thermodynamic constants for uranium beryllide UBe_{13} only the heat of formation [1] and the entropy at standard temperature, found by the calculation method of [2], are known.

In the present paper we present experimental data on the specific heat of UBe_{13} in the 13.5-303.4°K range and the values, calculated based on them, of the thermodynamic functions in the condensed state in the 0-300°K range.

Preparation and Identification of UBe_{13}

To prepare UBe_{13} we used uranium in the form of fragments cleaned of the surface oxides by electrolytic polishing in H_3PO_4, and electrolytic-beryllium powder. The impurity content in uranium and beryllium and their assumed phase composition are represented in Table 1.

A mixture of beryllium (33.09 wt.%) and uranium (66.91 wt.%) in a crucible of BeO was heated in a quartz ampoule in pure hydrogen (600 mm Hg) at 1300 ± 50°C for 1.5 h. Then, the hydrogen was pumped out at 600°C. The cooled product was ground in purified argon.

An x-ray investigation showed that the sample consists of a single phase – UBe_{13}. A metallographic investigation indicated that no visible impurities were present. The UBe_{13} sample was analyzed for uranium and beryllium content by chemical methods [3, 4], and for oxygen content by the neutron-activation method and vacuum melting in a graphite crucible with a platinum bath. We found 66.82% uranium, 32.42% beryllium, and 0.35% oxygen. The errors in the determination of uranium, beryllium, and oxygen equal ±0.2, 0.4, and 20%, respectively, where for oxygen this error refers to both methods of analysis. The total content of the component in the sample (taking into account the impurities introduced with the original uranium and beryllium) is 99.71%.

TABLE 1. Content of Impurities in Uranium and Beryllium and Their Assumed Phase Composition

Impurity	Content, wt. %			
	in uranium	in form of phase	in beryllium	in form of phase
Carbon	$6\cdot10^{-2}$	UC	$11\cdot10^{-2}$	Be_2C
Oxygen	$6\cdot10^{-3}$	UO_2	$22\cdot10^{-2}$	BeO
Nitrogen	$5\cdot10^{-5}$	UN	$6\cdot10^{-3}$	Be_3N_2
Silicon	$3{,}6\cdot10^{-2}$	U_3Si	$9\cdot10^{-3}$	Si
Iron	$1{,}4\cdot10^{-2}$	U_6Fe	$1{,}4\cdot10^{-2}$	Fe
Manganese	$3\cdot10^{-3}$	U_6Mn	$1\cdot10^{-3}$	Mn
Nickel	$6\cdot10^{-4}$	U_6Ni	—	—
Magnesium	$<1\cdot10^{-3}$	Mg	$2{,}3\cdot10^{-3}$	Mg
Copper	$9\cdot10^{-4}$	UCu_5	$2{,}8\cdot10^{-3}$	Cu
Chromium	—	—	$3\cdot10^{-3}$	Cr
Aluminum	—	—	$7\cdot10^{-3}$	Al
Boron	$5\cdot10^{-4}$	UB_2	—	—

In the calculation of the phase composition of the sample (on the basis of the composition of the mixture, the data of Table 1, and the results of the analysis) we took into account the amount of oxygen consumed during its preparation. At the same time we assumed that the oxygen was distributed in a stoichiometric ratio between the uranium and beryllium in the following way:

$$2UBe_{13} + 15O_2 \rightarrow 2UO_2 + 26BeO.$$

As is shown by calculations, the sample should contain 96.73 wt.% UBe_{13} and 2.97 wt.% impurity phases;

Translated from Atomnaya Énergiya, Vol. 37, No. 1, pp. 28-31, July, 1974. Original article submitted July 16, 1973.

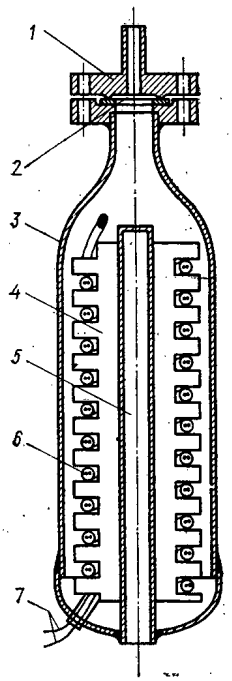

Fig. 1. Container with flanged seal. 1) Flange with connecting piece; 2) small copper sealing ring; 3) body of container; 4) impeller; 5) pocket for thermometer; 6) capillary containing heating element; 7) heating element made of constantan wire.

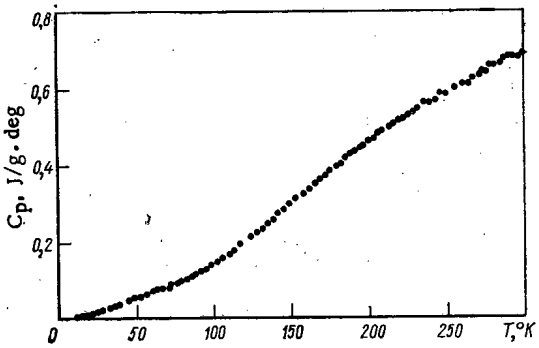

Fig. 2. Specific heat of uranium-beryllide sample.

the remaining 0.30 wt.%, taking into account possible errors in the analysis of the sample, refers to UBe_{13}. Below we present the composition of uranium beryllide (wt. %):

UBe_{13}	97.03
Be	0.29
UC	0.83
U_3Si	0.63
BeO	0.47
UO_2	0.34
U_6Fe	0.24
Be_2C	0.09
UN	0.06
Mn	0.002
Mg	0.002
Cu	0.002
Cr	0.001
Al	0.007
Remainder	0.006

Method of Measuring Specific Heat

The specific heat of UBe_{13} was measured in a vacuum adiabatic calorimeter; the apparatus and methods* of the work were reported in [5]. The difference consisted in the use of a semiautomatic system of controlling the adiabatic screens [6] and some structural changes in the container holding the sample (Fig. 1). First, the container was muffled by a flange, which enabled us to pressurize it comparatively easily in a chamber with inert gas. The flange was sealed using a copper gasket of thickness 0.1-0.15 mm, slightly coated with a vacuum lubricant. Second, the construction of the heater of the container was changed. The capillary in which the heating element had been placed was filled with BF-4 adhesive, with subsequent drying and polymerization, which allowed us to disconnect the platinum–glass from the vacuum inlets, made the construction more reliable mechanically and simplified the installation. Third, the container surface was silvered to improve its calorimetric qualities. The inside volume of the container was about 22 cm^3, and the weight was 51.81 g. To improve the heat exchange with the sample, the container was filled with purified helium up to a pressure of 200 mm Hg (at room temperature).

*The temperature was measured with a platinum resistance thermometer of type TSPN-2 No. 510, manufactured, calibrated, and certified at VNIIFTRI. The temperature in the 12-273.15°K range was measured in SST – 64 degrees, and above this range – in MPShT – 68 degrees.

TABLE 2. Thermodynamic Functions and Specific Heat of Uranium Beryllide

T, °K	S_T, J/mole·deg	$H_T - H_0$, J/mole	$(H_T - H_0)/T$, J/mole·deg	$-\Phi^*$, J/mole·deg	C_p, J/mole·deg	T, °K	S_T, J/mole·deg	$H_T - H_0$, J/mole	$(H_T - H_0)/T$, J/mole·deg	$-\Phi^*$, J/mole·deg	C_p, J/mole·deg
0	0,	0	0	0	0	160	69,00	6889,8	43,062	25,94	116,6
5	0,268	0,686	0,138	0,130	0,297	170	76,40	8111,4	47,714	28,67	128,1
10	0,632	3,473	0,347	0,284	0,862	180	84,04	9447,0	52,484	31,55	139,5
20	1,950	24,10	1,205	0,720	3,690	190	91,84	10891	57,321	34,52	150,5
30	3,690	67,61	2,255	1,435	8,054	200	99,81	12446	62,229	37,59	160,9
40	6,703	173,05	4,326	2,376	13,01	210	107,89	14101	67,149	40,74	170,8
50	10,19	329,95	6,598	3,590	18,37	220	116,04	15854	72,065	43,98	180,2
60	13,96	537,48	8,958	5,004	23,58	230	124,24	17700	76,952	47,29	189,2
70	17,99	798,98	11,414	6,573	29,08	240	132,48	19635	81,814	50,66	197,7
80	22,24	1117,8	13,975	8,268	35,31	250	140,72	21653	86,613	54,10	206,0
90	26,77	1503,1	16,702	10,07	42,55	260	148,95	23753	91,358	57,59	213,8
100	31,64	1965,1	19,652	11,98	50,54	270	157,16	25930	96,035	61,13	221,5
110	36,87	2514,8	22,861	14,01	59,89	280	165,37	28182	100,65	64,70	228,8
120	42,51	3163,3	26,363	16,15	70,25	290	173,47	30506	105,19	68,31	236,2
130	48,58	3922,3	30,171	18,41	81,50	298,15	180,12	32452	108,84	71,28	242,1
140	55,03	4793,6	34,242	20,78	93,05	300	181,63	32902	109,67	71,96	243,3
150	61,86	5783,5	38,556	23,31	104,9						

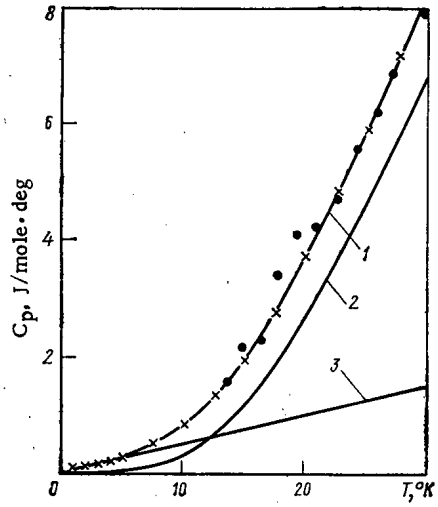

Fig. 3. Behavior of specific heat of UBe_{13} near absolute zero: •) experimental points; ×) calculated from the equation $C_p = \gamma T + 3D(\theta/T)$; 2) lattice component of specific heat; 3) electronic component of specific heat.

The specific heat of the container itself was measured over the entire range of temperatures investigated (13.52-299.6°K). During the control measurements of the specific heat of the standard – benzoic acid of mark K-2 – the maximum deviation from the standard values did not exceed ±1%. We can assume that for measurements of UBe_{13}, having higher thermal conductivity, the errors appear to be somewhat less because of the decrease in time of establishment of thermal equilibrium in the sample.

Results of Measuring Specific Heat and Calculating the Thermodynamic Functions

The specific heat of UBe_{13} (sample weight 43.507 g) was measured from 13.51 to 303.4°K at 95 points. The deviations of the experimental values from the smoothed curve in the 50-300°K range did not exceed ±0.5%. A spread of somewhat more than 2% was observed for 20-50°K. In the 17-20°K region we noted a deviation from the smoothed curve reaching 18% (an overestimate), which could hardly be a consequence of a systematic error. Experimental values of the specific heat of the uranium beryllide sample are given in Fig. 2.

To convert the specific heat to a value per mole of substance we introduce corrections to the specific heat of the sample for BeO [7], UO_2 [8], Be [9] and UN [10, 11] over the entire measured temperature range. The specific heat of the other impurities, owing to the absence of data in the measured temperature range, was assumed equal to the specific heat of the basic substance.

To extrapolate the specific heat from the lower measurement limit to 0°K we assumed that the metallic nature of the compound leads to a noticeable contribution of the electronic component to the specific heat of the sample. Actually, as follows from Fig. 3, the experimental values of the specific heat for UBe_{13} at low temperatures (13.51-25°K) can be represented by a sum of electronic and lattice components: $C_p = \gamma T + 3D(\theta/T)$. Extrapolation to 0°K according to this equation was made for values $\gamma = (3.60 \pm 1.21) \cdot 10^{-3}$ J/g·atm·deg^2 and $\theta = 176 \pm 5$°K. We should note that for beryllium, the coefficient for the electronic component of the specific heat equals $0.226 \cdot 10^{-3}$ J/g·atom·deg^2 [9], for uranium it is approximately $\gamma_U = 84 \cdot 10^{-3}$ J/g·atom·deg^2 (the estimate was made from the data of [12]).

The entropy and enthalpy of UBe_{13}, in the 0-13.51°K range were calculated using the given equation; above 13.51°K they were calculated by numerical integration of the smoothed curves $C_p/T = f(T)$ and $C_p = f(T)$. The molar values of entropy and enthalpy of UBe_{13} at T = 298.15°K are computed from the following quantities (in joules):

$$S^{\circ}_{13.51} = 0.96 \pm 0.25; \quad H_{13.51} - H_0 = 7.5 \pm 1.8;$$
$$S^{13.51}_{298.15} = 179.2 \pm 3.0; \quad H_{298.15} - H_{13.51} = 32\,440 \pm 580;$$
$$S^{\circ}_{298.15} = 180.1 \pm 3.3; \quad H_{298.15} - H_0 = 32\,450 \pm 580$$

(the given estimates are absolute, and are the maximum values possible).

These data refer to the UBe_{13} sample in which the content of the principal substance with the introduction of corrections to the specific heat for the impurities indicated above can be assumed equal to 98.17%. The error of the molar specific heat of uranium beryllide taking account of the purity of the sample, experimental errors, and errors connected with the introduction of the corrections, does not exceed 2%.

The thermodynamic functions calculated based on the specific heat obtained in the 0-300°K range are given in Table 2.

The values of specific heat and entropy can be determined somewhat more exactly at 298.15°K, since at this temperature we know the values for the entropy and specific heat of U_3Si [2] and UC [2, 13, 14] (the data of different authors differ by up to 10%), and also values of the entropy of U_6Fe [2] and Be_2C [15], obtained by a calculation method.

The final values for C_p and S at T = 298.15°K in this case are assumed equal to 244.3 ± 2.5 and 182.8 ± 1.7 J/mole·deg, respectively.

In conclusion the authors thank N. Kh. Samorukov, V. G. Shlyakov, A. G. Medvedevaya, and V. I. Grishin for help in the study.

LITERATURE CITED

1. M. I. Ivanov and V. A. Tumbakov, At. Énerg., 7, No. 1, 33 (1959).
2. M. Rand and O. Kubaschewski, The Thermochemical Properties of Uranium Compounds, Oliver and Boyd, London (1963).
3. V. K. Markov et al., Uranium, Methods for Its Determination [in Russian], Atomizdat, Moscow (1964).
4. W. F. Hillebrand and G. E. Lundell, Applied Inorganic Analysis, John Wiley (1953).
5. P. G. Strelkov et al., Zh. Fiz. Khimii, 28, 459 (1954).
6. Ya. M. Kraftmakher and P. G. Strelkov, Prikl. Matem. i Tekh. Fiz., No. 3, 194 (1960).
7. K. Kelly, J. Amer. Chem. Soc., 61, 1217 (1939).
8. W. Jouss, I. Gordon, and E. Song, J. Chem. Phys., 20, 695 (1952).
9. R. Hill and P. Smith, Philos. Mag., 44, 636 (1953).
10. E. Westrum and C. Barber, J. Chem. Phys., 45, No. 2, 635 (1966).
11. J. Counsell et al., Trans. Faraday Soc., 62, No. 523, 1736 (1966).
12. H. Flotow and H. Lohr, J. Phys. Chem., 64, 904 (1969).
13. T. Mukaido and K. Naito, J. Atomic Energy Soc. of Japan, 5, 601 (1963).
14. E. Westrum and F. Gronvold, Thermodynamics of Nuclear Materials, IAEA, Vienna (1962), p. 581.
15. J. Neely et al., J. Amer. Chem. Soc., 33, 363 (1950).

INCREASING THE EFFICIENCY OF SEPARATING ISOTOPE-CASCADES BY USING STEPS WITH MORE THAN TWO EMERGENT FLOWS

N. A. Kolokol'tsov*

UDC 621.039.31

In the ordinary type of isotope-separating cascade, a flow L of the mixture to be separated, with a concentration of the light component equal to c, passes in to each stage, while two flows – an enriched flow θL with a concentration c^+ and an impoverished flow $(1-\theta)$ with a concentration c^- – pass out; in passing along the separating channel, the mixture is impoverished with respect to the light isotope. As a result of this, the concentration of light isotope in the flow passing through the boundary of the channel in the cross section under consideration diminishes. This has the effect that considerable mixing of the light fraction takes place in the flow within the actual separating stage, and as the degree of impoverishment increases along the channel this leads to a reduction in the enrichment effect. This mutual relationship between the processes of impoverishment and enrichment leads to a loss of separating capacity, which, for a specific productivity of the separating stage, is proportional to $\delta^-\delta^+$, where $\delta^+ = c^+ - c = \varepsilon_0(1-\theta)/\theta \cdot \ln 1/(1-\theta)(c(1-c))$, $\delta^- = c - c^- = \varepsilon_0 \ln 1/(1-\theta)(c(1-c))$ [1, 2]. In symmetrical cascades in which the flow in each stage is divided in two, this internal mixing leads to the appearance of a factor $\ln 2$ $[\delta^+ = \varepsilon_0 \ln 2c(1-c)$ in the enrichment function (this being the so-called logarithmic effect), and the separating power is reduced by a factor of $\ln^2 2$, i.e., it is roughly halved. The mixing losses may be reduced by introducing asymmetrical cascades in which the enriched flow from the n-th stage is passed into the n + k-th stage, and the impoverished flow into the n–(p–1)th, where $k \geq 1$, $p \geq 2$ [2]. The most favorable flow separation coefficient θ is approximately equal to 0.8 (k = 1, p = 5), the separating power increasing relative to the symmetrical cascade by 33% [1-3], although the main proportion of the effect (~ 26%) is achieved for $\theta = 2/3$ (k = 1, p = 3). This version is constructionally far simpler and clearly more desirable [2]. The use of asymmetrical cascades does not actually eliminate the logarithmic effect, but provides an optimum combination of two asymmetries: that of the separation process, and that of the manner in which the stages are connected together. In an asymmetrical stage with $\theta > 0.5$ the internal mixing is greater than in the symmetrical stage, while the separating power increases owing to the intensification of the process of impoverishment along the channel.

There also is a fundamentally different way of increasing the separating power, based on the use of stages with three or more outflows. A stage with three outflows is shown in Fig. 1. In this system, the flow of the mixture to be separated, passing through the boundary of the channel θL, is in turn divided into two flows $\varkappa\theta L = D$ and $(1-\varkappa)\theta L = E$ with a concentration of $c + \delta^+$ and $c + \delta^0$ respectively, in which the δ^+ for $\varkappa \neq 1$ is greater than the δ^+ for $\varkappa = 1$, which corresponds to the ordinary stage with two outflows, and clearly $\delta^+ > \delta^0$. Thus the idea of introducing several outflows with respect to the light fraction enables us to reduce the internal mixing, while keeping the degree of impoverishment of the flow along the channel constant. If in the limit we take the number of outflows to infinity, we may entirely eliminate the logarithmic effect. This possibility was considered

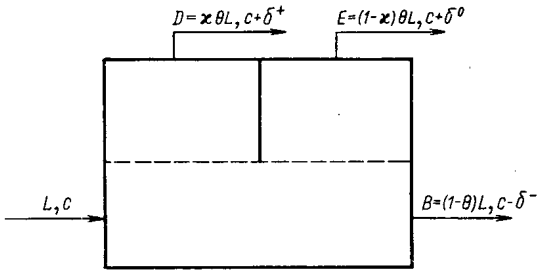

Fig. 1. Stage with three outflows.

*Deceased.

Translated from Atomnaya Énergiya, Vol. 37, No. 1, pp. 32-34, July, 1974. Original article submitted March 3, 1974.

TABLE 1. Versions of Cascade Schemes

Version	B_n is fed to stage	E_n is fed to stage	D_n is fed to stage	s	t
First	$n-1$	$n+1$	$n+2$	1	0
Second	$n-2$	$n+1$	$n+2$	1	1
Third	$n-1$	n	$n+1$	0	0
Fourth	$n-2$	n	$n+1$	0	1

theoretically in [3] for one of the cases of flow combinations.

Thus, by selecting the corresponding values and an appropriate method of connecting the stages into a cascade, we may achieve a material reduction in the total flow of the cascade, this being an important integrated characteristic (the quantity in question is proportional to the number of separating units and the energy consumed by the installation).

With increasing number of outflows the number of possible connecting schemes between the stages also increases; however, this process leads to additional difficulties of analysis. The complication of the schemes certainly increases the cost of making the apparatus and makes its applications more difficult. In this paper we shall consider the simplest stage-connecting schemes with limited numbers of flows which may be realized in practical cases without serious difficulty.

Let us consider four versions. In all these versions the stage has three outflows (Fig. 1). The flux $B_n = (1-\theta) L_n$ passes either to the previous $(n-1)$-th stage or the $(n-2)$-th. The enriched flow E_n passes either to the next $(n+1)$-th stage, and correspondingly D_n to the $(n+2)$-th, or else E_n is fed to the inlet of its own n-th stage and correspondingly D_n to the $(n+1)$-th. The balance equations of the total flows and the flows of the valuable component of the mixture in the section between the n-th and n + 1-th stages for all four versions may be written as follows:

$$sD_{n-1} + D_n + sE_n - B_{n+1} - tB_{n+2} = P, \tag{1}$$

$$sD_{n-1}(c_{n-1} + \delta^+_{n-1}) + D_n(c_n + \delta^+_n) + sE_n(c_n + \delta^0_n) - B_{n+1}(c_{n+1} - \delta^-_{n+1}) - tB_{n+2}(c_{n+2} - \delta^-_{n+2}) = Pc_P. \tag{2}$$

Here the quantities s and t have the specific values given in Table 1 for each version.

It is easy to show that the third version with $\varkappa = 1$ corresponds to the ordinary cascade with two communicating channels in the cross section, while the second with $\varkappa = 1$ also corresponds to a symmetrical cascade, but one having four such channels. We also note the fourth version with $\varkappa = 1$; this gives an asymmetric cascade with ordinary stages and $\theta = 2/3$.

Considering the separation coefficients as small for isotope mixtures, and, as usual, neglecting small quantities of higher orders, we obtain

$$\delta^+_n = \delta^+_{n-1} = \ldots = \delta^+,$$
$$D_n = D_{n-1} = \ldots = D,$$
$$c_{n-1} - c_{n-2} = c_n - c_{n-1} = \ldots = \frac{dc}{dn} \text{ etc.}$$

Then Eqs. (1) and (2) may be rewritten in the form

$$(1+s)D + sE - (1-t)B = P \approx 0, \tag{3}$$

$$(1+s)D\delta^+ + sE\delta^0 + (1+t)B\delta^- - \frac{dc}{dn}[sD + (1+2t)B] = P(c_P - c). \tag{4}$$

In the same way as for stages with two outflows, we may integrate the equation for the change of flow along the surface of separation and obtain an expression for the stage with three outflows:

$$\delta^+ = \varepsilon_0 c(1-c)\frac{E+B}{D}\ln\frac{D+E+B}{E+B}, \tag{5}$$

$$\delta^0 = \varepsilon_0 c(1-c)\frac{B}{E}\ln\frac{E+B}{B}, \tag{6}$$

$$\delta^- = \varepsilon_0 c(1-c)\ln\frac{E+B}{B}, \tag{7}$$

where ε_0 is the primary enrichment coefficient. Replacing D, E, and B in Eq. (3) by their values as indicated in Fig. 1 we have

$$(1+s)\varkappa\theta + s(1-\varkappa)\theta - (1+t)(1-\theta) = 0,$$

whence

$$\theta = \frac{1+t}{\varkappa+s+t+1}. \tag{8}$$

TABLE 2. Calculation of Cascade Schemes

No. of version	$\varkappa$																			
	0,1		0,2		0,3		0,4		0,5		0,6		0,7		0,8		0,9		1	
	α/β^2	θ	α/β^2	θ	α/β^2	θ	α/β^2	θ	α/β^2	θ	α/β^2	θ	α/β^2	θ	α/β^2	θ	α/β^2	θ	α/β^2	θ
First	1,048	0,476	1,093	0,455	1,138	0,435	1,182	0,417	1,227	0,400	1,272	0,385	1,319	0,370	1,365	0,357	1,413	0,345	1,460	0,333
Second	0,799	0,645	0,807	0,625	0,819	0,606	0,835	0,588	0,854	0,571	0,877	0,556	0,903	0,541	0,932	0,526	0,964	0,513	1,000	0,500
Third	0,941	0,909	0,789	0,833	0,760	0,769	0,767	0,714	0,791	0,667	0,823	0,625	0,862	0,588	0,905	0,555	0,951	0,526	1,000	0,500
Fourth	0,948	0,952	0,728	0,909	0,660	0,870	0,638	0,833	0,638	0,800	0,652	0,769	0,675	0,741	0,707	0,714	0,748	0,690	0,796	0,666

After an analogous transformation of Eq. (4) with the aid of (5)-(8) we write

$$\alpha \frac{dc}{dn} = 2\beta\varepsilon_0 c(1-c) - \frac{2P}{L}(c_P - c), \tag{9}$$

where

$$\alpha = \frac{s\varkappa(1+t)+(s+\varkappa)(1+2t)}{\varkappa+s+t+1}, \tag{10}$$

$$\beta = \frac{1+s+t(1-\varkappa)}{\varkappa+s+t+1}\ln\frac{\varkappa+s+t+1}{1+s+t(1-\varkappa)} + \frac{(1+s+t)(\varkappa+s)}{\varkappa+s+t+1}\ln\frac{\varkappa+s+t+1}{\varkappa+s}. \tag{11}$$

Equation (9) gives the concentration distribution for all versions of connecting the cascade stages under consideration. One characteristic of these schemes lies in the fact that three (rather than two) flows join at the entrance to each stage. If we introduce the concept of an ideal cascade, without any mixing of the concentrations at the inlet, we require that the concentrations of all three flows should be equal. It is not hard to show that a condition of this kind is quite impossible to fulfil, or, to be more precise, if it were fulfilled then the stage with three outflows would degenerate into an ordinary stage with two. Hence in analyzing the efficiency of the type of cascade under consideration we must abrogate the principle of nonmixing of the concentrations and confine ourselves to the less rigorous condition of a minimum total flow when working to specified external conditions. The imposition of this condition [3] is equivalent to finding a minimum of the function ΣL in Eq. (9). This function depends on the variable α/β^2 which varies over the range $\varkappa$, and also on s and t, which take fixed values for each version of the schemes in question.

Table 2 shows the results of some computer calculations. All the values of the function α/β are referred to its value corresponding to the ordinary symmetrical cascade (third version $\varkappa = 1$); the corresponding values of θ are also given. Of greatest interest are the third and fourth versions. The third version belongs to the series of combinations considered by Bouligand [3]. For an optimum value of $\varkappa$ slightly greater than 0.3 the total flow diminishes by roughly 32%, i.e., almost the same as in the asymmetrical cascade consisting of stages with two outflows for $\theta = 0.8$. The most efficient is the fourth version, which for $\varkappa \approx 0.45$ gives a 57% reduction in total flow. For this version the merits of the stage with three outflows and the merits of asymmetrical cascades are advantangeously brought together. It is interesting to note that the optimum result is obtained for a θ value of the order of 0.8, i.e., the same as in ordinary asymmetrical cascades, but with a less severe constructional complication [the back flow is passed not to the (n-4)-th but to the (n-2)-th stage]. It should be noted that the resultant optimum relationships may change slightly on using the gas-diffusion method of separation, if in effecting the optimization we consider not only the total productivity but also the area of the porous barriers.

LITERATURE CITED

1. K. Cohen, The Theory of Isotope Separation, New York (1951).
2. N. A. Kolokol'tsov, At. Énerg., 27, No. 1, 9 (1969).
3. G. Bouligand, CEA, Rep. 2622, UKAEA, Prod. Group, Inform. Ser. 16 (1965).

PRODUCTION OF ULTRACOLD NEUTRONS IN A STATIONARY (STEADY-STATE) REACTOR OF THE VVR-K (WATER-COOLED, WATER-MODERATED)TYPE

E. Z. Akhmetov, D. K. Kaipov, V. A. Konks, V. I. Lushchikov, Yu. N. Pokotilovskii, A. V. Strelkov, and F. L. Shapiro*

UDC 539.125.5.162.2:621.039.524.24

"Ultracold" neutrons are those experiencing total reflection for any angles of incidence on a vacuum-matter or vacuum-magnetic field boundary and having energies of

$$E \leqslant E_{\text{lim}} = \frac{h^2}{2\pi m} Nb \pm \mu B, \quad (1)$$

where N is the number of nuclei in unit volume, b is the coherent scattering length, m is the mass of a neutron, h is Planck's constant, μ is the magnetic moment of a neutron, B is the magnetic induction, the signs plus and minus relate to two orientations of μ relative to B.

This phenomenon of total reflection may be used for separating and storing such neutrons, either as a result of nuclear interaction with matter [1], or as a result of interaction with a magnetic field [2]. Equation (1) determines an energy range of ultracold neutrons until recently inaccessible on account of the difficulty of producing them.

The possibility of extracting and storing ultracold neutrons using nuclear interaction with matter was first verified experimentally in [3] using a reactor of the IBR class. Then some experiments with ultracold neutrons were carried out in the radial channels of a stationary reactor of the IRT type [4]. Neutrons with low energies close to the "ultracold" region were used in [5] to verify the 1/v law; certain characteristics of the behavior of ultracold neutrons were noted in [6, 7].

At the present time a first-order problem is that of creating fairly strong sources of ultracold neutrons. However, no methodical stage has yet been reached in the solution of this problem. In order to obtain ultracold neutrons the execution of methodical and scientific investigations in the VVR-K reactor has a number of favorable aspects. In particular, the open channel, tangential to the active zone of the reactor, with its comparatively large diameter (193 mm), enables us to increase the efficiency of the source by increasing the working surface of the ultracold-neutron converter and detector and reducing the losses in transporting the ultracold neutrons along the neutron guide.

In this paper we shall describe an apparatus for producing ultracold neutrons in the open horizontal tangential channel of a VVR-K reactor and shall present some initial results.

Description of the Apparatus

The arrangement of the apparatus is illustrated in Fig. 1. In the open tangential channel 193 mm in diameter we place an aluminum tube (5), 8 m long with an external diameter of 187 mm and a wall thickness of 3 mm. On one side of the tube in the center of the channel is the framework of the converter (ultracold neutron source) 4, 175 mm in diameter; either liquid nitrogen from the cooling system 7 (in the presence

*Deceased.

Translated from Atomnaya Énergiya, Vol. 37, No. 1, pp. 35-38, July, 1974. Original article submitted September 19, 1973.

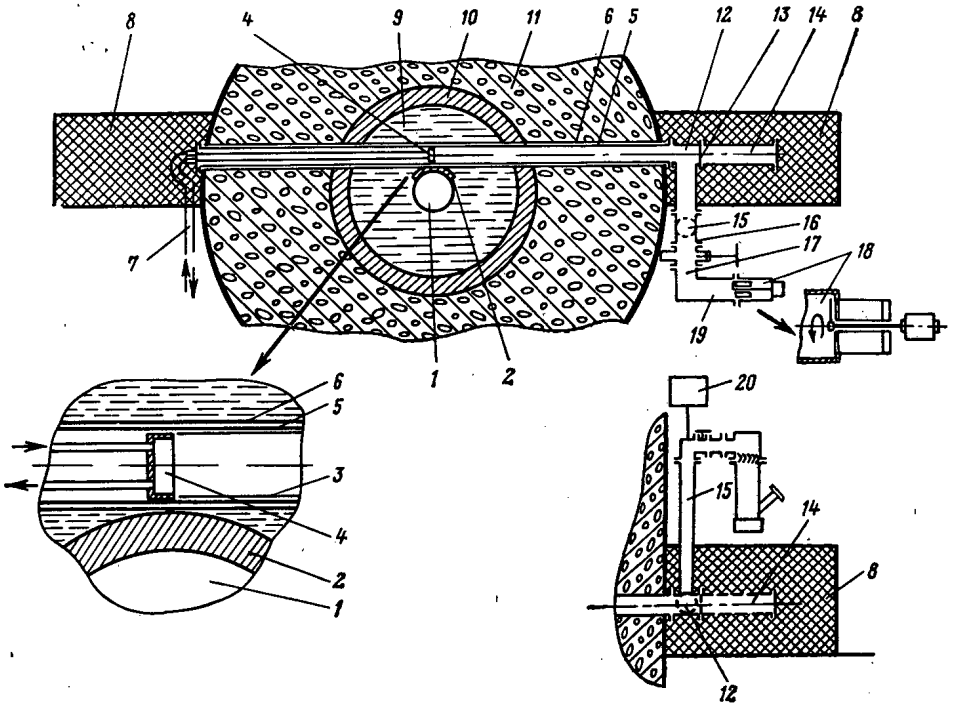

Fig. 1. Arrangement of experimental apparatus: 1) Active zone of the reactor; 2) lead layer 50 mm thick; 3) copper cylinders; 4) ultracold neutron converter; 5) aluminum tube; 6) open tangential reactor channel; 7) converter cooling system; 8) direct-beam shielding; 9, 10, 11) water, cast iron, and concrete shielding of the reactor respectively; 12), 16), 17), 19) copper parts of the neutron guide; 13) copper foil; 14) aluminum tube; 15) vertical part of the neutron guide for evacuation; 18) ultracold neutron detector; 20) system for filling with helium and monitoring the helium pressure.

of a solid moderator) or else liquid moderator pass to the converter along special tubes. From the other direction copper cylinders 175 mm in diameter, made of sheet copper 0.5 mm thick, are inserted into the tube 5 as far as the middle of the channel. Then the copper parts of the neutron guide, made of M2 type copper tubes 200 mm in diameter, are successively joined to this tube at the flanges. All the inner copper surfaces of the neutron guide are successively polished by chemical and electrolytic processes.

An additional aluminum tube (14) serves to reduce the background of scattered neutrons with energies $E > E_{lim}$ from the direct beam. In order to reflect the ultracold neutrons with $E \leq E_{lim}$ a copper foil (13) 50 μ thick is placed between the copper part of the neutron guide (12) and the tube (14).

For the diffuse reflection of neutrons from the walls of the neutron guide in transmission there is no major difference between the smooth bending of the tube indicated in [3, 4] and the direct rotation employed here.

The whole system is evacuated through a vertical internally polished tube (15) 135 mm in diameter, using a diffusion pump. In order to prevent oil vapor from falling on the copper surfaces and the converter, nitrogen and semiconducting traps are provided.

The working vacuum in the system is $5 \cdot 10^{-4}$ mm Hg. The total length of the copper neutron guide is a little greater than 6 m.

The ultracold neutrons from the converter (4) are transported along the neutron guide to the detector system (18), within the jacket of which lie two FÉU-13 photomultipliers with ZnS scintillators covered with a thin layer of a lithium compound (~ 0.05 mg/cm^2 Li) enriched with the ^{6}Li isotope [3]. The detectors are in turn covered with a thin (10 μ) copper slide. The pulses from the detectors are fed through amplifiers and discriminators to scalers or to a multichannel AI-100 pulse analyzer.

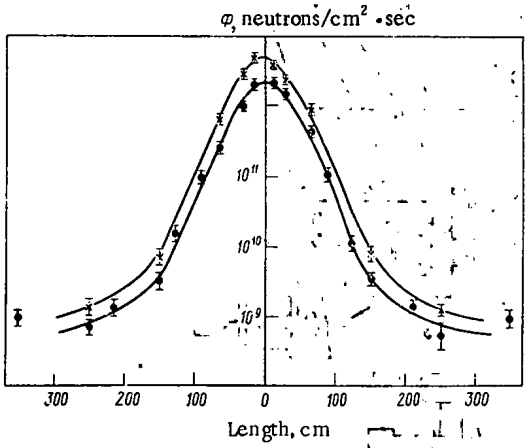

Fig. 2. Thermal neutron flux distribution along the open tangential reactor channel for two configurations of the reactor active zone.

In certain measurements high-purity helium from the filling system is passed into the neutron guide.

Measurements and Discussion

In order to calculate the expected yield of ultracold neutrons and the induced activity in various parts of the equipment, the distribution of neutron flux along the tangential channel was measured by the method of radioactive indicators [8]. For relative measurements we used copper indicators (5 mm in diameter and 15 μ thick). The absolute values of the neutron flux were obtained by measurements with gold indicators 0.26 mg/cm^2 thick at the ends of the tangential channel and in one of the vertical channels. The thermal neutron flux distribution was determined from measurements with indicators, either inside cadmium jackets or without any cover.

Figure 2 shows the thermal-neutron flux distribution along the tangential channel. In the center of the channel the thermal-neutron flux equals $(2.4 \pm 0.3) \cdot 10^{12}$ and $(4.8 \pm 0.4) \cdot 10^{12}$ neutrons/cm^2 · sec respectively for two typical configurations of the active zone of the reactor. The mean square errors of measurement, allowing for the normalization error, are indicated in the figure. The installation of a water moderator 175 mm in diameter and 300 mm long inside the channel, contrary to expectation, did not lead to any marked increase in the thermal neutron flux.

The energy spectrum of the neutrons in the tangential channel was not measured.

If we consider that a Maxwellian neutron energy distribution is established in the converter, with a value of $E_N = kT$, then according to [4] the maximum flux of ultracold neutrons is

$$\Phi_{UCN} = \frac{1}{8}\Phi_0\left(\frac{E_{lim}}{E_N}\right)^2 \frac{\bar{\sigma}_{cool}}{\sigma_a + \sigma_{heat}} \qquad (2)$$

where Φ_0 is the thermal neutron flux, E_{lim} is the limiting value of the energy, T is the effective temperature of the incident neutron spectrum, $\bar{\sigma}_{cool}$ is the scattering cross section involving the transfer of energy from the neutron to the converter, averaged over the thermal spectrum, σ_{heat} is the scattering cross section involving the transfer of energy from the converter to the neutron, σ_a is the neutron capture cross section. For example, in the case of an aluminum converter at 400°K, the flux of the ultracold neutrons

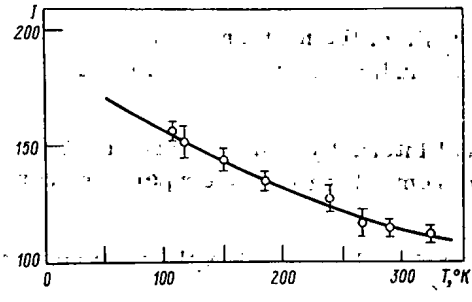

Fig. 3

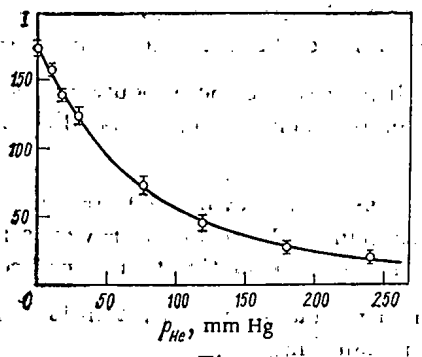

Fig. 4

Fig. 3. Dependence of the ultracold-neutron count rate (counts per 100 sec) on the temperature of a magnesium converter. The theoretical curve is normalized to the experimental value of I at room temperature.

Fig. 4. Dependence of the ultracold-neutron count rate (counts per 100 sec) on the helium pressure in the neutron guide. The theoretical curve is normalized to the experimental value of I for p = 0.

TABLE 1. Ultracold-Neutron Count Rate

Converter	Converter temperature, °K	Count rate, sec^{-1}	
		background	effect
$ZrH_{1.92}$	—	50±1	20±1
H_2O in aluminum ampoule	290	3,0±0,2	6,4±0,2
Aluminum ampoule	—	2,0±0,3	4,0±0,2
Magnesium	320	5,0±0,2	11,2±0,4

close to the converter equals 5 neutrons/$cm^2 \cdot sec$, which, on allowing for the transmission of the neutron guide (~0.2), agrees satisfactorily with the observed value of the ultracold-neutron flux at the outlet of the neutron guide.

Ultracold neutrons were first obtained in the foregoing apparatus and duly recorded in July 1971. By way of converters, use was made of water flowing through an aluminum container with a front wall 250 μ thick (water converter), zirconium hydride $ZrH_{1.9}$, and magnesium. Table 1 shows the ultracold-neutron count rate recorded by a scintillation detector with a working area of 14 cm^2 for a reactor power of 10 MW. In a four months work with a water converter and an average reactor power of 2.5 MW, theultracold-neutron count rate remained constant.

Figure 3 shows the dependence of the ultracold-neutron count rate on the temperature of the magnesium converter. The experimental results agree with the calculated curve [9].

In order to estimate the character of the ultracold-neutron diffusion from the converter to the detector, we measured the relationship between the ultracold-neutron count rate and the helium pressure in the neutron guide (Fig. 4). The resultant relationship $I(P_{He})$ shows that the intensity of the ultracold neutrons falls by a factor of two if the helium pressure in the neutron guide equals 60 mm Hg. This confirms the data of [4] and may indicate a considerable proportion of specular reflections from the tube walls.

A vacuum valve between sections 17 and 19 of the neutron guide with an open aperture 100 mm in diameter for the ultracold neutrons reduced the ultracold-neutron count rate by a factor of two. This also indicates the considerable proportion of specular reflections from the tube walls during the passage of the ultracold neutrons through the neutron guide.

A gradual but significant fall in the intensity of ultracold-neutron recording was noted in [4] over several months; in the opinion of the authors this was associated with the contamination of the surface of the neutron guide as a result of radiation-induced corrosion. In the apparatus here described there was no marked reduction in ultracold-neutron yield over six months (for an average reactor power of 2.5 MW).

The ultracold-neutron yield may be increased by cooling a number of converters to liquid-nitrogen temperature, and also increasing the thermal-neutron flux close to the converter. The efficiency of the apparatus as a whole may be greatly increased by using ultracold-neutron detectors with a better efficiency and a greater working area and by improving the construction of the system. According to estimations this should enable us to record as far as 10^3 ultracold neutrons per sec on the working surface of the detector.

The results of our measurements of the ultracold-neutron yields from several converters are now being analyzed.

Thus the foregoing results confirm the conclusions of [4] as to the possibility of extracting ultracold neutrons from the channels of a stationary reactor. The favorable characteristics of the arrangement utilizing the open horizontal tangential channel of a VVR-K reactor enable us to solve a number of both methodical and physical problems.

The authors wish to thank I. M. Frank for interest in the work and also all who assisted in its execution.

LITERATURE CITED

1. Ya. B. Zel'dovich, Zh. Éksp. Teor. Fiz., 36, 1952 (1959).
2. V. V. Vladimirskii, Zh. Éksp. Teor. Fiz., 39, 1062 (1960).
3. V. P. Lushchikov et al., JINR Preprint, R3-4127, Dubna (1968); ZhÉTF, Pis. Red., 9, 20 (1969).
4. L. V. Groshev et al., JINR Preprint, R3-5392, Dubna (1970).
5. A. Steyerl, Phys. Letters, 29B, No. 1, 33 (1969).
6. A. V. Antonov et al., Trudy Fiz. Inst. Akad. Nauk SSSR, 57, 270 (1972).
7. A. V. Antonov, D. E. Vul', and M. V. Kazarnovskii, ZhÉTF, Pis. Red., 9, 307 (1969).
8. R. B. Novgorodtsev et al., in: Transactions of the Second Coordinating Congress on the Dosimetry of Heavy Doses [in Russian], Izd. FAN, Tashkent (1966), p. 125.
9. V. V. Golikov, V. I. Lushchikov, and F. L. Shapiro, JINR Preprint R3-6556, Dubna (1972).

OPTIMIZING RESONATOR-SYSTEM POWER WHEN ACCELERATING WIDELY SPACED BUNCHES

V. L. Serov, Yu. F. Orlov, and A. I. Baryshev

UDC 621.384.6

Accelerated widely spaced dense charged-particle bunches can have various uses (both scientific and applied). For example, impact countercollisions of electron and positron bunches allow one to attain counterreaction luminosities which cannot be attained by other methods (with comparable rf-power expenditures) [1].

The process of accelerating dense bunches is accompanied by intense coherent energy radiation in a resonance cavity at the oscillation natural modes [2-8]; this reduces the acceleration efficiency and leads to a need for compensating significant integral energy losses by increasing rf-generator energy.

The integral energy-loss magnitude from a real elongated bunch, like the energy obtained by it from the field created by an external generator, depends on the number of particles and the bunch and resonator geometries.

The present paper considers the problem of optimizing energy transfer from the generator to the accelerated bunch, using as an example a system of independent resonators. We assume that the bunches are rather widely spaced and the generators are turned on only for a certain time τ_g before a bunch appears in a given resonator and are turned off immediately after its passage. The rf energy remaining in the resonator after the bunch passes is scattered in its walls and coupling unit in the time interval when the generator is not operating. Thus, the bunches are not linked to each other through the resonator field, so that the problem posed is solved for a single bunch.

Below, we optimize the quantity τ_g and find the optimal acceleration regime for a linear accelerator and also for proton and electron ring accelerators.

In the time τ_g, there accumulates in the resonator field energy W_r, which is then partially absorbed by the bunch in time Δt (we assume that $\Delta t \ll \tau_g$). Moreover, some generator energy W_g is absorbed in the resonator wall or is reflected from it and absorbed in the decoupling assembly. We consider below the case in which the decoupling assembly assures constant generator output power P_g, independent of the loading type:

$$P_g = \text{const}; \quad W_g = P_g t; \quad 0 < t < \tau_g. \tag{1}$$

We know that in this case the voltage on the tuned resonator increases exponentially when the generator is turned on, and the energy stored in it is determined by the following equation:

$$W_r(t) = \frac{CV_r^2}{2} = \frac{4Q_n P_g}{\omega_g Q_{ap}}(1 - e^{-\alpha_n t})^2, \tag{2}$$

where V_r is the resonator-potential amplitude; C is its equivalent capacitance; ω_g is the generator frequency; Q_0 and Q_{ap} are the intrinsic and applied Q; $Q_n^{-1} = Q_0^{-1} + Q_{ap}^{-1}$; α_n is the decay decrement taking into account coupling between resonator and generator. The maximum for the ratio in which we are interested $\eta(t) = W_r(t) \cdot W_g(t)^{-1}$ takes place when $t = \tau_g$ and $\alpha_n \tau_g = 1.25$; it is

$$\eta_{max} = 0.82 Q_0/(Q_0 + Q_{ap}). \tag{3}$$

Translated from Atomnaya Énergiya, Vol. 37, No. 1, pp. 39-42, July, 1974. Original article submitted June 19, 1973.

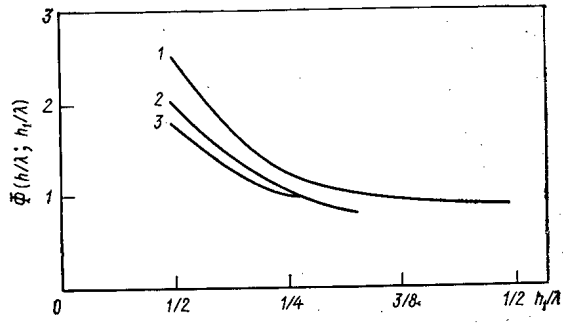

Fig. 1. Function $\Phi = \Phi(h/\lambda; h_1/\lambda)$ when $h/\lambda = 1/2(1); 1/3(2); 1/4(3)$.

It follows from this that the strong-coupling case is optimal:

$$Q_{ap} \ll Q_0; \quad \eta_{max} = 0.82; \quad (\tau_g)_{opt} = 2.5 Q_{ap}/\omega_g; \tag{4}$$

$$(P_r)_{opt} = 1.22 W_r (\tau_g)/\tau_g \approx 0.41 \omega_g W_g (\tau_g)/Q_{ap}. \tag{5}$$

Thus, when the coupling between generator and resonator increases, the system efficiency increases, and becomes greatest when $Q_{ap} \ll Q_0$. Here, to accumulate the required energy magnitude W_r in the resonator, the generator is turned on for a time $(\tau_g)_{opt}$ with power $(P_g)_{opt}$. Eighteen percent of the generator energy is lost in the resonator walls and to reflection (with absorption in the decoupling assembly).

In this case, the transient process proceeds as follows. At the instant the generator is turned on ($t = 0$), practically all the power is reflected from the resonator as from a short-circuited line. When $\alpha_n t = 0.69$, the reflection power with $Q_0 \gg Q_{ap}$ is close to zero, after which it increases anew. The energy lost in the walls in the time $(\tau_g)_{opt}$ is much less than W_r.

The average energy increment for one of N particles in a bunch having length h_1 and passing through a resonator can be written as follows [2]:

$$\Delta E = eMM_1 V_r \cos\varphi - \frac{8e^2N}{\pi\varepsilon_0 a}\psi\left(\frac{h}{\lambda}; \frac{h_1}{\lambda}\right); \qquad M = \frac{\sin\frac{\pi h}{\lambda}}{\frac{\pi h}{\lambda}}; \quad M_1 = \frac{\sin\frac{\pi h_1}{\lambda}}{\frac{\pi h_1}{\lambda}}. \tag{6}$$

Here, the second term describes losses to coherent radiation; the function ψ depends on the specific bunch and resonator parameters; ϕ is the equilibrium phase; a is the resonator radius; h its width; λ is the wavelength.

Multiplying Eq. (6) by the number of particles N and differentiating $N\Delta E$ with respect to N, we find that the energy transfer from the resonator to the entire bunch is maximal when the following relationship holds [2]:

$$N_{opt} = \frac{\pi\varepsilon_0 a M M_1 V_p \cos\varphi}{16 e\psi}. \tag{7}$$

When this relationship is invalid, the acceleration-system efficiency worsens. The average (over the bunch) energy increment for one particle in the optimal case, i.e., as in Eq. (7), is determined by the expression:

$$(\Delta E)_{opt} = \frac{eMM_1}{2} V_r \cos\varphi = \frac{8e^2N}{\pi\varepsilon_0 a}\psi. \tag{8}$$

In a linear accelerator, one usually strives to have maximal acceleration rate, so that, in practice, the assigned magnitude is allowable under field-potential breakdown conditions $(V_r/h)_{all}$. Then, it follows from Eq. (7) that

$$e(N/\lambda^2)_{all} = \frac{\pi\varepsilon_0}{16} MM_1 \left(\frac{V_r}{h}\right)_{all} \cos\varphi \frac{ah}{\lambda^2}\Big/\psi. \tag{9}$$

Thus, if the right side of Eq. (9) remains constant (a, h and h_1 proportional to λ), then the wavelength we choose must depend on the number of particles in the bunch as $N^{1/2}$.

The final energy E is determined by the total number of linear-accelerator resonators:

$$n = \frac{E}{(\Delta E)_{all}} = \frac{\pi\varepsilon_0 (a/\lambda)}{8e^2\psi} \cdot \frac{E\lambda}{N} = \frac{2\frac{\lambda}{h}\cdot\frac{E}{\lambda}}{eMM_1 \cos\varphi \left(\frac{V_r}{h}\right)_{all}}. \tag{10}$$

In the optimal case, when the most energy (taking radiation into account) is taken from the resonator, the efficiency is found as the following ratio:

$$(\varkappa)_{\text{opt}}=\frac{(N\Delta E)_{\text{opt}}}{P_g(\tau_g)_{\text{opt}}}=\eta_{\max}\frac{(N\Delta E)_{\text{opt}}}{W_r};$$
$$\frac{(N\Delta E)_{\text{opt}}}{W_r}=0.6\,\frac{(MM_1\cos\varphi)^2}{\psi}\cdot\frac{h}{\lambda};\qquad(11)$$
$$(\varkappa)_{\text{opt}}=0.6\,\frac{\eta_{\max}\cos^2\varphi}{\Phi\left(\frac{h}{\lambda};\ \frac{h_1}{\lambda}\right)}.$$

Figure 1 shows the function Φ; it is clear that its smallest values lie in the interval 0.8-1 and correspond to the case when $h_1/\lambda = 1/4-1/2$. Here, $(\varkappa)_{\text{opt}}$ depends, in fact, only on the phase value φ.

If two linear accelerators are used to obtain widely spaced impact collisions between opposed bunches (without their secondary use for counterreactions), then the reaction luminosities are, in the optimal regime, as follows:

$$L\approx 1.16\frac{N^2f}{s}F(h_1)=0.696\eta_{\max}\frac{\cos^2\varphi N\bar{\mathcal{P}}_g}{\Phi Es}F(h_1).\qquad(12)$$

where s is the transverse (right-angle) cross section of each of the beams at the point where the centers of both bunches meet; F(0) = 1 and as h_1 increases it decreases slowly; f is the bunch repetition rate; $\bar{\mathcal{P}}_g$ is the average accelerating-system power.

If one assigns the necessary luminosity value L at energy ε, the possible focusing area s, and the maximum value for $\bar{\mathcal{P}}_g$, then Eq. (12) determines the necessary number $N\cos^2\varphi$. Having additional physical considerations concerning the choice of equilibrium phase φ, we obtain from Eq. (9) the optimal value for wavelength λ.

Two accelerated proton bunches can be used after ejection to produce impact countercollisions between protons and secondary hadrons generated at the target; $p\pi$, pk, $p\bar{p}$, pn, etc., and also to produce encounters such as $\pi\pi$, * for example. Protons can be accelerated by using high-Q resonators placed around the orbit and operating at constant frequency. For this, it is necessary only that the field decay in the interval δt between two bunches: $\alpha_n\delta \gg 1$. In the time δt with the generator turned off, it is easy to achieve the necessary accelerating-field phase change (always less than π radians) so that the folllowing bunch will arrive at the right phase.

When the magnetic field increases linearly ($\dot{H}$ = const), the particle-energy increment per cycle is $(\Delta E)_{cy} = e/c(L_0R\dot{H} = \text{const}$, where L_0 is the orbit length. In this case, all the equations in the preceding section are satisfied with the difference that n now denotes the number of resonators in the orbit and E in Eq. (2) must be replaced by $(\Delta E)_{cy}$.

We will consider a ring accelerator for opposed electron and positron bunches. In this case, due to synchrotron radiation, the necessary value for energy transfer to a particle per cycle $(\Delta E)_{cy}$ does not remain constant, but increases sharply toward the end of acceleration. Therefore, one cannot obtain an optimum, constant efficiency value over the entire acceleration cycle. Taking this into account, we optimize the r-power magnitude, averaged over the acceleration cycle. We will take E, L_0, N, and λ as given; the number of resonators in the orbit n is subject to optimization. Energy losses to resonator excitation, on the one hand, are proportional to their number, while, on the other hand, the rf-energy magnitude needed to accelerate a small number of particles (when losses to coherent radiation in the resonators may be disregarded) falls in inverse proportion to the number of resonators in the orbit. However, if the number of resonators increases due to decreased magnetic length $2\pi R$, then the rf-energy dispersion increases to compensate for synchrotron radiation.

The generator energy expended during an acceleration cycle (for $k_{\max}$ particle revolutions) and optimized with respect to τ_g, is

$$W_\Sigma\approx 1.22n_1n\sum_{k=1}^{k_{\max}}W_r(k)=0.61Cn_1n\int_0^{k_{\max}}V_r^2(k)\,dk;\qquad(13)$$

here n_1 is the number of bunches in the orbit (in the case considered, $n_1 = 2$); C is the resonator equivalent capacitance. Now, we make the following definitions:

$$V_r(k)=\frac{1}{eMM_1\cos\varphi}\left[\frac{(\Delta E)_{cy}}{n}+\frac{8e^2N}{\pi\varepsilon_0 a}\psi\left(\frac{h}{\lambda};\ \frac{h_1(k)}{\lambda}\right)\right];\qquad(14)$$

*A. A. Naumov, whom the authors thank, pointed out that in the method using widely spaced impact collisions, which requires strong focusing of opposed particles, measurements are difficult at small scattering angles, which is a shortcoming of this method.

$$[\Delta E(k)]_{cy} = 30R\Delta H(k) + 0.88 \cdot 10^7 \frac{E^4(k)}{R} + \Delta E_{other}, \quad (15)$$

where R is the magnetic-track radius of curvature, in km; ΔH is the field increment per cycle, in kG; E and ΔE are expressed in gigaelectron-volts. The second term on the right describes synchrotron radiation in one cycle. The quantity ΔE_{other} includes all possible energy-loss mechanism, except for synchrotron and coherent radiation in the resonators.

When the bunch-acceleration cycle frequency is f, the average rf-system power is $\bar{\mathcal{P}} = W\Sigma f$. The condition for the average-power minimum takes the form:

$$\frac{\partial}{\partial n} n \int_0^{k_{max}} V_r^2(k)\, dk = 0 \quad (16)$$

or

$$\int_0^{k_{max}} dk \left[\frac{8e^2N\psi}{\pi\varepsilon_0 a} + \frac{(\Delta E)_{cy}}{n}\right]\left[\frac{8e^2N\psi}{\pi\varepsilon_0 a} - \frac{(\Delta E)_{cy}}{n} + 2\frac{\partial(\Delta E)_{cy}}{\partial R}\cdot\frac{\partial R}{\partial n}\right] = 0. \quad (17)$$

For the case when the magnet radius of curvature R = const is considered given, we can find the following expression from Eq. (17):

$$L_{acc} = hn_{opt} = \left(\frac{\int_0^{k_{max}} dk\,(\Delta E)_{cy}^2}{\int_0^{k_{max}} dk\,(N\psi)^2}\right)^{1/2} \frac{\pi\varepsilon_0 ah}{8e^2}. \quad (18)$$

The corresponding minimal value for the average rf power is:

$$\bar{\mathcal{P}}_{min} = \frac{1.22f}{4.8\cdot 10^2 \frac{n}{\lambda} e^2 M^2 4\pi c} \int_0^{k_{max}} \frac{\lambda n_{opt}}{(M_1\cos\varphi)^2}\left(\frac{(\Delta E)_{cy}}{n_{opt}} + \frac{8e^2N}{\pi\varepsilon_0 a}\psi\right) dk. \quad (19)$$

If the number of particles N, the bunch length h_1, and the phase value φ do not change over the acceleration cycle, then Eq. (19) takes on the form:

$$\bar{\mathcal{P}}_{min} = 1.04 \frac{NfF(k)\,\Phi\left(\frac{h}{\lambda};\ \frac{h_1}{\lambda}\right)}{\cos^2\varphi}, \quad (20)$$

where

$$F(k) = \left(k_{max}\int_0^{k_{max}} dk\,(\Delta E)_{cy}^2\right)^{1/2} + \int_0^{k_{max}} (\Delta E)_{cy}\, dk;$$

$$\Phi = \frac{\psi\left(\frac{h}{\lambda};\ \frac{h_1}{\lambda}\right)}{M^2 M_1^2 \frac{h}{\lambda}}.$$

Clearly, the minimal-power value is not directly dependent on the wavelength, but is a function of the parameters h/λ and h_1/λ, the assigned energy increment in the cycle, and the equilibrium phase. However, the bunch length cannot be assigned arbitrarily; it depends on the phase-stability-region magnitude, which is $2\pi h_1/\lambda \leqslant 3\varphi$. The smallest value for the function $\Phi/\cos^2\varphi$ occurs when $\varphi \approx 30$–$40°$.

If the breakdown voltage $(V/h)_{all}$ can be considered given and independent of λ, then we again obtain $\lambda^2 \sim N$. Actually,

$$\left(\frac{V}{h}\right)_{all} \geqslant \frac{(\Delta E)_{cy} + \frac{8e^2N}{\pi\varepsilon_0 a}\psi n_{opt}}{L_{acc}}. \quad (21)$$

If we take Nn_{opt}/a from Eq. (18), then the numerator of this ratio will not depend on N or λ. Consequently, $L_{acc} \sim h/V$ is independent of N and λ, and we obtain from Eq. (18): $\lambda^2 \sim N$.

Equation (18) remains approximately true in the case when the assigned quantity is not R, but the orbit length L_0, if only the number of particles is large enough that $L_{acc} \ll \pi R$. In this case $R = (L - L_{acc} - l)/2\pi$ is practically independent of L_{acc} and can be considered approximately constant (l is the total length of intervals not occupied by accelerating resonators). If N is so small that Eq. (18) gives $L_{acc} > \pi R$, then one should use the general equation, Eq. (17). In particular, if we wholly disregard coherent radiation

in the resonators (and also magnetic-field variation over time), then when L_0 = const we obtain the familiar condition

$$hn_{opt} = \pi R. \tag{22}$$

We will consider a synchrotron with opposed electron and positron bunches $N^- = N^+ = 2 \cdot 10^{13}$; E = 100 GeV; R = km, magnetic-field sinusoidal-oscillation (with magnetiziation) frequency f_H = 200 Hz; H_{max} = 0.875 kG; H_{ej} = 1.67 kG. In this case, at the end of acceleration, the losses to synchrotron radiation per cycle are $\Delta E\gamma$ = 4.4 GeV and the particle-energy increment at the end of acceleration is U = 1.6 GeV. The relative energy fraction expanded on synchrotron radiation is rather small and equals $W_\gamma/E \approx 0.2$, $\Delta\varepsilon_\gamma/U = 0.55$. When λ = 75 cm, $h/\lambda = 0.25$, and $h_1/\lambda = 0.25$ (in principle, h_1 can, with the help of damping, be made almost constant over the acceleration cycle) from Eq. (18) we obtain $n \approx 8 \cdot 10^3$ and $hn \approx 1.5$ km, i.e., $hn \ll \pi R = 6.3$ km. The losses from a single particle to coherent radiation in all resonators are 4.14 GeV /cycle; $(V_r)_{max}$ = 1.8 MeV; V_r/h = 96 kV/cm; the total peak power without generators is equal to $4.5 \cdot 10^3$ MW.

The average power is $\bar{\mathcal{P}} = 2.2 \cdot 10^6$ f W, where f is the bunch-accelerations frequency, $f \ll f_H$. The average beam power is $0.64 \cdot 10^6$ f W; $\varkappa_{max} \approx 29\%$. When f = 20 Hz, $\bar{\mathcal{P}}$ = 44 MW, and of that about 13 MW goes into the beam, ~7 MW to synchrotron radiation, and 16 MW to coherent radiation (the losses ΔE_{other} were considered to be zero).

We note that a similar calculation for a proton accelerator gives $\varkappa_{max}$ = 37%. The worsened $\varkappa$ in the electron accelerator is due to synchrotron radiation. The small value of this worsening ($\varkappa_{electron}/\varkappa_{proton} \approx 0.8$) is due in the present case to the choice of a high magnetic-field variation frequency f_H (with widely spaced bunch triggering, $f = 0.1\ f_H$).

LITERATURE CITED

1. A. I. Alikhanyan et al., VII International Conference on High-Energy-Particle Accelerators (Erevan-Tsakhkadzor) [in Russian], Vol. 2, Izd. AN ArmSSR, Erevan, (1970), p. 103.
2. V. L. Serov and A. I. Baryshev, Izv. AN ArmSSR, Fizika, 7, No. 6, 406 (1972).
3. L. N. Kazanskii, A. V. Kisletsov, and A. N. Lebedev, At. Énerg., 30, No. 1, 31 (1971).
4. O. A. Kolpakov and V. I. Kottov, Zh. Tekh. Fiz., 34, No. 8, 1387 (1964).
5. G. P. Fomenko, Izv. VUZ. Fizika, No. 4 (1966).
6. S. B. Rubin and V. N. Mamonov, Preprint OIYaI D-3346-2, Dubna (1967).
7. V. I. Kartin in: Accelerators and Physical-Experiment Radio Electronics [in Russian], No. 2, Atomizdat, Moscow (1972), p. 60.
8. V. L. Serov and G. A. Nagorskii, Izv. AN ArmSSR, Fizika, 7, No. 8 (1973).
9. J. Altman, Superhigh-Frequency Apparatus [Russian translation], Mir, Moscow (1968).

INTRODUCTION OF THE METHOD OF PREPLANTING GAMMA IRRADIATION OF SEEDS AND THE COMMERCIAL KOLOS GAMMA APPARATUS INTO AGRICULTURAL PRACTICE

N. M. Berezina, A. M. Kuzin, and D. A. Kaushanskii

UDC 577.3:539.12.04

One of the realistic and extremely promising ways of utilizing atomic energy in agriculture is the preplanting γ irradiation of seeds of agricultural plants to increase their yield and improve the quality of production.

The possibility of the utilization of ionizing radiation to stimulate development and increase the yield of agricultural plants has been indicated by the observations of many authors [1-4].

The investigations of N. M. Berezina et al. [5-10] have convincingly demonstrated the stimulating effect of small doses of ionizing radiation on the yield of a number of agricultural crops. In [11], on the basis of the analysis of data on the stimulating effect of definite doses of ionizing radiations, it was concluded that only preplanting γ irradiation of dry seeds can be considered as a possible agricultural method.

In 1955, under the general supervision of the Scientific Council on Problems of Radiobiology of the Academy of Sciences of the USSR, investigations of the method of preplanting irradiation of seeds of agricultural crops were organized in various climatic zones of the Soviet Union: the Latvian SSR, the Gor'kii region (RSFSR), Azerbaidzhan SSR, Uzbek SSR, etc. At the present time, there are theoretical representations of the mechanism of the stimulating effect of radiation on the development of seeds and the yield of crops [12, 13]. According to the modern data, the development of a plant from a dry seed up to the moment of ripening of the yield is determined by the following factors.

1. The hereditary program of development, encoded in the DNA of the cells of the seeds, entirely determining the sequence of phases of development (formation of morphological forms, initial composition and type of metabolism of the given plant variety).

2. The influx of nutrients from the external environment.

3. The influx of energy essential for processes of development and synthesis of the basic substances in the plant.

4. The formation during metabolism of effector triggers – substances that produce a specific and nonspecific derepression of the genes, their deblocking, or the disappearance of inhibitors inducing repression of genes, which also determines the transition of the entire plant or individual parts of it from one phase of development to another, i.e., its ontogenesis.

How does preplanting γ irradiation of seeds influence these leading factors of development?

Numerous investigations have shown that the genetic program of development, the code lodged in the structure of DNA, is practically unchanged at the low doses of irradiation that have a stimulating effect. Individual, very rare changes in the DNA, arising randomly after irradiation in stimulating doses in few cells, are repaired by the repairing enzymes or are eliminated in the process of development. On the basis of numerous studies over many years with stimulating doses of irradiation, the practically important

Translated from Atomnaya Énergiya, Vol. 37, No. 1, pp. 43-51, July, 1974. Original article submitted August 24, 1973.

conclusion has been drawn that the program of development, encoded in the genotype of the given species and the given varieties, is preserved at the low doses of irradiation that give an effect of stimulation.

The influx of nutrients to planted seeds and the plants that develop from them is determined by two circumstances; the content of these substances in the surrounding medium and the permeability of the seed coat and numerous biomembranes of its internal structures. Of course, preplanting irradiation of seeds has no influence on the content of substances needed by the plant in the surrounding medium; all the requirements for fertilizers, moisture content, and working of the soil remain in force. However, the changes in the permeability of the biomembranes after γ irradiation, demonstrated in a number of experiments, and the acceleration of the influx of nutrient substances from the surrounding medium into the tissues of the developing seeds and plants will play an important role in the stimulation of germination and development of the seedlings. The third factor – the influx of energy – is provided for during the period of ontogenesis through the energy of sun rays, accumulated in the process of photosynthesis, and in the initial stages of germination, through the energy of stored nutrients consumed in the process of respiration. Of course, the energy of the absorbed γ quanta is immeasurably small in comparison with these sources and is not a direct cause of stimulation; however, indirectly by inducing an acceleration of the utilization of stored nutrients and a more rapid and intensified formation of chloroplasts, as well as by increasing the leaf surface, it promotes a better assimilation of the energy of sun rays during the process of photosynthesis, which makes a significant contribution to the stimulation of development and the formation of the yield. The earlier and intensified formation of nonspecific and specific effector triggers in the germinating seed and then in the developing plant, which play the role of a starter mechanism in the process of deblocking and derepression of genes, will also be a leading factor in the expression of the effect of γ stimulation. In a dormant seed, all the information encoded in DNA is in a repressed, blocked state. The first oxidative processes arising in the seed during its soaking and access to oxygen, form nonspecific effects, which induce a deblocking of many genes, providing information for the synthesis of a number of enzymes essential at the beginning of respiration and the preparation of the cells for division. The free radicals formed in the irradiated seeds readily give hydroperoxides, hydroquinones, and oxyquinones after the intake of oxygen; these substances react with the histones of the nuclei and their sulfhydryl groups, which leads to conformational changes in their molecules and a nonspecific deblocking of DNA, essential for the beginning of development. As is well known, irradiated seeds germinate earlier; the primary biochemical processes in the seeds are accelerated. The formation of a specific effector trigger in the embryo – gibberellic acid – is also accelerated. Its earlier influx to the aleurone layer of the seed leads to a repression of specific genes controlling the synthesis of α-amylases, proteases, and a number of other enzymes that mobilize the stored nutrients of the seeds – starch and proteins. A more rapid and intensified formation of sugars and amino acids and an acceleration of their influx to the embryo have been noted in γ-stimulated seeds, which is vital for stimulation. In seeds irradiated with stimulating doses, tryptophan synthetase is synthesized more actively, as a result of which indolylacetic acid – auxin, which is a specific synthetic effector trigger, is formed in greater amounts [8]. In view of the same factors, in γ-irradiated seeds the processes of synthesis of DNA and RNA and protein synthesis are accelerated, the mitotic index is increased, and growth processes are intensified. The earlier and more intensive development of the root

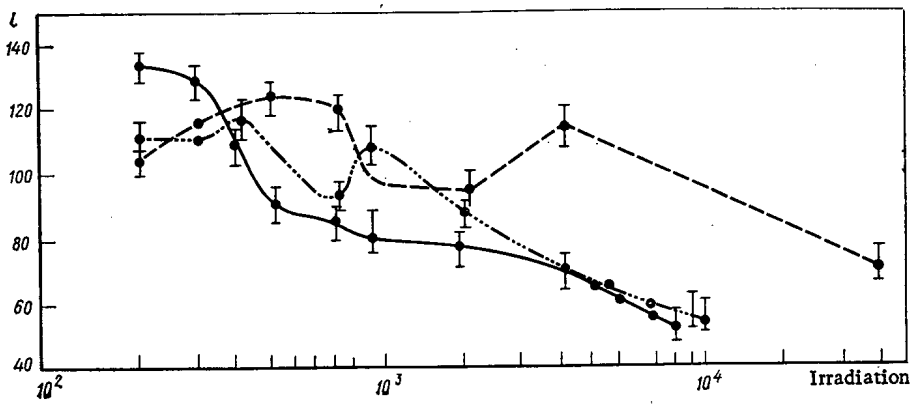

Fig. 1. Changes in the values of the optimum stimulating doses of γ irradiation with changing moisture content of the seeds: ——) 25%; – – – – –) 10%; –·· · ··–·· · ··–··) 5%; (l is the length of the roots, % of control).

TABLE 1. Effects of Ionizing Radiations on Corn Seeds of Different Ages

Year of crop	Year of irradiation	Length of roots of seedlings, mm			
		500 R	control	% of control	t*
1958	1959	26,5±0,9	20,3±0,8	131	5,3
1956	1959	22,6±1,1	19,8±0,9	114	2,0
1955	1959	16,5±2,0	18,0±0,9	91	0,7

*t here and henceforth is the criterion of significance of the difference.

system in stimulated seedlings, the formation of the chloroplasts, and the development of the leaf surface lead to an acceleration of the development of the plants and, correspondingly, to a more intensive formation of effectors, which act not only on the apical growing point, but also induce the beginning of the development of lateral buds, which promotes a greater branching of the stimulated plants, a greater formation of generative organs [9]. Stimulation of the preceding stages of development leads to an earlier formation of effector triggers responsible for the beginning of flowering (flowering factor). As a rule, plants from seeds γ-irradiated in a stimulating dose bloom several days earlier, which shortens the vegetation period and is important for better formation of the yield [10].

The theory being developed of the leading role of accelerated synthesis of effector triggers as the basic cause of the stimulating effect of low doses of radiation also well explains the fact that, as a rule, the content of the component, toward the production of which the given crop was evolutionarily directed, is increased in the yield from stimulated seeds. In the case of irradiation of carrot seeds, the concentration of carotene in the yield is increased [7], in the sugarbeet the concentration of sucrose [14], and in potato tubers the concentration of starch. This is explained by the fact that the type of metabolism determined by the genetic information contained in the given selected variety is unchanged by irradiation with stimulating doses. However, the early and intensified formation of effectors leads to a more accelerated realization of the genetic information, which is also expressed in an increase in the component in the yield, for the sake of which the given crop is grown. For a long time, a serious obstacle to the recommendation of preplanting irradiation of seeds as an agricultural method was the poor reproducibility of the effect of stimulation, detected in the original experiments on the study of the biological effects of x-rays, which served as the basis for the cessation of work along this line abroad. In the USSR, on the contrary, intensified investigations of the causes of the poor reproducibility of the stimulaating effect of low doses of irradiation were begun and showed that the biological action is determined not only by the value of the integral dose of irradiation, but is also inseparably linked with and easily changed by a complicated assortment of modifying factors [2].

The lack of knowledge of the role and mechanism of the action of modifying factors in the first attemps at the practical utilization of radiation stimulation was the main cause of the poor repeatability of the positive effect of stimulating doses of radiation. The role of the following modifying factors has now been elucidated: the moisture content and age of the seeds, the interval of storage of the irradiated seeds and the degree of their maturity, seasonal variations of radiation sensitivity, type variety, and planting qualities of the seeds. The significance of regionalized varieties in the stabilization of the effects of stimulation has also been demonstrated.

At the present time the complex of modifying factors has been far from fully studied, but what is already known permits such a stabilization of the results obtained that preplanting irradiation can be recommended for introduction for a number of crops as a new economically profitable agricultural method. In studying the effects of modifying factors individually, it can be stated that one of the main ones is the moisture content of the irradiated seeds.

Modern radiobiological concepts consider the radiolysis of water as one of the mechanisms of radiation damage to the organism, and attribute great significance to the water content in the object at the moment of irradiation [12].

The experiments conducted have shown that the value of the stimulating doses of irradiation varies depending on the water content.

In the case of the irradiation of corn seeds of the Sterling and Bukovinskii-3 hybrid varieties with controlled moisture content 10-12%, the optimum stimulating dose is 500 R, at a dose rate of 700 R/min. Drying the seeds to a 5% moisture content lowers the value of the optimum dose to 400 R. In this case the additional growth of the roots of six-day old seedlings was also changed, comprising 6% instead of 18%. At a moisture content of the seeds of up to 25%, their radiosensitivity increased even more, and a dose of 250 R had a stimulating effect while at a dose of 500 R, instead of the stimulation that arose in the seeds

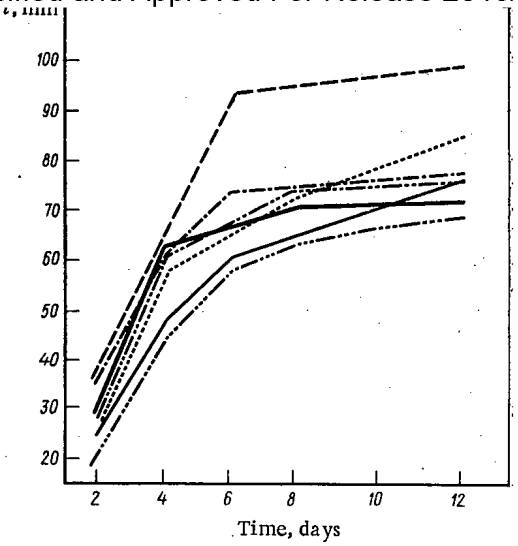

Fig. 2

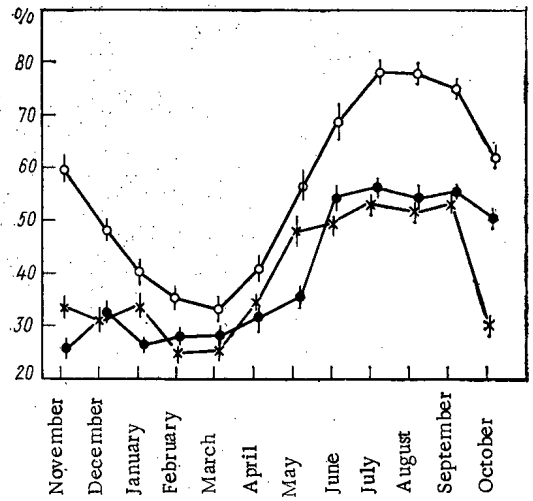

Fig. 3

Fig. 2. Dependence of the additional growth of corn roots on the value of the stimulating dose of γ irradiation (l is the length of the roots): ----) planting immediately after irradiation; -.-.-.-) after storage for one day; -..-..-) two days; ....) three days; ——) seven days; —— ... — ... —) 14 days; ——) control.

Fig. 3. Dependence of the change in the radiation sensitivity on the time of year; ○) castor plant; ●) sunflower; ×) soybean.

with the 10-12% moisture content, an inhibition of growth of the roots was observed. The changes in the values of the optimum stimulating doses of γ radiation with changing moisture content of the seeds is shown in Fig. 1.

Considering the fact that under commercial conditions the moisture content of the seeds can readily vary, the methodological instructions developed for the preplanting irradiation of seeds [15, 16] recommend irradiation of seeds at air-conditioned humidity to obtain repeatable effects of stimulation. Deviation of the moisture content from the norm requires a preliminary refinement of the optimum doses of irradiation of seeds.

The age of the irradiated seeds also proved to be an important factor for obtaining unambiguous results. During the aging of seeds, i.e., when the period of storage is lengthened, their radiation sensitivity was increased, together with a lowering of the germination rate (Table 1).

As can be seen, seeds of the crop of the preceding year gave a 31% additional growth of the roots of the seedlings, for those stored for three years 14%, while irradiation had no stimulating effect on seeds stored for four years after harvesting, with a 64% germination rate.

On the basis of these data, confirmed by repeated subsequent experiments, it is recommended that seeds of the crop of the preceding year be used for preplanting irradiation. In experiments conducted without considering the age of the seeds, this factor may be one of the causes of the nonrepeatability of stimulation.

The stimulating effect of γ radiation also varies with the periods of storage of the irradiated seeds. At the initial stages of development, radiobiologists believed that the effect of the dose remains unchanged in irradiated seeds. The modern representations have shown that slow metabolic processes occurred in irradiated seeds, the course of which depends on the periods and conditions of storage of the irradiated seeds. Corn seeds of the Sterling variety of air-conditioned humidity, form the yield of the preceding year, irradiated with a source of γ radiation from ^{60}Co at a dose of 500 R, dose rate 700 R/min, were planted 1, 2, 3, and 14 days after irradiation, and immediately after irradiation. The change in the effect of the stimulating dose was determined according to the additional growth of the roots at 2, 4, 6, 8, and 14 days of development (Fig. 2). Maximum additional growth of the roots was observed when the corn was planted directly after irradiation. In the case of planting 1, 2, 3, and 8 days after irradiation, the gain in length of the roots was sharply lowered, being stabilized at a level of 12-20% in comparison with the control.

TABLE 2. Effects of Preplanting γ Irradiation of Seeds on the Yield of Corn after Various Periods of Storage of Irradiated Seeds

Periods of planting of irradiated seeds	Yield		
	centners /hectare	% of control	t
Control (nonirradiated seeds)	310±12,4		
Directly after irradiation	407±12,0	128,0	5,6
After two days	350±3,5	112,0	3,1
After one year	294±4,1	99,6	—

In a field experiment in the Moscow region, the results of storage of seeds of irradiated corn were compared (Table 2).

In the case of planting directly after irradiation, the maximum additional yield of green mass was obtained; after two days the effect of stimulation was reduced, while in the case of planting of irradiated seeds after a year, there was no stimulating effect.

Analogous data were obtained in the growth of tomatoes under conditions of hydroponics. In the case of planting of irradiated seeds directly after irradiation, the height of the seedlings exceeded the control by 20.5%, while after 14 days this gain was reduced to 6%.

A study of the effects of storage on a wider assortment of agricultural plants showed that it is specific for various crops. For corn, sunflower, and tomatoes, the best indices were obtained when the irradiated seeds were planted immediately after irradiation, while in wheat, on the contrary, to obtain the optimum results it was necessary to expose the irradiated seeds before planting. In experiments of the Scientific-Research Institute of Agriculture of the Georgian SSR [5], it was shown that the storage of irradiated seeds for a month after irradiation lowered the yield of grain of corn and increased the yield of wheat of the Bezostaya 1 variety up to 33.5%.

The data obtained indicate a strong modifying effect of storage of irradiated seeds, which under definite conditions may induce various degrees of reduction of the yield instead of stimulation. The study of the effect of storage for a wide assortment of agricultural plants is one of the most urgent problems in the utilization of preplanting irradiation of seeds in practice.

One of the factors that changes the biological effect of doses is the dose rate of irradiation. In the case of irradiation of corn seeds of the Sterling variety with a source of γ radiation from ^{60}Co with a dose of 13 kR with sharply different dose rates (600 and 4.6 R/min), pronounced differences were observed; low dose rates of irradiation had a stronger inhibiting effect than high ones.

In determining the values of the optimum stimulating doses for various crops, it is quite essential to indicate the dose rate of irradiation.

In the case of planting of irradiated seeds in various soil-climatic zones, variations of the optimum stimulating doses were established. Thus, when irradiated corn seeds were planted in the Moscow, Gor'kii, and Leningrad regions, the Latvian and Moldavian SSR, the optimum stimulating dose for the Sterling variety was 500 R. On the Apsheronsk penninsula, stimulation arose at a higher dose of irradiation of the corn seed – 4 kR.

The stimulating dose for cucumbers in the middle belt is 300-500 R. In the Kirgiz and Azerbaidzhan SSR, with different temperature and light conditions and with a high level of insolation and natural radioactivity of the soils (Kirgiz SSR), the optimum stimulating dose is 10 kR.

Among the modifying factors we should also include the degree of maturity of the irradiated seeds, since this factor changes their radiosensitivity. Planting sunflower seeds from immature yellow and brown calathides, an inhibition of the seedlings of 10-15% in comparison with the control was observed; ripened seeds served as the control.

Finally, we should take up still another modifying factor, which has an effect on the change in the radiosensitivity and depends on the time of year. The effects of stimulating and inhibiting doses, established in the winter months, are not repeated in summer experiments. Assuming that these changes are a consequence of the different light and temperature conditions, an experiment was conducted, planting a number of oil crops – castor oil, soybean, and sunflower – under conditions of luminostat, monthly for a year with irradiation at a dose of 40 kR; the temperature and light conditions were maintained at the same level. The criterion for evaluating the effects of irradiation according to months was a measurement of the height of the plant after 20 days of vegetation (Fig. 3). In Fig. 3 it is distinctly evident that the same dose of 40 kR has an appreciable inhibiting effect during the winter months, and that the injurious effect of the same dose is weakened in the spring to summer months. These valuable data indicate the necessity of conducting initial determinations of the optimum stimulating doses of irradiation, considering the seasons of

Fig. 4. General view of the Kolos mobile commercial γ apparatus.

TABLE 3. Comparative Study of the Effects of the Radiation of ^{60}Co and ^{137}Cs on the Growth, Commercial Properties, Shifts of Phases of Development, and Yield of Cabbage of the Slava Variety

Variations of experiment	Yield of commercial planting, % of control	Phases of development, % of control			Yield, % of control
		without heads	with underdeveloped heads	formed heads	
Irradiation: ^{60}Co, E_γ = 1,33; 1,17 MeV, dose 2000 R	100	56,5	26,5	17,0	100
^{137}Cs, E_γ = 0,66 MeV, dose 2000 R	154	12,5	38,0	49,5	120
	172	7,5	34,0	38,5	121

the year, and of introducing only those doses that have been established or verified during the spring and summer months into field experiments and commercial tests.

Finally, experiments on the comparative evaluation of the biological effects of radiations with various energies were of vital importance.

Field experiments in the Moscow region with head cabbage [7] showed that there are essentially no differences between the effects of γ irradiation with energies 1.25 and 0.66 MeV (Table 3).

Thus, a study of modifying factors showed the necessity of a multi-faceted consideration of the conditions accompanying irradiation, which permit stable gains in yield to be obtained.

In 1958-1960, the GUPOS Experimental Gamma Apparatus was designed [17], with an output of 20 kg/h, with the aid of which a large number of laboratory and field experiments on the preplanting irradiation of seeds has been conducted. In the USSR in 1966-1967, the first Kolos γ apparatus in world practice was developed [18, 19], designed for the preplanting irradiation of seeds of grain, grain-pod, technical, and other crops in the collective forms, mounted on the chassis of a ZIL-131 truck (Fig. 4).

The setup consists of a unit for irradiation of seeds, an electric feed system, devices for conveying the seeds to irradiation, and control systems. Before the beginning of the work, the seeds are poured into the receiving dosing hopper (Fig. 5), from which the seed is delivered by a bucket conveyor to the hopper of the irradiation unit. In the irradiation unit an irradiator of ^{137}Cs sources with a total activity of 3500 Ci is mounted, which permits the treatment of about one ton of seeds per hour at a dose of 750-1000 R. The seeds pass in a continuous stream through the working chamber and are sent to a collecting conveyor belt, which delivers them to the hopper for treated seeds. The required dose can be varied from 200 to 5000 R by regulating the rate of flow. All the systems and devices of the setup are accommodated in the heated body of the truck with openings for the delivery of electricity from the external network of the container of the loading hopper, etc. The setup has an autonomous electric power plant for work under field conditions. Feed from an outside source of alternating current with voltages 220 and 380 V is possible; the power consumed is 1 kW. The setup is serviced by one driver and two operators. The shielding of the installation ensures a dose rate of γ irradiation of no more than 0.28 mR/h at the surface of the body.

TABLE 4. Results of Production Tests of Preplanting Irradiation of Agricultural Crops in the Moldavian SSR in 1972

Crops	Area		Yield		Additional yield		Gross additional yield, centners	Total monetary profit, rubles
	planted with irradiated seeds, hectares	control plantings (nonirradiated seeds), hectares	from area planted with irradiated seeds, centners/hectare	from control plantings, centners/hectare	centners/hectare	% of control		
Corn								
for grain	7454	6521	41,8	37,6	4,2	11,2	20300	131950
for silage	560	295	270,4	202,7	67,7	33,4	29300	26077
Sunflower	4864	5060	19,8	17,6	2,2	12,5	10109	161744
Sugarbeet	717	920	412,3	384,8	27,5	7,1	23811	69052
Total	13595	12796						388823
Introducing (planting without control)								
Corn								
for grain	5291	—	—	—	4,2*	11,2	22222	144443
for silage	970	—	—	—	67,7*	33,4	65669	58445
Sunflower	1646	—	—	—	2,2*	12,5	3621	57936
Sugarbeet	80	—	—	—	27,5*	7,1	2200	6380
Total	7987	—	—	—				267204

*The additional yields on the areas of introduction were taken from the results of production tests in the same year.

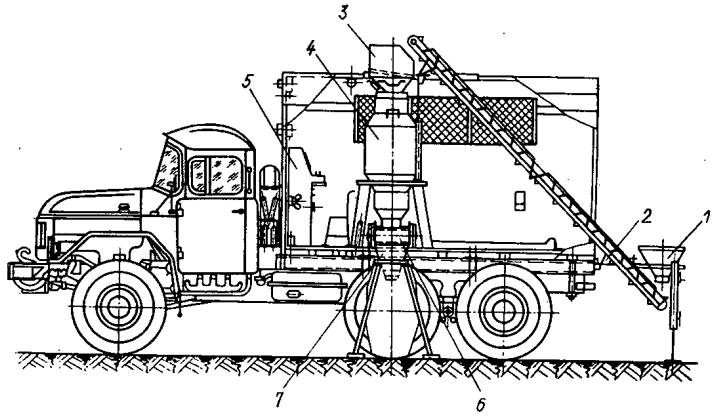

Fig. 5. Scheme of the Kolos mobile commercial apparatus: 1) receiving dosing hopper; 2) delivering transporter; 3) hopper of irradiation unit; 4) irradiation unit; 5) control panel; 6) collecting transporter; 7) hopper for treated seeds, under which a burlap container is fastened.

The Kolos setup is designed for the irradiation of dry flowing seeds (grain, legume, technical and other crops) with an average dry weight of the seeds 0.7 g/cm^3, moisture content 10-12%, and size of seed 5-15 mm. The total weight of the installation with the truck is 10.3 tons. According to the requirements of the All-Union Standards, the Kolos setup according to its weight parameters can be operated on all highways.

To determine the absorbed doses in the irradiation of seeds in a continuous flow, the method of thermoluminescence dosimetry is used [20, 21]. Five-year tests of a commercial Kolos γ setup have shown that it corresponds to the requirements of modern agricultural production and have permitted its recommendation for series manufacture [12].

A preliminary evaluation of the economic effectiveness of the use of the Kolos installation on the basis of the average values of the crop yield, cost of production, and additional yield have shown that the expenditures of the farms for the acquisition of the setups pay for themselves during the first season of their operation. Moreover, the expenditures for irradiation of the seeds per hectare for winter wheat, corn for grain and silage, sugarbeets and peas are 1.96, 0.09, 0.11, 0.06, and 0.84 rubles, respectively.

In 1968 28 tons of seeds of 15 different agricultural crops were irradiated in the Moldavian SSR and used to plant 760 hectares of field areas. In 1969, 47 tons of seeds were irradiated, and in 1970 102 tons, which were used to plant 1249 and 4000 hectares, respectively. The bulk of the plantings was taken up by corn. The average additional weight of the yield of grain for these years was 11.1, 8.1, and 13.3%, respectively, which shows the high effectiveness of the method of preplanting irradiation [23].

In 1971 and 1972, the tests and introduction, financed by the Ministry of Agriculture of the Moldavian SSR, were continued on a wider scale. In 1972, about 35 thousand hectares were involved in the experiment (with a control) (Table 4) [24]. The average weight gain of the yield of corn was 15.8%, in 1971 and 11.2% in 1972. The pure profit using the four Kolos installations was 547 thousand rubles.

In February 1973 the Scientific and Technical Council of the Ministry of Agriculture of the Moldavian SSR adopted a resolution on the wide introduction of preplanting irradiation of corn seeds and the expansion of production tests on the sugarbeet and sunflower.

Since 1970, the testing of the method of preplanting irradiation of seeds in the Pavlodar region, situated in an arid zone of the Kazakh SSR, with average annual atmospheric precipitation 226 mm, has been begun. The plantings with irradiated seeds in 1971 was conducted on an area of about 7000 hectares. Irradiated millet, buckwheat, sunflower, barley, and wheat seeds, and corn for silage, were planted. The additional yield for the crops ranged from 10 to 20%. The pure profit from the preplanting irradiation, using one Kolos installation, was 84 thousand rubles. In 1972 the area under production tests was about 20,000 hectares. Seeds of millet, wheat, sunflower, buckwheat, and corn for silage were irradiated. The additional yield (in % of the control) was 27, 10, 14, 17, and 16%, respectively [25], while the pure profit using two Kolos installations was 221,000 rubles. In 1972 the Regional Agricultural Administration resolved to introduce preplanting irradiation of seeds into practice. At the present time, the Pavlodar Regional Agricultural Administration has eight Kolos installations at its disposal.

In 1972-1972, broad production tests using a commercial Kolos γ installation were conducted in the Kirgiz SSR [26, 27]. The irradiation of corn seeds for grain increased the average yield of grain in the ears by 9.4 centners/hectare, and the silage mass by 64.5 centners/hectare, which, according to the data of the Kirgiz Scientific-Research Institute of Agriculture, yielded a supplementary profit of about 40 rubles per hectare. The Industrial and Technical Council of the Main Administration of Agriculture of the Ministry of Agriculture in 1973 recommended introduction of the preplanting irradiation of corn seeds.

The materials cited show that the first examples of the wide utilization of the achievements of radiobiology and atomic technology in agricultural practice are positive, and are an effective form of intensification of agricultural production.

LITERATURE CITED

1. L. P. Breslavets, The Plant and X-rays [in Russian], Izd-vo AN SSSR, Moscow–Leningrad (1946).
2. N. M. Berezina, Preplanting Irradiation of Seeds of Agricultural Plants [in Russian], Atomizdat, Moscow (1964).
3. Materials of the First Scientific and Practical Conference on the Use of Isotopes and Ionizing Radiations in Agriculture [in Russian], Kishinev (1970).
4. Summaries of Reports at the All-Union Conference on the Use of Radiation Technology in Agriculture [in Russian], Vols. 1 and 3, Kishinev (1972).
5. N. M. Berezina and F. A. Dedul', in: Transactions of the Georgian Scientific-Research Institute of Agriculture [in Russian], Vol. 25, Tbilisi (1968).
6. N. M. Berezina, [3], p. 5.
7. N. M. Berezina and R. R. Riza-zade, in: Preplanting Irradiation of Agricultural Crops [in Russian], Izd.-vo AN SSSR, Moscow (1963), pp. 194-198.
8. A. F. Revin and N. M. Berezina, Biologicheskie Nauki, No. 1, 54 (1971).
9. N. M. Berezina et al., Radiobiologiya, 11, No. 6, 332-337 (1971).
10. N. M. Berezina, in: Ionizing Radiations in Horticulture [in Russian], "Kuban," Krasnodar (1966), p. 138.
11. A. M. Kuzin, First Geneva Conference [in Russian], (1955), Report.
12. A. M. Kuzin, Radiobiologiya, 12, No. 5, 635 (1972).
13. A. M. Kuzin et al., Stimulation Newsletter, 4, 1-11 (1972).
14. A. T. Miller, [4], Vol. I, 38.
15. N. M. Berezina et al., Methodological Instructions for the Preplanting Gamma Irradiation of Seeds of Agricultural Plants [in Russian], Atomizdat, Moscow (1970).

16. N. M. Berezina et al., Methodological Instructions for the Preplanting Gamma Irradiation of Seeds of Agricultural Plants [in Russian], Kishinev (1972).
17. A. V. Bibegral' et al., Atomnaya Énergiya, 12, No. 2, 159 (1962).
18. D. A. Kaushanskii and B. G. Zhukov, Atomnaya Énergiya, 28, No. 4, 366 (1970).
19. D. A. Kaushanskii, [3], p. 19.
20. D. A. Kaushanskii and Li Don Khva, Atomnaya Énergiya, 30, No. 5, 479 (1971).
21. D. A. Kaushanskii and Li Don Khva, [4], Vol. 3, p. 112.
22. D. A. Kaushanskii and A. V. Antonovich, [4], Vol. 1, p. 17.
23. V. N. Dysikov et al., [3], p. 17.
24. G. Ya. Rud, V. N. Lysikov, and K. I. Sukach, Sel'skoe Khozyaistvo Moldavii, No. 3, 32 (1973).
25. Yu. A. Martem'yanov and A. V. Kalashnikov, [4], Vol. 1, p. 37.
26. A. S. Sultanbaev, [4], Vol. 3, p. 38.
27. L. A. Sergeeva, A. S. Sultanbaev, and A. N. Gulyaev, [4], Vol. 3, p. 144.

SPUTTERING OF MATTER BY FISSION FRAGMENTS

V. A. Bessonov

UDC 539.211:546.79

Metal-surface-sputtering regularities under the influence of charged particles are of interest for various branches of science and technology; they were considered in [1-3]. However, little research has been done on sputtering of uranium and other fissionable-material surfaces during nuclear fission and fragment yield into the surroundings. Knowing the laws of this phenomenon can be important, for example, in radiation chemistry when realizing radiation-chemical processes using fission-fragment kinetic energy [4, 5] and in some other branches, where thin layers of uranium-containing materials are used or where nuclear fuel is not enclosed in a special envelope.

There is still no perfected and rigorous theory concerning surface sputtering under the influence of fission fragments, but it has been established that the sputtering or ejection ratio K, which is defined as the number of fissionable-material atoms carried away by one fission fragment leaving the surface, is related to several experimental parameters. The present paper briefly considers the sputtering ratio's dependence on the emitter (fission fragment source) surface state. It is also shown how crystal structure and emitter-material properties influence the ratio K and how the sputtering ratio and integral neutron-irradiation dose are interrelated. An attempt is made to analyze the state of sputtered-material nuclei gathered at the collector and to delimit the probable ejection mechanism from these data.

F. S. Lapteva and B. V. Ershler [6] were the first to confirm experimentally the fissionable-material ejection phenomenon. They showed that on the order of a thousand uranium atoms may leave a pure polished ^{233}U or ^{239}Pu surface with one fission fragment. If the simple surface is covered with an oxide film, this value is on the average 24 atoms per fragment. B. Lastman [7], referring to [8], names a similar figure – 45 molecules of uranium dioxide per fission event in a surface layer with thickness equal to the recoil-atom mean free path.

The concepts of radiation-damage theory [9, 10] are used to explain surface-sputtering effects under the influence of fission fragments. Fissionable-material surface-layer sputtering can be explained by using the "thermal-peak" hypothesis [9-12] or the "displacement-peak" theory proposed by Brinkman [13-15]. Another explanation for ejection (sputtering) is based on the theory of atomic expulsion at the expense of recoil-atom energy; these atoms produce displacement cascades [9, 10]. Whaphan and Makin [16] believe damage may occur to a surface from which high-energy charged ions emerge at the expense of expelling larger particles. If we accept the proposition that there exists a high-temperature region along the fission-fragment motion trajectory, then in the "peak" region there arises instantaneously an explosive pressure. This may give rise to motion in the solid-state layers surrounding the track and lead to particle expulsion from the material surface layer. When the temperature in the "thermal-peak" region exceeds 10,000°C, one can expect particles larger than 40 Å to be ejected.

Lapteva and Ershler evaluated the applicability of the "thermal-peak" theory for explaining the phenomena observed and found that the experimentally determined quantities of vaporized uranium atoms require an expenditure up to 17% of the total fission-fragment kinetic energy; this much exceeds the theoretical value. Using Lapteva and Ershler's results and assuming the ejection ratio is 2000 and that, of all the possible "displacement-peak" formation variants, only peaks near the surface lead to material vaporization, S. T. Konobeevskii [9] calculated the "displacement-peak" length. The value he found – $2.7 \cdot 10^{-6}$ cm – agrees well with other evaluations of this quantity.

Translated from Atomnaya Énergiya, Vol. 37, No. 1, pp. 52-56, July, 1974. Original article submitted December 7, 1972; revision submitted December 6, 1973.

Since the fission fragments carry uranium from the uppermost thin layer of material, many researchers have tried to pursue the relationship between the sputtering ratio and this layer's properties. As we noted already, it was shown in [6] that purifying the emitter surface from oxide film increases the ejection capability, raising K from 24 to thousands of atoms. Rogers and Adam [17] confirmed this result and also showed the dependence between the sputtering ratio and the emitter integral irradiation dose by neutrons. Peterson and Thorpe [18] studied the effect of the oxide film at the sample surface on sputtering. The authors observed increased uranium-ejection rate when there is additional emitter oxidation by moist helium during irradiation. A relationship between ejection rate and irradiation dose was also discovered. It was established that during irradiation in air in the presence of moisture and oxygen, the emitter surface properties can change due to chemical reactions. This confirms the data on surface-property and K-magnitude variation due to interaction between the emitter and reactive gases or air [19, 21, 22]. The emitter surface may also be acted on by radiolysis products which accumulate in the evacuated vessel during irradiation. The experimental material allowed Nilsson [19, 20] to conclude that emitter-surface grinding and the degree of polishing do not significantly change the uranium dioxide sputtering ratio. Increasing the oxygen concentration in the vessel, on the contrary, is accompanied by its increase. Nilsson also found that matter ejection from metallic uranium with an unoxidized surface, or, rather, a surface whose oxide film is thinner than 160 Å, is noticeably higher than from the same sample whose surface had undergone more prolonged oxidation. Nilsson's data disagree with those in [23], which studied matter vaporization in targets prepared using ^{244}Cm salts. It was shown in [21, 23] that when targets having layer thickness in the order of 10^{-6} cm are used, the fraction of sputtered atoms increases due to fission fragments passing parallel to the target surface. In a vacuum, the rate of atom sputtering from a target decreased much more slowly than in air; this was related to the change in microrelief and its properties when fission fragments act on the surface in air and when the samples are evacuated. The disagreement with Nilsson's data [Nilsson did not observe the surface-relief effect (various degrees of polishing) [19] on the sputtering factor] can be explained by the insignificance of the contribution from fission fragments, which pass parallel to the emitter surface in his experiments, to the total uranium-atom-ejection effect due to fission fragments.

V. K. Gorshkov and L. N. L'vov [23] confirm the thermal-vaporization model for emitter material acted on by fission fragments and alpha particles; they estimate the "crater" size at sites from which fission fragments are emitted to the material surface. However, because the sputtered layers are different in nature, it is hardly possible to compare rigorously the results given in [21, 23] with those obtained on metallic surfaces.

In work with short-lived spontaneously decaying targets based on ^{252}Cf oxides, a dependence between the ejection ratio and the source thicknesses was observed [24, 25]. Thus, in [24], changing the Cf-oxide layer thickness from 0.2 to 8 $\mu g/cm^2$ caused K to increase from 50 to 3800. A similar ejection ratio with initial increase in emitter thickness was obtained qualitatively in [23]. If the layer thickness from which ejection occurs is comparable to the depth of the "crater" left in the surface by the emitted fragment, then the magnitude of K depends on the emitter thickness.

There is not yet a single opinion concerning "crater" formation on the emitter surface after fission fragments are emitted. Suppositions concerning "crater" existence are expressed in [6, 23]. Zimen and Mertens [26] observed "crater" funnels at fission-fragment emission sites on the surface. Riehl [27], in studying gold samples irradiated by fission fragments, could not find such "craters," but he expressed the hypothesis that there exists a possible damage region around the site from which the fragment leaves the material. Concluding our consideration of whether "craters" really exist at fission-fragment exit sites to the surface, we should say that the published data are too scanty to support a final conclusion. The "craters" observed by several authors in materials with ionic bonding (in particular, in curium salts and uranium dioxide) and their absence on a metallic surface (gold) can be due to the character of absorption and energy transport in various materials from a high-energy charged particle (which is what a fission fragment is) to kernels of a crystal subjected to irradiation..

The results of electron-microscopic research on fission-fragment traces in thin layers indirectly confirms this. It has been shown [9, 12, 28, 29] that visible tracks form where the fissionable-material layer consists of very small crystallites in which yielded energy may be localized. The tracks disappear as the crystallite dimensions increase. It has been established [30] that the track width depends on the fission-fragment mass and the physical characteristics of the material in which deceleration occurs. The finest tracks were observed in carbon. These data together with observations on the effect of sputtered-material structure and nature on the ejection ratio (using ^{239}Pu compounds as a model, a relationship was

TABLE 1. Dependence of Sputtering Ratio on Emitter Properties and Irradiation Conditions

Pellet-preparation method	Average grain size, μ	Integral dose with respect to thermal neutron	Sputtering ratio		Reference
			K_N	$K_{steady-state}$	
Vacuum deposition; air oxidation to UO_2; film thickness up to 400 Å	0,05	$<10^{16}$	$5\cdot10^4$		[33]
		$>5\cdot10^{16}$		30	
UO_2 sintering	10	$<10^{16}$	110		
		$>5\cdot10^{16}$		4,5	[34]
UO_2 sintering; annealing at 1000°C in hydrogen atmosphere	7—8	$8\cdot10^{17}$		9	[19]
UO_2 deposition	<0,2	$<10^{15}$	2800		
		$>10^{15}$		38,5	[18]
UO_2 sintering		$8\cdot10^{18}$		70	[32]

established in [24] between the ejection ratio and the sputtered-element compound type) allow one to formulate a hypothesis concerning a possible relationship between the ejection process and the nature of the chemical bond. Kaminskii [1] and Pleshivtsev [2] studied the relationship between sputtering efficiency and crystal-axis orientation with respect to accelerated ions incident on the surface. A Soviet group [31] confirmed experimentally and theoretically justified this effect, as applied to large-crystal-uranium sputtering when bombarded by argon ions. Further study is needed concerning the effect of the material's nature (metal or nonmetal) on "crater" formation and ejection ratio.

Since none of the authors gave special proof that oxide film was absent from the uranium surface studied, the divergence noted in K values for a nominally unoxidized surface (Lapteva and Ershler: 1200; Rogers: 1000; Nilsson; 43; Gautsch and Ruedl: 34 [32]), can be ascribed in part to indeterminacy with respect to the emitter-surface states. Thus, information concerning physical properties and surface state for sputtered materials is very important for explaining experimental results obtained in studying ejection. Therefore, experimental studies on ejection from uranium-dioxide pellets having known crystal structure and composition are of interest. Table 1 shows results of these studies. It is clear that even with identical composition for a material whose surface properties depend little on short-term contact with air, various authors found significant divergences in the ejection ratio. The cause for these differences is apparently in the different grain sizes for sample crystals. It was shown in [35] that uranium emission from a collector used as an emitter in secondary emission, occurs at much greater rates. Since uranium on the collector, according to electron-microscopic studies of deposits on carbon collectors [36, 37], forms clusters, "spots" several tens of angstroms in size, the passage of high-energy particles through such clusters may completely vaporize them. Rogers [33], using the "thermal peak," explains in this way the vaporization of UO_2 grains smaller than 90 Å which are hit by fission fragments. Describing ejection as an instantaneous-metal-crystallite vaporization process under conditions formulated in studies of track formation in thin films (see, for example, [9, 12, 37, 38]), requires, in particular, that there exists between crystallites in the sample a boundary resistance which worsens the conditions for electron-excitation dissipation into the volume. On the other hand, one cannot raise the crystal-lattice temperature at the expense of fission-fragment energy higher than 100°C [39]. If the sample consists of large grains, while the energy absorbed by them during fragment passage is insufficient to completely vaporize them, then material ejection must, apparently, decrease noticeably. In this case, uranium may be carried off due to only the process of expelling atoms from the upper layers at the expense of recoil atoms. This is how Rogers [34] and Nilsson [19, 20] explain the low values for sputtering ratio from UO_2 sintered samples. Atom expulsion from the UO_2 surface by fission fragments due to cascade collisions is confirmed by experiment and calculations in [26]. Thus, starting by representing the ejection process as a complex phenomenon dependent on emitter crystal structure and its surface properties and composition, one can explain the sputtering-ratio variation with increased irradiation dose: as the fraction of small crystallites is depleted in the sample structure, a transition occurs, from ejection of crystals having subcritical size by the "vaporization" mechanism to expulsion from the surface layer due to recoil. Nilsson's experiments [20] used UO_2 samples which had been treated for 4.5 h at 1000°C in a hydrogen atmosphere. This could lead to increased emitter-crystallite dimensions and, according to the concepts developed above concerning the effect of crystallite size on the ejection ratio, it could decrease the sputtering effect even at initial sample-irradiation stages; this was, in fact, observed. Also observed was change in the uranium crystallite dimensions from 50 to 180 Å after irradiation up to integral dose $2.5\cdot10^{17}$ neutrons $\cdot$ cm^{-2} [33].

When the number of vaporized-material nuclei on the collector increases, the probability increases that uranium atoms will be expelled from this layer due to fission fragments which arise in it and fission fragments which arrive from the emitter. This process, called reejection, establishes a certain steady-state quantity of matter on the collector. Therefore, as the integral irradiation dose increases, the value of the ejection ratio decreases. According to data in [17], the reejection factor begins to play a noticeable role with integral fluxes with respect to thermal neutrons equal to 10^{15} neutrons/cm^2. Its effect may be decreased by changing the ratio of emitter to collector surfaces. Unfortunately, there are now no experimental findings which explain how reejection and emitter-surface crystallite size affect the sputtering ratio.

Electron-microscopic research data on deposits gathered by the collector do not now allow us to formulate exactly in what form the uranium atoms are first fixed by the collector surface. Most studies show that not separate atoms, but conglomerates, are present on the collector. Verghese and Pasik [40] discovered that there are present on the collector, single atoms and atom accumulations which, when the collector is irradiated again, form defect accumulations, "clusters," on the collector. The existence of uranium-atom accumulations cannot be explained by expulsion theory, since, in this case, as shown by the calculations in [41], it is difficult to expel atoms from the third or deeper crystal-lattice layers. Neither does the "vaporization" model lead to accumulation formation. One should either assume an explosive surface damage mechanism under the conditions formulated in [16] or recognize the possibility of atom migration and coalescence at the surface during irradiation. The latter is supported by experiments [22] on varying the UO_2 film state during irradiation, and also by studies on "inlet" migration for some heavy metals on carbon and silicon-oxide surfaces during prolonged heating in a high vacuum [42]. Electron-microscopic studies on uranium expelled from an emitter and deposited on a carbon-collector surface, support, in some experiments [36] the hypothesis concerning "islet" migration and agglomeration into large fragments.

It is, apparently, too early to draw final conclusions on the particle form in which material sputtered by fission fragments leaves the emitter surface. The observed particle size and composition [32-36] allow one to affirm that their state is determined by many factors, among which emitter-material chemical composition and its crystalline structure, the collector-surface nature, the integral irradiation dose, and the gas pressure and composition in the capsule, may be significant. The ejection of material may in some cases be decreased significantly by forming the fissionable-material surface from the largest possible crystallites. Another possible way to decrease the ejection ratio is related to using inert coatings whose composition and thickness are chosen such that the greatest shielding effect is assured with minimal thickness. Gold, nickel, and carbon have been used for such coatings [32, 33]. An amorphous-carbon layer, 200 Å thick, deposited on an emitter surface made of uranium, its oxide, or carbide, completely excludes emitter-material atom ejection. Using rather thick (up to 1.9 μ) gold coatings did not completely exclude ejection, and reproducibility was poor. Using nickel films 0.4-0.5 μ thick, completely stopped fissionable-material vaporization.

We are just beginning to study the phenomena observed in studying ejection for emitters coated by shielding layers. However, we can already say that the shielding film's decelerating power and its atomic composition can have a significant effect on atom-expulsion processes. It is known, for example [43], that a material's ability to form visible tracks when heavy charged particles pass through it depends on a critical energy-loss quantity $(dE/dx)_{cr}$, characteristic for every substance, and which, in turn, depends on several physical characteristics of the material. Several papers [1, 2] have established relationships among bombarding-particle energy, energy and number of vaporized atoms, their position on the particle table, and the target-atoms heat of sublimation. Garber et al. [44] confirmed that monocrystalline materials are more subject to damage when acted on by fission fragments, than polycrystals of the same metals. This conclusion seems to need additional checking. Little research [24, 25] has been done on the effect of emitter electrical potential on ejection and the sputtered-material nuclear charge.

In conclusion, we must say that by changing crystalline properties and coating composition, and the crystalline structure and physicochemical properties of a fissionable-material surface and its nature, one can regulate damage processes in thin fuel elements and heavy-particle sources.

LITERATURE CITED

1. M. Kaminskii, Atomic and Ionic Collisions on a Metal Surface [in Russian], Mir, Moscow (1967).
2. N. V. Pleshivtsev, Cathode Sputtering [in Russian], Atomizdat, Moscow (1968).

3. G. Garter et al., Rad. Res. Rev., 3, No. 1, 1 (1971).
4. M. Steinberg, Adv. Nucl. Sci. Tech., 1, 247 (1962).
5. V. I. Gol'danskii et al., Isotopy v SSSR, No. 12, 7 (1968).
6. F. S. Lapteva and B. V. Ershler, At. Énerg., No. 4, 63 (1956).
7. B. Lastman, Radiation Phenomena in Uranium Dioxide [in Russian], Atomizdat, Moscow (1964), p. 105.
8. W. Lewis, DM-58 (1960).
9. S. T. Konobeevskii, Effect of Radiation on Materials [in Russian], Atomizdat, Moscow (1967).
10. M. Thompson, Defects and Radiation Damage in Metals [Russian translation], Mir, Moscow (1971), p. 242.
11. F. Seitz, Disc. Faraday Soc., 5, 271 (1949).
12. A. Goland, Studies in Radiation Effects, Ser. A, Phys. and Chem., 1, 159 (1966).
13. J. Brinkman, J. Appl. Phys., 25, 961 (1954).
14. J. Brinkman, Amer. J. Phys., 24, 246 (1956).
15. J. Brinkman, Rep. NAA-SR-6642 (1962).
16. A. Whaphan and M. Makin, Phil. Mag., 7, No. 81, 1441 (1962).
17. N. Rogers and J. Adam, J. Nucl. Mater., 16, 182 (1962).
18. P. Peterson and M. Thorpe, Nucl. Sci. and Eng., 29, 425 (1967).
19. G. Nilsson, J. Nucl. Mater., 20, 215 (1966).
20. G. Nilsson, J. Nucl. Mater., 20, 231 (1966).
21. V. K. Gorshkov, L. N. L'vov, and P. A. Petrov, At. Énerg., 22, No. 1, 24 (1967).
22. T. Bierlein and B. Mastel, J. Appl. Phys., 31, 2314 (1960).
23. V. K. Gorshkov and L. N. L'vov, At. Énerg., 20. No. 4, 327 (1966).
24. B. M. Aleksandrov et al., At. Énerg., 33, No. 4, 821 (1972).
25. S. Pauker and N. Steiger-Shafrir, Nucl. Instr. and Meth., 91, No. 4, 557 (1971).
26. K. Zimen and P. Mertens, Z. Naturforsch., 26a, 773 (1971).
27. N. Riehl, Kerntechnik, 3, 618 (1961).
28. J. Kelsch et al., J. Appl. Phys., 33, 1475 (1962).
29. E. Ruedl, P. Delavignette, and S. Amelinckx, J. Nucl. Mater., 6, 46 (1962).
30. N. Pravdyuk and V. Golyanov, in: Proc. Intern. Conf. on Properties of Reactor Materials and Effects of Radiation Damage, Leningrad (1962), p. 160.
31. Yu. Sokurski et al., J. Nucl. Mater., 9, 59 (1963).
32. O. Gautsch and E. Ruedl, J. Nucl. Mater., 32, 290 (1969).
33. M. Rogers, J. Nucl. Mater., 16, 298 (1965).
34. M. Rogers, J. Nucl. Mater., 22, 103 (1967).
35. M. Rogers, J. Nucl. Mater., 12, 332 (1964).
36. T. Bierlein and B. Mastel, J. Nucl. Mater., 7, 32 (1962).
37. M. Rogers, J. Nucl. Mater., 15, 65 (1965).
38. A. Goland and A. Paskin, J. Appl. Phys., 35, 2188 (1964).
39. I. M. Lifshits, M. I. Kaganov, and L. V. Tanatarov, At. Énerg., 6, No. 4, 391 (1959).
40. K. Verghese and R. Pasik, J. Appl. Phys., 40, 1976 (1969).
41. N. S. Bespalova and A. G. Gurvich, Dokl. AN SSSR, 202, No. 4, 804 (1972).
42. W. Phillips, J. Appl. Phys., 39, 3210 (1968).
43. R. Fleischer et al., Phys. Rev., 133, Al 443 (1964); J. Appl. Phys., 36, 3645 (1965).
44. R. I. Garber et al., At. Énerg., 28, No. 5, 406 (1970).

ELECTRICAL CONDUCTIVITY OF A MULLITE-CORUNDUM CERAMIC AT ELEVATED TEMPERATURES DURING IRRADIATION

U. G. Gulyamov, N. S. Kostyukov, and A. P. Sokolov*

UDC 621.315.61

Because of the widespread application of ceramic materials in nuclear technology, reliable data relating to their radiation stability are essential, in particular, data about changes of their electrical properties under the action of radiation.

In this present paper, the relation was investigated between the electrical conductivity of a mullite–corundum ceramic (MG-2), irradiated in the VVR-SM reactor at a neutron flux of $1.3 \cdot 10^{13}$ n/cm$^2 \cdot$ sec, and the temperature (over the range 100-600°C), intensity and duration of the reactor radiation.

The measurement results of the electrical conductivity $\sigma_{n\gamma}$ for a constant intensity of the reactor radiation are described by the equation $\sigma_{n\gamma} = 1.6 \cdot 10^{-9} e^{-0.17/kT} + 6.3 \cdot 10^{-2} e^{-0.92/kT} + 10^{3} e^{-1.82/kT}$.

It is shown that as a result of irradiation in the temperature range up to 200°C, the electrical conductivity of MG-2 increases by a factor of 100-1000. This is due to the presence in MG-2 of boron, which has a high interaction cross-section with neutrons and which leads to an increase of conductivity not only because of the γ-components of the reactor radiation, but also owing to the neutron component. A significant change of behavior of the $\log \rho - 1/T$ curves in the low temperature region, obviously confirms the change of conductivity mechanism under the action of radiation.

The dependence of the electrical conductivity of MG-2 on the intensity of the reactor radiation at temperatures below 227°C is of an exponential nature, but at higher temperatures it is a power dependence.

ANALYTICAL CALCULATION OF THE RANGE OF IONS AND THE PARTIAL LOSS OF ENERGY DURING RETARDATION

A. P. Balashov†

UDC 539.101

In order to solve the wide class of problems associated with the calculation of the ranges of ions and the formation of structural defects and electron-hole pairs in dielectrics under the action of radiation, it is necessary to take into account the distribution of energy contributed between ionization and excitation

*Translated from Atomnaya Énergiya, Vol. 37, No. 1, pp. 57-61, July, 1974. Original article submitted April 25, 1972.

†Original article submitted May 28, 1973; abstract submitted January 3, 1974.

processes of atomic electrons and elastic interaction processes with atomic nuclei, leading to the displacement of atoms and faulting of the material structure. A calculation of the specific energy losses of heavy charged particles with energies less than 1 MeV, by a nucleon, can be carried out within the framework of the Lindhard–Scharff model; however, the application of the model to the solution of this type of problem is made difficult by the absence of an analytical representation of the ranges and of the partial energy losses.

In this paper, based on the Lindhard–Scharff model, easily derived expressions are obtained for the total ranges of heavy charged particles and for the magnitude of the energy lost during retardation in elastic interaction events with the atoms of the medium. For simplification, the dimensionless representation of the energy ε and the range ρ is used.* For an ion with an initial energy in the range $\varepsilon_{i-1} < \varepsilon \leq \varepsilon_i$ (i = 1, 2, 3), the energy transferred to the atomic subsystem during retardation, $g(\varepsilon)$, is determined by the expression

$$g_i(\varepsilon) = f_i(\varepsilon) + \delta_i,$$

where

$$f_i(\varepsilon) = \frac{a_i}{K} \ln \frac{\lambda_i^2 + \varepsilon}{\lambda_i^2 + \varepsilon_{i-1}}; \quad \lambda_i^2 = \frac{a_i}{K} + b_i$$

and

$$\delta_i \equiv g_{i-1}(\varepsilon_{i-1}) = \sum_{j=0}^{i-1} f_j(\varepsilon_j)$$

[Here $g(\varepsilon)$ is the energy transferred to the atomic subsystem in dimensionless units; K is the electron retardation parameter; a_i, b_i and ε_i are constants.]

For the region $\varepsilon > \varepsilon_3$:

$$g(\varepsilon) = \frac{1}{K}\left[0.94 - \frac{2 + \ln 1.294\varepsilon}{\varepsilon^{1/2}}\right] + \sum_{j=0}^{3} f_j(\varepsilon_j).$$

The expression for the range of heavy particles in an atmospheric medium, taking into account the concurrence of excitation processes of the electron subsystem and interaction with atoms of the medium, can be represented in the form

$$\rho = \frac{2}{K}\varepsilon^{1/2} - \Delta(K_i\varepsilon).$$

The first term of the expression corresponds to the case of purely electron retardation, and the second term carries a correction which takes account of retardation due to the transfer of energy to the atomic subsystem. $\Delta(K_i\varepsilon)$ for a particle with energy in the range $\varepsilon_{i-1} < \varepsilon \leq \varepsilon_i$ has the form

$$\Delta_i(K_i\varepsilon) = \frac{2a_i}{K^2\lambda_i} \operatorname{arctg} \frac{(\varepsilon^{1/2} - \varepsilon_{i-1}^{1/2})}{\lambda_i^2 + (\varepsilon\varepsilon_{i-1})^{1/2}} + \Delta_{i-1}(K_i\varepsilon_{i-1}).$$

The expressions obtained are applicable for an arbitrary combination of particle-medium over a wide range of energies. The error of these expressions, in comparison with the results of numerical calculations, does not exceed 3 to 5%.

*J. Lindhard and M. Scharff, Phys. Rev., 124, 128 (1961).

DESTRUCTIVE EFFECT OF HYDROGEN ON THE CLADDING DURING REPROCESSING OF THE FUEL ELEMENTS OF A WATER-COOLED /WATER-MODERATED POWER REACTOR

A. T. Ageenkov and V. F. Savel'ev

UDC 621.039.54

The results are given of investigations into the destructive action of hydrogen on the zirconium alloy cladding during fuel element reprocessing. It is shown that the accelerated interaction of the alloys with hydrogen begins at 600°C; at a temperature of 700-800°C, the hydrogen content in the alloy approaches the limiting value during one hour: 1.7 to 2.0 wt.%. Absorption of hydrogen by tubular claddings is accompanied by an increase of their size (Fig. 1). In physico-chemical properties, the material of composition $ZrH_{1.8-2.0}$ is characterized by a low mechanical strength ($\sigma_b < 10$ kg/mm^2), brittleness and shortness; a high microhardness (300-310 kg/mm^2), low wearability and stability in oxygen and air up to a temperature of 700°C. The structure of the hydrogen-containing alloy has been studied by an autoradiographic method (Fig. 2).

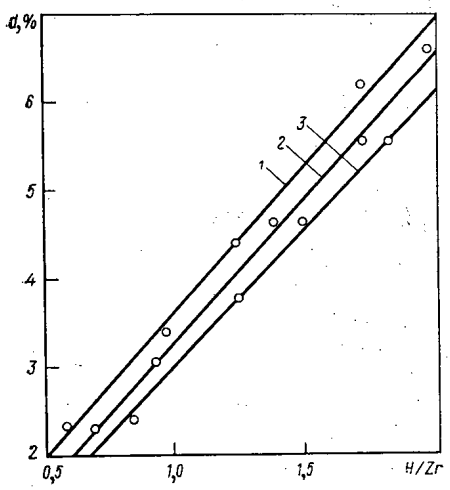

Fig. 1

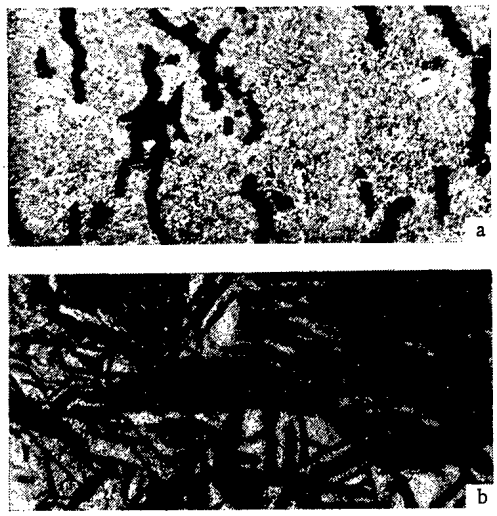

Fig. 2

Fig. 1. Dependence of increase of cladding diameter d on the hydrogen content in the alloy: 1) Alloy Zr—1% Nb; 2) alloy Zr—2.5% Nb; 3) alloy Zr—0.6% Fe—0.6% Ni.

Fig. 2. Autoradiographs of the hydrogen-containing alloy Zr—1% Nb (×200): a) hydrogen content 0.016 wt. %, hydrides take the form of individual disconnected inclusions; b) hydrogen content 1.2 wt.%, hydride phase spread throughout the whole alloy structure.

Original article submitted June 28, 1972; revision submitted December 28, 1973.

LINEAR PERTURBATION THEORY FOR FUEL BURNUP PROBLEMS IN A FAST REACTOR

V. V. Khromov, A. A. Kashutin and V. B. Glebov*

UDC 539.125.5.162.5:621.039.526

A method is presented for fast-reactor optimization calculations, taking account of the changes in reactor characteristics during operation.

Equations for the importance functions and formulas for small perturbations are derived from a variational principle [1, 2]. These formulas permit an estimate of the perturbation of various functionals of the neutron distribution and the neutron flux at any time t due to changes in reactor characteristics (composition, reactivity compensation parameters) at a time $t_0 \leq t$.

These estimates are performed rapidly by using polynomial approximations of the time behavior of the neutron flux and importance functions [3]. The time dependence of various reactor characteristics can be approximated as exactly as desired. The spatial dependence of the solutions is described by the Bubnov–Galerkin method, using a set of coordinate functions to take account of the specific nature of the problem being studied [4].

The calculation is programmed in FORTRAN for a BÉSM-6 computer. The program is designed for fast-reactor optimization calculations in the multigroup diffusion approximation for one-dimensional geometry. The burnup processes are analyzed for the average change in isotopic composition within the boundaries of the reactor zones. The program permits the study of the effect of isotopic composition and reactivity controls on the time behavior of the neutron distribution. The method is illustrated by examples of calculations for large fast reactors. An analysis of the results shows that the method makes efficient use of machine time and memory, and gives results which are accurate enough for optimization calculations.

LITERATURE CITED

1. G. Pomraning, J. Math. Phys., 8, 149 (1967).
2. G. Pomraning, Nucl. Sci. and Engng., 29, 220 (1967).
3. I. S. Akimov and E. I. Grishanin, Atomnaya Énergiya, 16, 500 (1964).
4. V. V. Khromov, A. A. Kashutin, and V. B. Glebov, Atomnaya Énergiya, 36, 385 (1974).

^{40}K GAMMA DISTRIBUTION AT THE OCEAN–ATMOSPHERE BOUNDARY

A. S. Vinogradov, K. G. Vinogradova, and B. A. Nelepo†

UDC 551.463:539.1

Measurements of the gamma activity of sea water and the atmospheric layer near the surface of the ocean require detailed information on the ^{40}K gamma distribution which determines the main part of the background radiation in the water, and a significant part of it in the atmosphere near the water surface.

*Original article submitted July 10, 1973.
†Original article submitted July 16, 1973.

The differential spectra and integral fluxes of primary and scattered ^{40}K gamma radiation have been calculated by the Monte Carlo method for a lower half-space filled with water of salinity and composition corresponding to the average for sea water, and the upper half-space occupied by a uniform atmosphere of a perfectly black absorber. The calculations were performed by random sampling using analytic averaging of absorption and the collision density method. The energy intervals in the differential spectra were 10 keV wide.

The effect of the surface on the flux in water appeared more strongly in the flux directed downward from the surface. The flux toward the ocean surface was larger at all levels, and for energies above 500 keV did not depend on the distance from the surface. The flux of scattered radiation reflected from the atmosphere was zero for energies above 800 keV. At a depth of 10 mfp the spectra of scattered radiation were in good agreement with results obtained by solving the kinetic equation for an infinite uniform medium [A. S. Vinogradov, Studies in Oceanic Physics [in Russian], MGI AN UkrSSR, Sevastopol (1969). p. 106].

In the atmosphere the gamma flux directed from the ocean surface is larger. The flux toward the ocean surface vanishes for energies above 600-800 keV, depending on the distance from the surface.

The surface affects the direct measurements of the ^{40}K gamma distribution in the ocean only up to a depth of about 2 m. In measurements of the gamma activity in atmospheric layers near the water the height of the detector above the ocean surface must be taken into account since the ^{40}K gamma distribution varies appreciably with height.

THE DEVELOPMENT OF ACTIVITY GENERATORS FOR INDUSTRIAL RADIATION CIRCUITS WITH POWER-GENERATING CHANNEL-TYPE REACTORS

A. Kh. Breger, S. P. Dobrovol'skii,
E. L. Ivanter, V. S. Petrov,
N. I. Rybkin, A. M. Sidorov,
and Yu. I. Tokarev*

UDC 621.039.553.573

One of the most promising paths for the complex utilization of thermal neutron reactors [1] is the creation in them of radiation circuits, in which a nonfissionable working substance is activated by neutron leakage from the active zone and the γ-radiation produced by the radioactive isotopes is used for carrying out various radiation-chemical processes on an industrial scale [2, 3].

In the present paper, the results are discussed of design developments of one of the principal units of industrial radiation circuits – the activity generator – in power-generating reactors of the channel type (RBMK) used in nuclear power generation in the Soviet Union at the present-day stage [1].

The activity generators are installed in the third row of graphite blocks of the reflector, in channels with water designed for cooling the reflector, as a result of which the temperature of the working substance does not exceed 70°C. The construction of the activity generator is sectional-tubular. Each section consists of three U-shaped tubes, made in the form of a spiral coil.

The channels of the activity generator are joined by collectors for the supply and removal of the working substance (Fig. 1). For convenience of grouping of the collectors and of access to them, and also for

*Original article submitted July 23, 1973.

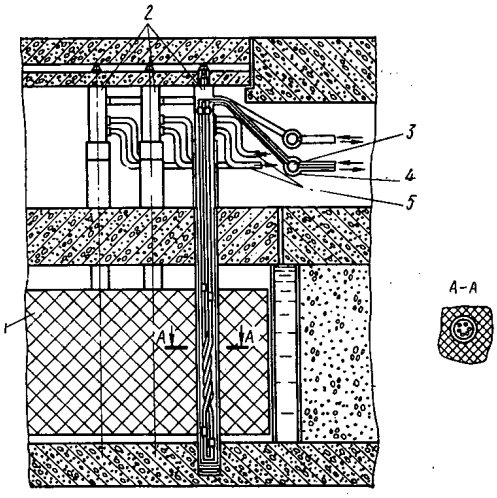

Fig. 1. Arrangement of activity generator channels in the reactor: 1) reflector; 2) activity generator channels; 3) alloy collector; 4) cooling water collector; 5) cooling channel piping.

the purpose of introducing the minimum changes into the design of the RBMK reactor, the activity generator section-channels (54 pieces) are arranged on approximately 1/3 of the perimeter of the active zone of the reactor. The disposition of an activity generator and its design, in the case of necessity, permits individual channels to be disconnected without stopping the power generation of the reactor. The total independence of the radiation circuit is ensured also by the presence of an intrinsic water cooling system of the activity generator channels, separate from the overall system, for cooling the graphite masonry of the reflector.

The physical calculations of the activity generator, with the working substance in the form of a liquid metal indium–gallium alloy of eutectic composition, carried out on a computer showed that the installation of this type of generator in the reactor leads to a reduction of the burnup of the fuel by not more than 1%. The calculated magnitude of the γ-output of the radiation circuit from such a generator is about 10 million g-equiv. of radium.

Thus, the planned studies have shown the technological feasibility of installing activity generators in power-generating reactors of the RBMK type, which gives realistic prerequisites for the creation of industrial radiation circuits with these reactors, the production possibilities and the basic economic indexes of which are shown in [3-7].

LITERATURE CITED

1. A. M. Petros'yants et al., Atomnaya Énergiya, 31, No. 4, 315 (1971).
2. A. P. Aleksandrov, Atomnaya Énergiya, 25, No. 5, 356 (1968).
3. A. Kh. Breger, in: Radiation Chemistry [in Russian], Atomizdat, Moscow (1972), p. 403.
4. E. L. Ivanter et al., in: Problems of Atomic Science and Technology. Series "Planning" [in Russian], Izd. TsNIIatominform, Moscow, No. 4, 60 (1971).
5. L. P. Poluektova et al., in: Radiation Chemistry [in Russian], Atomizdat, Moscow (1972), p. 551.
6. A. Kh. Breger et al., Conference on the Radiation Modification of Polymers [in Russian], Theses of Reports, Nauka, Moscow (1968), p. 99.
7. S. M. Berlyant et al, Conference on the Radiation Modification of Polymers [in Russian], Theses of Reports, Nauka, Moscow (1968), p. 92.

DETERMINATION OF FISSION PRODUCT CHARGE DISTRIBUTION PARAMETERS

A. B. Koldobskii, V. Yu. Solov'ev, and V. M. Kolobashkin*

UDC 539.173.8

The most accurate way of determining the charge distribution parameters of the elements of an isobaric chain of fission products is to calculate these from the experimental values of the independent and cumulative fission product yields. However, no universal algorithm for such a calculation has been described in the literature. We have developed a procedure for calculating the charge distribution parameters based on the method of maximum probability. The algorithm is convenient for work on a computer and permits the use of experimental information on both the independent and cumultative yields. Results of the calculation are presented for isolated chains.

SPATIAL AND SPECTRAL DISTRIBUTIONS OF GAMMA RAYS REFLECTED BY SHIELDS OF LIGHT MATERIALS

D. B. Pozdneev and M. A. Faddeev†

UDC 539.122:539.121.72

Differential energy spectra of reflected gamma rays leaving various parts of the surfaces of slab shields of beryllium, carbon, and concrete have been calculated by the Monte Carlo method. The primary energies of the gamma rays frompoint, isotropic and monodirectional sources were 0.279, 0.661, and 1.25 MeV. The program can take account of single, double, and multiple scattering.

Integration of the differential energy spectra gives data on the angular distribution and the integral spectra of the reflected gamma rays.

The dependence of the integral number current albedo on the shield thickness and the distance from the point of incidence of the primary gamma rays on the shield are presented in a form convenient for practical engineering calculations.

*Original article submitted September 24, 1973.
†Original article submitted October 25, 1973.

PERTURBATION THEORY OF VARIOUS APPROXIMATIONS IN STEADY-STATE NEUTRON TRANSPORT

V. Ya. Pupko

UDC 539.125.52:621.039.51.12

Perturbation theory calculations of neutron physics problems are frequently limited to the first approximation. We discuss a general method for constructing perturbation theories of various approximations. We do this by expanding a perturbed eigenfunction of the neutron flux in terms of the eigenfunctions of the quasi-stationary neutron transport equation for the unperturbed medium. The treatment of this problem and the notation, follow [1].

We write the equations for the eigenvalues and eigenfunctions of the forward and adjoint neutron transport operators in the form

$$-\hat{L}F(x)=\frac{\alpha}{v}F(x); \tag{1}$$

$$-\hat{L}F^{+*}(x)=\frac{\alpha}{v}F^{+*}(x). \tag{2}$$

Here $x = (r, E, \Omega)$ is the set of arguments (coordinates, energy, direction of velocities) on which the neutron flux F and the importance F^{+*} depend, $\hat{L}$ and $\hat{L}^{+}$ are operators taking account of all the neutron interaction processes in the medium and their variation with velocity $v\Omega$, and the α's are the eigenvalues of these operators.

We write the perturbed Eq. (1) in the form

$$-(\hat{L}+\delta\hat{L})F'(x)=\frac{\alpha'}{v}F'(x). \tag{3}$$

For fixed boundary conditions we use Eqs. (2) and (3) to obtain the expression for the variation $\delta\alpha = \alpha' - \alpha$ [2]:

$$-\delta\alpha=\frac{\int F^{+*}\delta\hat{L}F'\,dx}{\int\frac{1}{v}F^{+*}F'\,dx}. \tag{4}$$

Equation (4) is exact if the perturbed function F'(x) is substituted into it. We determine this function from Eq. (3) together with the adjoint equation for the Green's function

$$-\hat{L}^{+}\Phi^{+}(x;\,x_0)=\delta(x-x_0). \tag{5}$$

Using (3) and (5) it is easy to obtain

$$F'(x_0)=\int\Phi^{+}(x;\,x_0)\left(\frac{\alpha'}{v}+\delta\hat{L}\right)F'(x)\,dx. \tag{6}$$

Thus F' and α' are found by solving Eqs. (4) and (6) simultaneously.

We express $\Phi^{*}(x; x_0)$ as a Fourier expansion in the eigenfunctions of Eq. (2)*:

$$\Phi^{+}(x;\,x_0)=\sum_{k=1}^{M}C_k(x_0)F_k^{+*}(x)+\int\limits_{\mathrm{Re}\,\alpha=\alpha_B}^{\infty}C_\alpha(x_0)F_\alpha^{+*}(x)\,d\alpha, \tag{7}$$

*It is assumed that the set of eigenfunctions belonging to the discrete and continuous spectrum of the eigenvalues of the operators of Eqs. (1) and (2) is complete.

Translated from Atomnaya Énergiya, Vol. 37, No. 1, pp. 63-65, July, 1974. Original letter submitted March 6, 1973.

where in general M is the finite number of eigenfunctions of the discrete spectrum, and $\alpha_B = \min(v\Sigma_t) > \operatorname{Re}\alpha_k$ is the boundary of the continuous spectrum [1, 3]. The expansion coefficients are determined by using the biorthogonality conditions which follow from the fact that the operator L^+ of Eq. (2) is the adjoint of $\hat{L}$ in Eq. (1):

$$\begin{gathered}\int \frac{1}{v} F^{+*}F_k\,dx = N_m\delta_{mk};\\ \int \frac{1}{v} F_\alpha^{+*}F_{\alpha'}\,dx = N_\alpha\delta(\alpha'-\alpha);\\ \int \frac{1}{v} F_\alpha^{+*}F_m\,dx = \int \frac{1}{v} F_k^{+*}F_\alpha\,dx = 0.\end{gathered} \tag{8}$$

Substituting (7) into (5) and using Eqs. (1), (2), and (8) we find

$$C_m(x_0) = \frac{F_m(x_0)}{\alpha_m N_m};\quad C_\alpha(x_0) = \frac{F_\alpha(x_0)}{\alpha_{N_\alpha}}. \tag{9}$$

Using (6), (7), and (9) we obtain for a perturbed eigenfunction of the neutron flux a Fourier expansion in the eigenfunctions of the unperturbed Eq. (1)

$$F'_m(x) = \sum_{k=1}^{M} A_{km}F_k(x) + \int\limits_{\operatorname{Re}\alpha=\alpha_B}^{\infty} A_{\alpha m}F_\alpha(x)\,d\alpha, \tag{10}$$

where

$$\begin{aligned}A_{k,m} &= \frac{1}{\alpha_k N_k}\int F_k^{+*}\left(\frac{\alpha'_m}{v} + \delta\hat{L}\right)F'_m\,dx;\\ A_{\alpha,m} &= \frac{1}{\alpha N_\alpha}\int F_\alpha^{+*}\left(\frac{\alpha'_m}{v} + \delta\hat{L}\right)F'_m\,dx.\end{aligned} \tag{11}$$

Using (4) we obtain

$$A_{k,m} = \frac{\alpha_m}{\alpha_k}\cdot\frac{N'_{k,m}}{N_k} + \frac{1}{\alpha_k}\cdot\frac{\varepsilon'_{k,m}}{N_k} - \frac{1}{\alpha_k}\cdot\frac{\varepsilon'_{m,m}}{N_k}\cdot\frac{N'_{k,m}}{N'_{m,m}}, \tag{12}$$

where

$$N'_{k,m} = \int \frac{1}{v} F_k^{+*}F'_m\,dx;\quad \varepsilon'_{k,m} = \int F_k^{+*}\delta\hat{L}F'_m\,dx. \tag{13}$$

The expression for $A_{\alpha,m}$ is similar to (12). For k = m, Eq. (12) gives

$$A_{m,m} = \frac{N'_{m,m}}{N_m}. \tag{14}$$

The method presented is easy to generalize to the case of inhomogeneous equations:

$$\begin{aligned}-\hat{L}\psi(x) &= Q(x);\\ -\hat{L}\psi^+(x) &= P(x).\end{aligned} \tag{15}$$

The perturbation theory formula for a linear functional of the neutron flux $\psi(x)$ has the form [4]

$$\delta I = \int (P'\psi - P\psi)\,dx = \int \psi^+(\delta Q + \delta\hat{L})\,dx + \int \delta P\psi'\,dx. \tag{16}$$

Hence using the solution of Eq. (5) we find

$$\delta\psi(x) = \int \Phi^+(x_0;\ x)(\delta Q + \delta\hat{L}\psi')\,dx_0, \tag{17}$$

with $\psi^+(x) = \int \Phi^+(x_0; x)P(x_0)dx_0$. As in the preceding case we obtain

$$\psi'(x) = \sum_{k=1}^{M} B_kF_k(x) + \int\limits_{\operatorname{Re}\alpha=\alpha_B}^{\infty} B_\alpha F_\alpha(x)\,d\alpha, \tag{18}$$

where

$$B_k = \frac{1}{\alpha_k N_k}\int F_k^{+*}(Q' + \delta\hat{L}\psi')\,dx.$$

The expression for B_α is similar to that for B_k.

We discuss the use of expansion (10) for constructing perturbation theories of various approximations. For simplicity we consider the widely used age-diffusion approximation. In this case there is no integral in Eq. (10), and M = ∞. In addition the expansion index is separated into energy and geometric indices.* Taking account of Eqs. (12) and (14) we rewrite Eq. (10) in the form

$$F'_{ml}(x)=\frac{N'_{ml;\,ml}}{N_{ml}}F_{ml}(x)+\sum_{\substack{k=1\\k\neq m}}^{\infty}\sum_{\substack{n=1\\n\neq l}}^{\infty}A_{kn;\,ml}F_{kn}(x), \tag{19}$$

where $k \neq m$ and $n \neq l$ simultaneously.

The expression for $A_{kn,ml}$ is similar to (12) with the addition of the geometric indices n and l. In the zero approximation $\hat{\delta L} = 0$ and $F^{(0)}_{ml} = F_{ml}(x)$, which can also be obtained from (12) and (14) since $A^{(0)}_{mm} = 1$ and $A_{kn,ml} = 0$, $k \neq m$, $n \neq l$. In the first approximation we substitute $F'_{ml}(x) \approx F_{ml}(x)$ into Eqs. (12) and (14). Then by using (8) we obtain from (19)

$$\delta F^{(1)}_{ml}(x)=F^{(1)}_{ml}(x)-F_{ml}(x)=\sum_{\substack{k=1\\k\neq m}}^{\infty}\sum_{\substack{n=1\\n\neq l}}^{\infty}A^{(1)}_{kn,\,ml}F_{kn}(x), \tag{20}$$

where

$$A^{(1)}_{kn;\,ml}=\frac{1}{\alpha_{kn}}\cdot\frac{\varepsilon_{kn,\,ml}}{N_{kn}}. \tag{21}$$

The generalization of this method to s-th approximation perturbation theory gives

$$\delta F^{(s)}_{ml}(x)=\sum_{\substack{k=1\\k\neq m}}^{\infty}\sum_{\substack{n=1\\n\neq l}}^{\infty}A^{(s)}_{kn,\,ml}F_{kn}(x),\quad s=1,\ 2,\ 3\ \ldots, \tag{22}$$

where

$$A^{(s)}_{kn,\,ml}=A^{(1)}_{kn,\,ml}+\sum_{\substack{k'=1\\k'\neq m}}^{\infty}\sum_{\substack{n'=1\\n'\neq l}}^{\infty}A^{(1)}_{kn,\,k'n'}A^{(s-1)}_{k'n',\,ml}$$

$$+A^{(s-1)}_{kn,\,ml}\frac{\alpha_{ml}}{\alpha_{kn}}\left[1-A^{(1)}_{ml,\,ml}-\sum_{\substack{k'=1\\k'\neq m}}^{\infty}\sum_{\substack{n'=1\\n'\neq l}}^{\infty}A^{(1)}_{ml,\,k'n'}A^{(s-1)}_{k'n',\,ml}\right]. \tag{23}$$

The coefficient $A^{(1)}_{ml,ml}$ is found from Eq. (21), and $A^{(0)}_{kn,ml} = 0$.

We note that in the sum over the energy index (k, k', m) the eigenvalues and eigenfunctions appear with their complex conjugates [1]. This leads to the separation of Eq. (22) into its real and imaginary parts, and to the vanishing of the imaginary expressions in the summation over the indices k and k'.

The construction of perturbation theories of various approximations for k_{eff} of a reactor requires the equation for the reactivity given in [1]

$$\delta\rho=\delta\left(\frac{k_{\text{eff}}-1}{k_{\text{eff}}}\right)=-T'_1\delta\alpha_1-\alpha_1\delta T'_1, \tag{24}$$

where $\delta\alpha_1$ is found by using (4), and the variation $\delta T'_1$, a parameter analogous to the neutron generation time, is determined from the perturbation theory formulas for a bilinear functional [5]. The main difficulty in the practical application of the theory is the necessity of knowing the set of eigenfunctions of Eqs. (1) and (2). In a number of problems this can be done analytically (a bare reactor of [1]), but in general it can only be done numerically. For many practical problems there is sufficient information only on the discrete spectrum of eigenvalues and eigenfunctions of the neutron flux. In this case both the real and the complex conjugate eigenvalues and eigenfunctions must be known to describe the perturbation of the neutron spectrum correctly.

The author thanks V. G. Zolotukhin, S. B. Shikhov, É. E. Petrov, and A. A. Abagyan for a helpful discussion of the work.

LITERATURE CITED

1. V. Ya. Pupko, in: Theoretical and Experimental Problems in Nonstationary Neutron Transport [in Russian], Atomizdat, Moscow (1972), p. 66.
2. E. Pendlebury, Proc. Phys. Soc., 68A, 474 (1955).
3. S. B. Shikhov and A. A Shkurpelov, cf. [1], p. 97.
4. G. I. Marchuk, Methods of Making Nuclear Reactor Calculations [in Russian], Gosatomizdat, Moscow (1961).
5. L. N. Uzachev, Atomnaya Énergiya, 15, 472 (1963).

EFFECT OF REACTOR IRRADIATION ON THE DISSOCIATION PRESSURE OF ZIRCONIUM HYDRIDE

V. S. Karasev, V. G. Kovyrshin, and V. V. Yakovlev

UDC 621.039.532

An earlier study of the temperature dependence of the dissociation pressure of zirconium hydride and its dependence on hydrogen content showed that during irradiation with a neutron flux of intensity $\sim 10^{14}$ neutrons/cm^2·sec ($E \geq 0.1$ MeV) the equilibrium pressure was greater than under the same conditions without irradiation [1]. These and other data presented in the present paper were obtained when studying samples of zirconium hydride irradiated in hermetic ampoules furnished with a system of pressure measurement and a controllable rate of hydrogen extraction, enabling the hydrogen content of the samples to be varied.

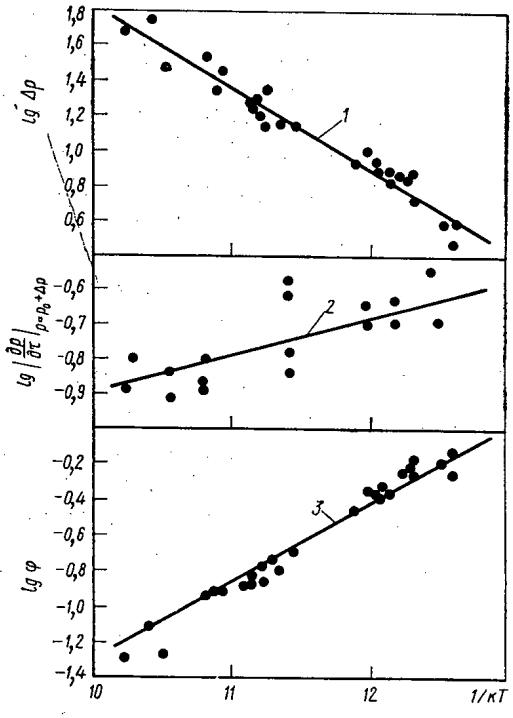

Fig. 1. Temperature dependence of the radiation-induced increase in the dissociation pressure of zirconium hydride (1), the rate of fall of hydrogen pressure on absorption by the sample at the increase $p = p_0 + \Delta p$ (2), and the parameter φ (3).

Since the apparatus error encountered when measuring the equilibrium hydrogen pressure in the ampoule was considerably smaller than the total error associated with determining the sample temperature, special attention was paid to the latter. In experiments without irradiation the error in measuring the sample temperature was no greater than ±2°C. During irradiation the temperature was monitored by reference to three or four Chromel–Alumel thermocouples distributed over the sample surface, with continuous recording of the readings, and periodic testing of the latter by means of a class-0.05 potentiometer. The existence of thermal contact between the thermocouples and the sample was checked by reference to the electrical resistance of the contact. The influence of the hydrogen atmosphere on the readings of the thermocouples was checked at the melting point of NaCl (800.8°C); it remained constant for ~200 h. During the period required to establish the equilibrium hydrogen pressure after taking the hydrogen from the ampoule, the sample temperature was kept constant to within of ±2°C by means of a special system designed to regulate the thermal conditions of irradiation [2].

The total error committed in determining the sample temperature during irradiation (allowing for the temperature drop over the sample thickness due to radiative energy transfer of the order of 4 W/g [3]) never exceeded ±5°C, which corresponded to a change of ~1.5 mm Hg in the equilibrium pressure during the experiments without irradiation at, for example, ~1000°K, this being considerably less than the radiative effect (~10 mm Hg) at the same perature [1].

Translated from Atomnaya Énergiya, Vol. 37, No. 1, pp. 65-66, July, 1974. Original letter submitted May 21, 1973; revision submitted January 22, 1974.

A comparison between the influence of hydride composition and temperature on the equilibrium hydrogen pressure with and without irradiation was made in identical ampoules, using the same samples. As irradiation temperature we took the value corresponding to the maximum readings of the thermocouples placed in the sample (the temperature drop over the sample was 5-10°C), which underestimated the actual radiation effect.

The character of the isotherms and the error committed in determining the sample composition prevent us from making a reasonably accurate judgment of the change in equilibrium pressure which occurs on irradiating hydrides with hydrogen contents greater than that corresponding to the composition $ZrH_{1.5}$; we shall therefore simply present the results obtained in the range $ZrH_{0.9}$ to $ZrH_{1.4}$, in which the dissociation pressure does not depend on the hydrogen content (at constant temperature), while on varying the irradiation temperature T from 900 to 1100°K the equilibrium pressure p exceeds the corresponding value in the absence of irradiation p_0 by Δp = 3-50 mm Hg. The temperature dependence of Δp (Fig. 1) is described by an exponential function (curve 1) with an activation energy of (1.07 ± 0.05) eV and a preexponential factor of $(1.9 \pm 1.7) \cdot 10^6$ mm Hg.

The rise in equilibrium pressure which occurs on irradiation is associated with compensation of the additional (irradiation-induced) hydrogen evolution at a rate v_p, equal to the difference in the rates of the thermally-activated absorption and evolution of hydrogen with the absence of irradiation for the same value of v_p. The quantity $(\delta p/\delta\tau)_p = p_0 + \Delta p$ mm Hg/sec, proportional to v_p, was determined in these experiments by analyzing the kinetic characteristics of the absorption of hydrogen by equivalent samples of zirconium hydride in the temperature range indicated. These results are described by the expression $(-\delta p/\delta\tau)_p = p_0 + \Delta p = K_0 \exp(E_p/kT)$ with $E_p = 0.2 \pm 0.05$ eV (curve 2). The value of v_p is related to the velocity of the thermally-activated process limiting the evolution of hydrogen from the hydride under radiationless conditions $v = v_0 \exp(-E_v/kT)$ by the equation $\varphi = v_p/v \approx (p/p_0)^{0.5} - 1$, derived by analyzing the kinetic establishment of equilibrium, with due allowance for the adsorption, desorption, and chemisorption of hydrogen on the surface of the hydride, and also for the reversible transition of hydrogen from the hydride into the chemisorbed state [4, 5]. For the range of compositions and temperatures under examination the function φ derived from the experimental values of p_0 and $p = p_0 + \Delta p$ is described by the equation $\varphi = \varphi_0 \exp(E_\varphi/kT)$ with $\varphi_0 = (2.1 \pm 0.3) \cdot 10^{-6}$ and $E_\varphi = (1.00 \pm 0.05)$ eV (curve 3). A comparison between the experimental values of E_p and E_φ shows that the value of $E_v = E_\varphi - E_p$ agrees closely with the activation energy for the diffusion of hydrogen in the hydride ~0.8 eV [6], which (as we should expect) determines the kinetics of hydrogen evolution from the sample.

LITERATURE CITED

1. R. A. Andrievskii et al., Fourth Geneva Conference (1971), Soviet Report 49/R/452.
2. V. S. Karasev et al., At. Énerg., 22, No. 6, 492 (1967).
3. V. M. Kolyada and V. S. Karasev, At. Énerg., 26, No. 1, 55 (1969).
4. J. Becker and C. Harfman, J. Phys. Chem., 57, 157 (1953).
5. E. Ehrlich, J. Phys. Chem., 59, 473 (1955).
6. P. Paetz and K. Lucke, J. Metallkunde, 62, No. 9, 657 (1971).

OPTIMAL BRINGING OF REACTOR INTO THE STATIONARY REGIME OF FUEL RELOADING

B. P. Kochurov

UDC 621.039.516

As is shown [1], the operation of a reactor in the stationary regime with continuous reloading of fuel allows us to considerably increase (by a factor of 3/2-2) the burnup and to reduce the consumption of uranium compared with the regime in which all the fuel is reloaded at the same time. There is interest in investigating the transient regime of the reactor from the moment of its start-up to the output in the stationary regime (questions connected with the investigation of the optimal regimes for reloading fuel were studied in [2-4]).

Below we consider the following problem. For a sufficiently large time interval, we wish to find the strategy of reloading for which the minimum amount of fresh fuel is spent. The principal requirements are that the solution be positive and that the reactivity of the reactor not be below a certain value. We can superimpose on the burnup a constraint to be determined by the stability of the fuel elements. Additionally we can require that the reactor be found in a stationary regime from some fixed moment on.

Let $F(s, \tau)$ be a distribution function giving the fraction of fuel with burnup less than s at the moment τ, where s and τ are single-scale quantities, to be measured, for example, by the energy release from 1 ton of fuel (MW·days/ton). If there is no reloading, then in an interval $\Delta\tau$, fuel with burnup s produces an increment of burnup $\Delta\tau$, so that

$$F(s, \tau) = F(s - \Delta\tau, \tau - \Delta\tau).$$

We fix $\Delta\tau$, dividing the segment of the "time" axis over the period for which we are considering the history of the reactor, into N equal intervals with separate moments $\tau_j = j\Delta\tau$, and we perform the following Laplace transformation with respect to the variable s:

$$F(s, \tau_j) \to \int e^{-\lambda s} dF(s, \tau_j) = \sum_m e^{-\lambda \Delta\tau m} x(\Delta\tau m, \tau_j) = \sum_m z^m x_j^m \equiv x_j(z).$$

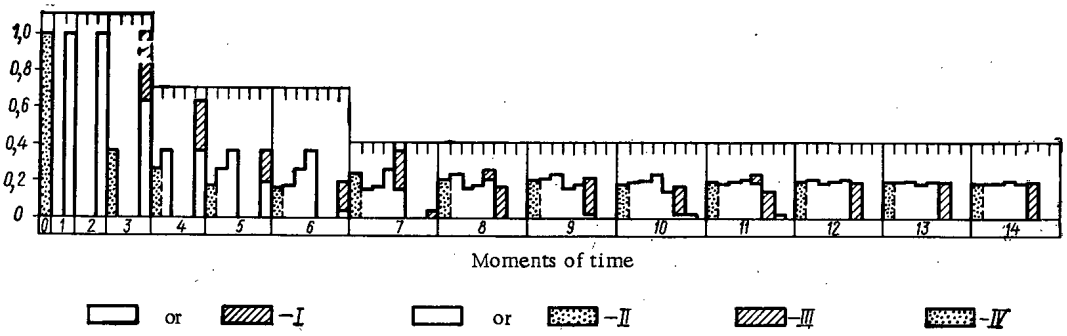

Fig. 1. Example of optimal strategy of reloading of fuel for the initial stage of operation of the reactor; I) distribution of fuel according to burnup, up to reloading [the ordinates correspond to values of the coefficients of the polynomials $zx_{j-1}(z)$]; II) distribution of fuel based on age after reloading [$x_j(z)$]; III) fuel removed [$u_j(z)$]; IV) fresh fuel (u_j^0).

Translated from Atomnaya Énergiya, Vol. 37, No. 1, pp. 66-68, July, 1974. Original letter submitted June 25, 1973.

TABLE 1. The Function k(s)

S, MW • days /ton	k (s)	S, MW • days /ton	k (s)
0	1,030	3000	0,998
750	1,034	4500	0,961
1500	1,029	6000	0,924
2250	1,015	7500	0,893

TABLE 2. Maximum Values of ΔP (%) as a Function of Various Factors

M	NS	τΔ·MS, MW • days/ton		
		3000	6000	3000 *
8	23	0	0	0
9	23	20,8	22,1	22,4
10	23	23,2	25,0	25,3
11	23	23,7	25,6	25,9
11	15	21,1	23,6	24,1
11	12	17,2	18,6	19,1
11	10†	0	0	0

*Linear function k (s) = 1.03-0.00002 s.
†The standard regime is realized.

The integral equals the sum if $F(s, \tau_j)$ had discontinuities only at the points $\Delta\tau m$. After introduction of the formal variable $z \equiv e^{-\lambda\Delta\tau}$ the dependence with respect to s is represented by the coefficients x_j^m of polynomial $x_j(z)$, determining the fraction of fuel with burnup m (for fixed $\Delta\tau$ the burnup can be characterized by the number m). The functions $F(s-\Delta\tau, \tau-\Delta\tau)$ correspond to the polynomial $zx_{j-1}(z)$ such that $x_j(z) = zx_{j-1}(z)$. If at moment j there occurs unloading of the fuel, characterized by the polynomial* $u_j(z) = \sum_{m=1}^{M} u_j^m z^m$, with it being replaced by fresh fuel, then

$$x_j(z) = zx_{j-1}(z) + Bu_j(z) \qquad (1 \leqslant j \leqslant N), \tag{1}$$

where $x_0(z) = 1$; the operator B acts as follows:

$$Bu_j(z) = \sum_{m=1}^{M} u_j^m \cdot 1 - u_j(z). \tag{2}$$

The number M determines the maximum admissible burnup of fuel (we assume $z \cdot z^M = 0$). The polynomial $zx_{j-1}(z)$ characterizes the state at the moment j up to reloading of the fuel, $x_j(z)$ characterizes the state after reloading. It is natural to require that the inequalities

$$0 \leqslant u_j^m \leqslant 1, \quad \forall j, m, \tag{3}$$

and also the inequalities $zx_{j-1}(z) \geq u_j(z)$ be satisfied, which with account of (1) is equivalent to the solution

$$x_j^m \geqslant 0, \quad \forall j, m \tag{4}$$

being nonnegative. We form the vector†

$$x = [x_0(z), x_1(z), \ldots, x_N(z)] \Leftrightarrow$$
$$\Leftrightarrow (x_0^0; x_1^0, x_1^1; \ldots, x_M^0, \ldots, x_M^M; \ldots; x_N^0, x_N^1, \ldots, x_N^M)$$

and we introduce the scalar product

$$(x, y) = \sum_i \langle x_i(z), y_i(z)\rangle; \quad \langle x_i(z), y_i(z)\rangle = \sum_m x_i^m y_i^m.$$

It is advisable that we rewrite inequalities (4) in the form

$$(\delta_{ij} z^m, x) \geqslant 0, \quad \forall j, m.$$

Let, as a result of the calculation of the kinetics, there be known the dependence of the neutron multiplication constant on the burnup k(s), in particular, let it be given by the polynomial k(z).‡ Then the constraint on the reactivity can be represented in the form

$$\langle k(z), zx_j(z)\rangle \equiv (\delta_{ij} z^+ k(z), x) \geqslant \bar{k} \quad (0 \leqslant j \leqslant N), \tag{5}$$

where the operator z^+ reduces the power of z by one power, and the zero power of z vanishes.

The constraints (4) and (5) are inconvenient because they depend on the phase variable x, and not on the control u. Taking into account that each of them is given by a linear functional of the form (f, x), with the help of the adjoint functions

$$\psi_j^f - z_{j+1}^+ \psi_{j+1}^f(z) = f_j(z) \quad (0 \leqslant j \leqslant N-1) \tag{6}$$

*The coefficient u^m corresponds to the fraction of unloaded fuel with burnup m.
†The variable length of the vectors $x_i(z)$ is connected with the fact that at moment i, burnup m > i is unattainable.
‡The coefficients $k^m \equiv k(\Delta\tau m)$ of the polynomial k(z) give the neutron multiplication constant as a function of the burnup m.

we transform (4), (5) into the form

$$(f,\ x)=\sum_{j=1}^{N}\langle\psi_j^f(z),\ Bu_j(z)\rangle; \tag{7}$$

at the same time we must multiply Eq. (6) by $x_j(z)$, sum over j, and use the property of adjoint operators and Eq. (1).

The functions $\psi_i^{m,j}=z^{m-j+1}$ correspond to the functionals in (4); this gives

$$\begin{aligned} u_i^0&=\sum_{m=1}^{M}u_{i+m}^m \quad (0\leqslant i\leqslant N-M),\\ u_i^0&\geqslant\sum_{m=1}^{N-i}u_{i+m}^m \quad (N-M+1\leqslant i\leqslant N-1), \end{aligned} \tag{8}$$

where

$$u_i^0=\sum_{m\geqslant 1}u_i^m. \tag{9}$$

The relations (8) have the following sense: fresh fuel, loaded at moment i, has burnup m at moment i + m, where the quantity of fuel drawn off at all moments i + m should not exceed the value u_i^0. The sign of the equality arises in connection with the fact that the maximum admissible burnup equals M.

The functions $\psi_i(z)=\sum_{M-1\geqslant m\geqslant j-i}k^{m+1}z^{m-j+1}$ correspond to the functionals in expression (5), and the constraints on the reactivity take the form

$$\sum_{j=i-L(i)}^{i}k^{i-j+1}u_j^0-\sum_{i\geqslant j\geqslant i-L(i)+1}\ \sum_{m=1}^{L(i)-i+j}k^{i-j+m+1}u_j^m\geqslant\bar{k},\quad\forall i, \tag{10}$$

$$L(i)=\begin{cases} i & i\leqslant M-1,\\ M-1 & i\geqslant M.\end{cases}$$

The calculation of the minimum of the total fuel consumption

$$P=\sum_{i=0}^{N}u_i^0 \tag{11}$$

as a function of the components of the vector u for linear constraints (3), (8)-(10), represents a problem in linear programming [5]. If in addition we require that $u_i^0=u_i^{MS}=1/MS$ from some moment $i\geq NS$, then at the moment NS + MS (or earlier) the reactor will be found in a stationary regime. There exists some standard method of bringing the reactor to a stationary regime through MS intervals: $u_0^0=1$; $u_i^0=u_i^i=1/MS$ $(1\leq i\leq MS)$, requiring a single excess loading [in the discrete representation $(MS-1)/MS$] in comparison with an infinite stationary regime. Therefore, to calculate an optimal strategy, the topic of discussion is the economy of a certain part of this loading $\Delta P=P_{stand}-P<1$.

In Fig. 1 we represent a typical example of an optimal strategy,* calculated based on a VORS program (Fortran, BÉSM-6). The values of k^m for $\Delta\tau=600$ MW·days/ton were determined based on the data of Table 1, the value of MS was assumed equal to five (this corresponds to a burnup of 3000 MW·days/ton in a stationary regime), M = 7, $k=k_{stat}=\sum_{m=1}^{MS}k^m/MS$, $\Delta P=20\%$; the moment NS was not fixed.

In Table 2 we represent optimal values of ΔP for division of the burnup in the stationary regime with equilibrium burnup of 3000 and 6000 MW·days/ton for eight intervals (MS = 8), where for the last column we replace the dependence represented in Table 1 by the linear function k(s).

On the basis of the calculations performed we can draw the following conclusions. The form of the function k(s) has a very weak effect on the magnitude of ΔP. If the admissible burnup does not exceed its maximum value in the stationary regime (M = MS), then the gain of ΔP proves to be zero. To obtain the principal part of the gain it is sufficient to increase the admissible burnup by 10-15%; its further increase (up to ~40%) leads to a rather weak variation of ΔP. For the optimal output in the stationary regime we require about two and a half runs (see Fig. 1). If we require a more rapid approach in the stationary regime, i.e., if we must reduce NS, then ΔP at first will vary weakly, and then sharply fall to zero.

*The function k(s) represented in Table 1 is characteristic of the reactor of the A-1 Atomic Electric Power Plant in Czechoslovakia [6].

LITERATURE CITED

1. B. L. Ioffe and L. B. Okun', At. Énerg., No. 1, 80 (1956).
2. D. Tabak, IEEE Trans. Nucl. Sci., NS-15, 60 (1968).
3. T. Sauar, Nucl. Sci. and Engng., 46, 274 (1971).
4. A. Suzuki and N. Kiyose, ibid., 11.
5. S. I. Zukhovitskii and L. I. Avdeeva, Linear and Convex Programming [in Russian], Nauka, Moscow (1967).
6. V. M. Abramov et al., At. Énerg., 36, No. 3, 163 (1974).

OPERATIONAL MEASUREMENT OF BIOMEDICAL PROTON BEAM INTENSITY

Ya. L. Kleinbok and V. M. Narinskii

UDC 621.384.668

Since 1968, a beam of protons with energies from 70 to 200 MeV has been used at the Institute of Theoretical and Experimental Physics for biological studies and for radiation therapy of cancers. The pulse duration of the extracted proton beam is 1.6 μsec, the repetition rate 0.25 Hz, the intensity range $2 \cdot (10^8-10^{11})$ protons/pulse; the transverse dimension of the beam varies from 3 to 90 mm, and the energy range is 70-200 MeV [1, 2].

The performance of biological studies required the creation of an operational system providing measurement of intensity in practically single beam pulses (reciprocal duty factor, $25 \cdot 10^5$) under conditions of strong electromagnetic interference produced by the proton extraction system at the very time of measurement. The requirements imposed on the measurement system were determined not only by the technical conditions but also by the particular use of the beam. During radiation therapy, the measuring system is a medical instrument upon the accuracy, operational simplicity, reliability, and flexibility of which the patient's health depends.

The system must ensure measurements having an accuracy better than ±3% over the entire range of energies, intensities, and transverse beam dimensions without any readjustment of the input device (sensor). The sensor must not have any effect on beam characteristics. The method for monitoring the effectiveness of the system must be simple and ensure checking of the entire channel. The method for constructing the measuring system is determined mainly by the choice of the sensor which directly senses the beam [3].

The so-called transmission sensors – electromagnetic and electrostatic – fill these requirements most completely. The use of an electromagnetic sensor in the system developed (current transformer) made it possible to create an interference-proof system for operational measurement of the intensity of the biomedical proton beam using comparatively simple equipment.

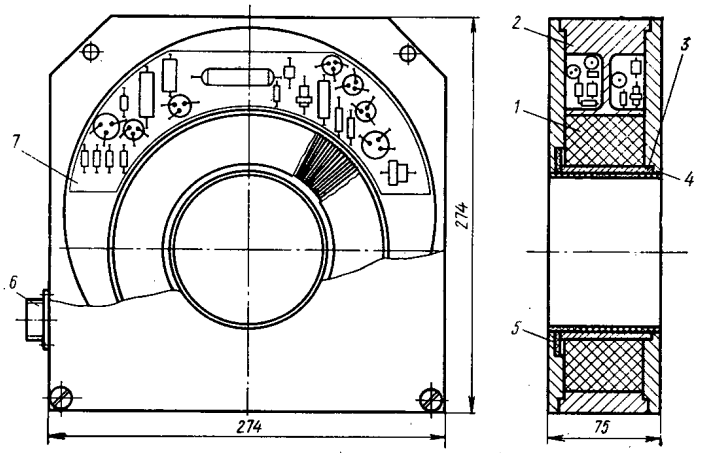

Fig. 1. Electromagnetic sensor.

Translated from Atomnaya Énergiya, Vol. 37, No. 1, pp. 69-70, July, 1974. Original letter submitted July 2, 1973; revision submitted February 4, 1974.

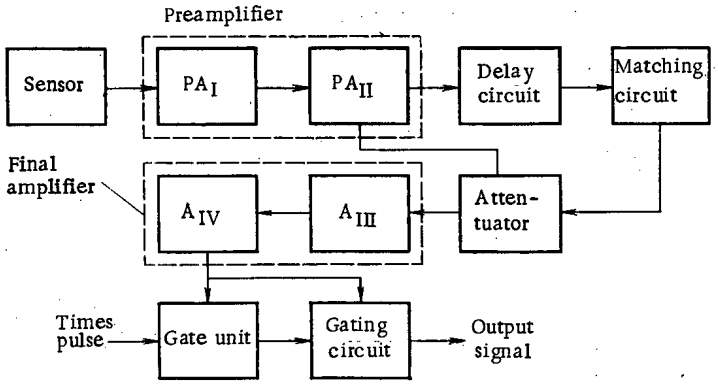

Fig. 2. Block diagram of system for operational measurement of intensity.

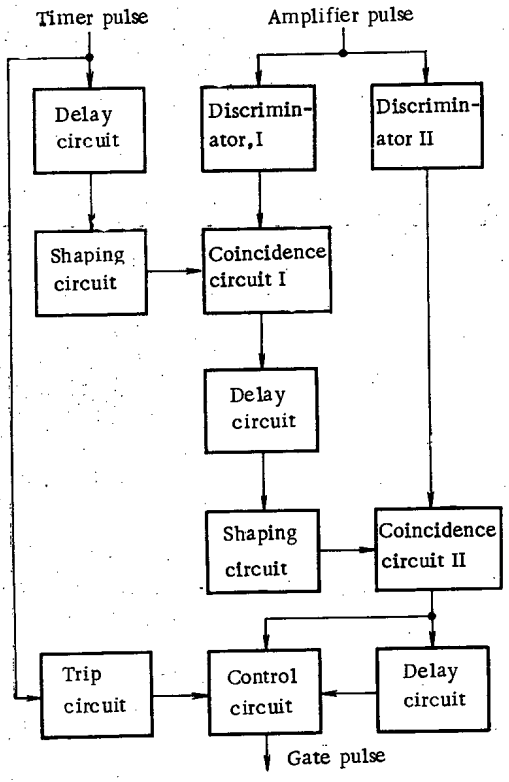

Fig. 3. Block diagram of gate unit.

The electromagnetic sensor (Fig. 1) consists of the permalloy ring 1 (external and internal diameters 168 and 120 mm, width 52 mm) with a winding uniformly distributed over its circumference. The winding is made of PÉLShO-0.14 conductor; the number of turns is 89 and the sensor inductance is ~14 mH. The sensor is inside the duraluminum housing 2. Openings in the housing covers correspond to the internal diameter of the ring. In the internal cavity of the ring, there is the metal bushing 3 one edge of which is directly adjacent to the cover 4. Between the second edge and the cover there is the circular plastic washer 5, which is 2.5 mm thick and creates a "slit" in the solid shield providing interaction between the beam and current transformer. The emf induced in the transformer winding determines the voltage pulse at the sensor output. The amplitude of the voltage is proportional to the intensity of the proton beam. The operating principles of an electromagnetic sensor are described in detail in [3] and reasons for the choice of design are presented.

To record the pulses from individual signals, it is convenient to use the VCh-17 pulse digital voltmeter, which is commercially produced. The minimum pulse amplitude recorded by this instrument is 0.05 V which calls for the use of special amplifiers (Fig. 2). The choice of electronic units for the measuring system and their layout is mainly determined by the presence of high-intensity pulsed interference produced by the beam extraction devices. To reduce these effects to a minimum, the electromagnetic sensor is thoroughly shielded; the preamplifiers PA_I (K = 7) and PA_{II} (K = 30), the delay circuits, and the matching circuits are located directly in the sensor housing 7 (see Fig. 1). Connection to the final amplifiers at the control panel and the power feed to the electronic circuits is accomplished by means of a special cable through the 2RM14B4Sh1V1 connector 6 (see Fig. 1) attached to the sensor housing. The signal is fed over a shielded RK-75-2-12 cable which accompanies the power conductors and is enclosed in a common external shield. The signal is fed to the VCh-17 by the amplification stages A_{III} (K = 7) and A_{IV} (K = 12) of the final amplifier through the gating circuit. Attenuators are introduced into the preamplifier and final amplifier in order to expand the dynamic range of the amplification channel. The preamplifier attenuators have two fixed values (1 : 1 and 1 : 10) and the final amplifiers attenuators have four fixed values (1 : 1, 1 : 2, 1 : 5, and 1 : 10). The gating circuit (Fig. 3) opens the recording channel only at the time of a useful signal. For effective operation of the gating circuit, a circuit to delay the signal by 8 μsec is introduced into the preamplifier.

The introduction in the gate unit, of circuits to discriminate against amplifier pulse height (two discriminators with thresholds $U_{thresh\,I} = 0.2$ V and $U_{thresh\,II} = 0.7$ V) and the selection of this pulse in time, made it possible to identify a useful signal from the amplifier at the output of the gating circuit and to ensure effective selection of it. These measures completely protected the measurement system from interference, which made it possible to automate control of their irradiation procedures – to carry out the accumulation of a total dose with automatic beam shutoff in accordance with a previous setting, to perform programmed control (with respect to dose) of patient rotation, etc.

To check the dynamic range of the measuring system and to evaluate the accuracy of the attenuators and the stability of the entire system, a VCh-7 pulse digital voltmeter was used having a basic error $\Delta = \pm 0.5\% U_{meas} \pm 1$ ml of discharge.

In studies, the beam was simulated by a current pulse from a G5-15 oscillator transmitted along a conductor passing through the sensor opening. Measurements were made at a pulse repetition rate of 1 kHz. The tests show the error in measurements of proton beam intensity over the range $2 \cdot (10^8 - 10^{11})$ protons/pulse, does not exceed ±3%.

In order to determine the accuracy of direct measurement of proton beam intensity, a comparative calibration of the measuring system was made using the induced activity in ^{12}C for a broad range of beam intensities. The test results indicated agreement within the limits of accuracy of the method of induced activity (±6%).

LITERATURE CITED

1. S. I. Blokhin et al., in: Dosimetry and Radiation Processes in Dosimetric Systems [in Russian], Fan, Tashkent (1972), pp. 71-75.
2. V. S. Khoroshkov et al., Meditsinskaya Radiologiya, No. 4, 56 (1969).
3. V. G. Brovchenko et al., Electronic Devices in Electrostatic Accelerators [in Russian], Atomizdat, Moscow (1968).

LEAD TRANSMISSION CURVE FOR 31-GEV ELECTRONS

A. S. Belousov, E. I. Malinovskii,
S. V. Rusakov, S. P. Kruglov,
and V. D. Savel'ev

UDC 539.121.7

The radial distribution of absorbed energy and the transmission curve in lead were measured for a beam of 31-GeV electrons from the Serpukhov synchrotron [1]. Measurement of the radial distribution of absorbed energy, E(r, t), was made with LiF thermoluminescent detectors (TLD) placed within a lead absorber. The absorber was made of lead disks 200 mm in diameter. Since the TLD are small (diameter 3.5 mm and thickness 1.2 mm), their introduction into the absorber satisfies the requirements of the Bragg–Cray principle [2] and consequently permits a determination of the energy losses in the surrounding medium from the energy losses in the TLD. In addition, shower distortion associated with transition effects at the LiF – Pb boundary is negligibly small according to [3] for our detectors having a thickness $0.6 \cdot 10^{-2}$ X_0.

Figure 1 shows the radial distribution E(r, t) of absorbed energy for various absorber thicknesses. The measurement error is 3% or less.

The transmission curve Π(t) can be obtained from the relation

$$\Pi(t) = \frac{\int_0^\infty E(r, t)\, r\, dr}{\int_0^\infty \int_0^\infty E(r, t)\, r\, dr\, dt}. \qquad (1)$$

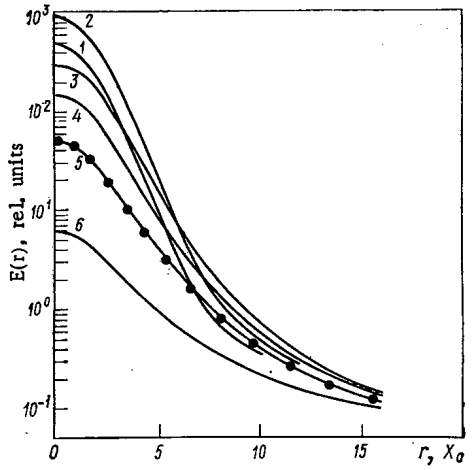

Fig. 1

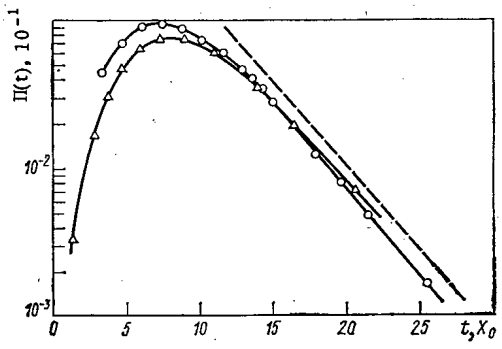

Fig. 2

Fig. 1. Radial distribution of absorbed energy for various values of t: 1) 3.4 X_0; 2) 6.2 X_0; 3) 13.7 X_0; 4) 16.4 X_0; 5) 19.6 X_0; 6) 25.5 X_0.

Fig. 2. Transmission curve: ○) experimental data from this work; Δ) theoretical data from [4]; ----) exponential function with an attenuation factor $\mu_{min} = 0.47$ cm^{-1}.

Translated from Atomnaya Énergiya, Vol. 37, No. 1, pp. 71–72, July, 1974. Original letter submitted July 9, 1973.

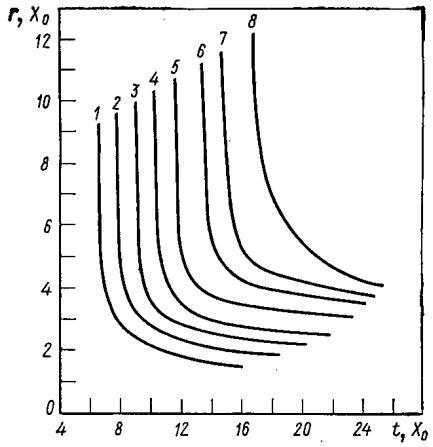

Fig. 3. Isoenergy curves: 1) 30%; 2) 40%; 3) 50%; 4) 60%; 5)70%; 8) 80%; 7) 85%; 8) 90%.

A numerical method was used for the integration; the resultant transmission curve is shown in Fig. 2. In the calculations, a radiation length $X_0 = 0.562$ cm was used. Beyond its maximum, the experimental transmission curve is given by an exponential function with an attenuation factor $\mu = 0.48 \pm 0.01$ cm^{-1}, the value of which is in good agreement with the value for the minimum attenuation coefficient in lead $\mu_{min} = 0.47$ cm^{-1}.

Results of an analytic calculation of cascade curves have been given [4], i.e., the total number of shower electrons as a function of lead absorber thickness, $\Phi_e(t)$, for primary electrons having energies from $3 \cdot 10^8$ to 10^{14} eV. The calculation took into account the Compton effect, the effect of incomplete screening on the pair-production cross section, and the magnitude of radiation losses for photons and electrons with energies $< 10^{18}$ eV. In addition, multiple scattering and ionization losses were taken into account in approximate fashion. Ionization losses were assumed constant, i.e., all electrons lost an energy ε_0 (critical energy) over a path length X_0.

A calculated transmission curve for electrons of energy $E_0 = 31$ GeV was obtained from the relation

$$\Pi_p(i) = \frac{\Phi_e(t)\,\varepsilon_0}{E_0}, \qquad (2)$$

and is shown in Fig. 2. A value $\varepsilon_0 = 7.6$ MeV, the same as that used in [4], was used in the calculations. One of the reasons for the difference between the theoretical transmission curve and the experimental curve may be the fact that in the calculations the ionization losses were assumed to be $\varepsilon_0 = 7.6$ MeV while the energy lost by electrons over a path X_0 exceeds the critical energy for small thicknesses.

To determine the efficiency of a total absorption detector, it is necessary to know the value of the absorbed energy

$$\frac{\Delta E}{E_0} = \frac{\int_0^r \int_0^t E(r, t)\, r\, dr\, dt}{\int_0^\infty \int_0^\infty E(r, t)\, r\, dr\, dt} \qquad (3)$$

for cylindrical volumes of given dimensions. Isoenergy curves are given in Fig. 3 which were obtained from experimental results.

In conclusion, the authors thank M. Ya. Borkovskii for valuable discussions.

LITERATURE CITED

1. S. S. Gershtein et al., IFVÉ Preprint 72-93, Serpukhov (1972).
2. F. Spiers in: Radiation Dosimetry, G. Hine and G. Brownell, editors [Russian translation], Izd. Inostr. Lit., Moscow (1958).
3. K. Pinkau, Phys. Rev., 139, No. 68, 1548 (1965).
4. Z. Buja, Acta Phys. Polon., 24, No. 3, 381 (1963).

RADIATION AND THERMAL TESTS OF ELECTRON-EMISSIVE NEUTRON DETECTORS AND CABLES WITH MAGNESIAL INSULATION

I. Ya. Emel'yanov, V. I. Vlasov, Yu. I. Volod'ko, S. G. Karpechko, L. V. Konstantinov, V. V. Postnikov, and V. I. Uvarov

UDC 539.1.074.88

Electron-emissive neutron detectors (EDN) [1-5] are used widely for monitoring the neutron flux distribution in the active zones of nuclear reactors. The signal from the EDN in the bounds of the active zone and biological shield is transmitted through cables with an internal and external conductor of corrosion-resistant steel and magnesium oxide insulation [6]. The technology used for the production of cables with magnesial insulation is used frequently for the manufacture of EDN; this technology permits the serial production of EDN to be organized almost without limitation in length of the sensitive part of the detector.

For a separate study of the radiation and thermal effects on the electrical properties of detectors and cables under active zone conditions of power reactors, an experimental device was designed and installed in a dry channel inserted in the active zone of the water-cooled/water-moderated research reactor IVV-2. For a specified level of the radiation intensity, this permitted different temperature values to be obtained by means of electric heaters, i.e., the temperature of the EDN and cables could be varied within known limits, independently of the radiation intensity.

Four EDN samples with a silver emitter were tested, representing a section of KDMS(S) cable, made to technical specifications TUMI 098-69. The cable has a core of silver Sr 999 GOST 7222-54 with a diameter of 0.55 mm, magnesium oxide insulation, analytical grade GOST 4526-67 and is clad with corrosion-resistant steel Kh18N10T with a thickness of 0.5 mm; the external diameter of the cable is 3.0 mm. In addition, four samples of KNMS(S) cable, to technical specifications TU15-06-467-69, were tested. The material of the core and cladding was corrosion-resistant steel Kh18N10T and the insulation material was fused magnesium oxide, periclase electrotechnically in accordance with GOST 13236-67. The diameter of the core was 0.5 mm, cladding thickness 0.6 mm and the external diameter of the cable was 3.0 mm. The EDN and cable samples, before testing, were outgassed for 7 h at a temperature of 750-800°C.

The V-I characteristics of the EDN and cables were obtained at different levels of radiation intensity and temperatures (over the range of voltages from −50 to +50V) and proved to be close to linear. The short-circuit current – the EDN current, or background current of the cable – and the insulation resistance were calculated on the basis of the V-I characteristics.

The experimental data on the resistance of the EDN insulation (Fig. 1) were processed in accordance with the theoretical dependence of the conductivity of a mineral insulator on temperature and radiation intensity [7]. The relation is based on the assumption that the conductivity σ of the insulation consists of a thermal σ_t and radiation-thermal σ_{rad} component, i.e., the resistance of the insulation is expressed in the following way (for a specified temperature and radiation intensity):

$$R_{In} = \left(\frac{1}{R_{rad}} + \frac{1}{R_t}\right)^{-1}, \quad (1)$$

Translated from Atomnaya Énergiya, Vol. 37, No. 1, pp. 72-76, July, 1974. Original article submitted July 19, 1973.

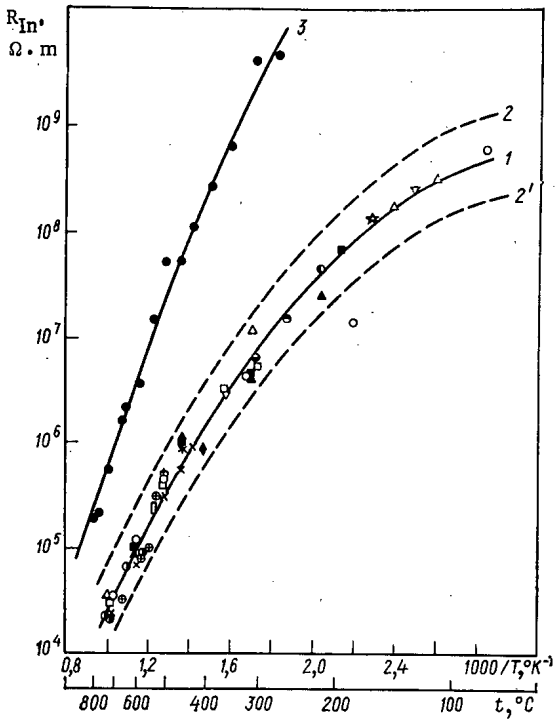

Fig. 1. Temperature dependence of the EDN insulation resistance for the following values of γ-radiation intensity and thermal neutron flux.

Arbitrary symbols	γ-radiation dose intensity, rad/sec	Neutron flux, n/cm² · sec
	outside reactor	
○	2,8·10³	1,7·10¹²
▲	8,4·10³	5,1·10¹²
▽	1,1·10⁴	6,7·10¹²
△	1,4·10⁴	8,5·10¹²
☆	1,7·10⁴	1,0·10¹³
■	2,2·10⁴	1,4·10¹³
◐	2,8·10⁴	1,7·10¹³
◓	3,4·10⁴	2,0·10¹³
◒	4,8·10⁴	2,9·10¹³
□	5,0·10⁴	3,1·10¹³
◇	6,7·10⁴	4,1·10¹³
◆	7,8·10⁴	4,8·10¹³
×	8,4·10⁴	5,1·10¹³
✳	9,0·10⁴	5,4·10¹³
⊛	1,0·10⁵	6,3·10¹³
⊕	1,1·10⁵	6,8·10¹³
⊡	1,2·10⁵	7,3·10¹³
◑	1,4·10⁵	8,5·10¹³

Note. 1) Curve, corresponding to calculations by formula (1), using formulas (2)-(4); 2 and 2') confidence limits, with confidence coefficient of 0.99; 3) curve obtained from formulas (3) and (4).

where R_t is the insulation resistance at a given temperature outside the reactor.

It can be seen from Fig. 1 that the radiation-thermal component of the conductivity is much greater than the thermal component and R_{rad} mainly determines the magnitude of the total resistance of the insulation. Empirical temperature relations between R_{rad} and R_t for EDN have been obtained:

$$R_{rad} = T^{-3/2} \exp(10.6 - 2.0 \cdot 10^6/T^2 + 12000/T); \quad (2)$$

$$R_t = \exp(9900/T + 4.6), \quad 300 < T < 750°K; \quad (3)$$

$$R_t = \exp(13700/T - 0.44), \quad 750 < T < 1100°K, \quad (4)$$

where T is the absolute temperature, °K; R_{rad} and R_t refer to 1 m length of detector and are expressed in Ω·m. The curves plotted in Fig. 1 are calculated by formula (1), using formulas (2)-(4), and also the values of R_{In} outside the reactor calculated by formulas (3) and (4), with confidence limits in the calculation of R_{In} in the reactor, and with a unidirectional confidence coefficient of 0.99.

The considerable difference, with identical temperature, between the value of the resistance outside the reactor and inside the reactor (see Fig. 1) and the weak stratifcation of points corresponding to different radiation intensities, are explained by the change of conductivity mechanism of magnesium oxide during its irradiation with fast electrons, outgoing from the emitter.

The current in the EDN, with a constant neutron flux, increases with increase of temperature, and the temperature dependence of the current at temperatures above 400°C is close to exponential. The sensitivity of the EDN, defined as the EDN current referred to unit neutron flux and to unit length, depends considerably more weakly on the intensity of the reactor radiations than on the temperature, and with increase of radiation intensity it decreases. The growth of the EDN current with increase of temperature for a constant neutron flux may occur on account of the increase of the velocity of the nuclear reaction of the neutron absorption in the silver as a result of Doppler broadening of the neutron resonances [8]. Over the temperature range from normal to 750°C, the Doppler broadening of neutron resonances for silver leads to an increase of neutron absorption by 15-20% which, clearly, does not adequately explain the observed increase of the EDN current. Analysis of the experimental data showed that the dependence obtained for the sensitivity of the EDN on the temperature and neutron flux, can be interpreted conveniently by using the product of the thermal neutron flux and the resistance of the EDN insulation, $\varphi_T R_{In}$, which is proportional to the magnitude of the electric potential barrier in the EDN insulation [9]. It was established (Fig. 2) that with a constant value of $\phi_T R_{In}$, the sensitivity of the EDN depends weakly on the temperature and the neutron flux. By processing the measurement results, shown in Fig. 2, by the method of least squares, the following empirical dependence of the EDN current on the neutron flux and the factor $\phi_T R_{In}$ was obtained:

$$i_{EDN} = 1.2 \cdot 10^{-15} \phi_T \exp\left[0.15 \left(\lg \frac{\phi_T R_{In}}{1.7 \cdot 10^{13}}\right)^2 - 2.5 \lg \frac{\phi_T R_{In}}{1.7 \cdot 10^{13}}\right], \quad (5)$$

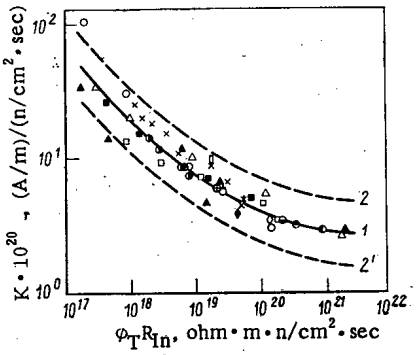

Fig. 2. Dependence of EDN sensitivity on $\phi_T R_{In}$. 1) curve corresponding to formula (5); 2 and 2') confidence limits for a confidence coefficient of 0.99. The nomenclature of the experimental points is the same as in Fig. 1.

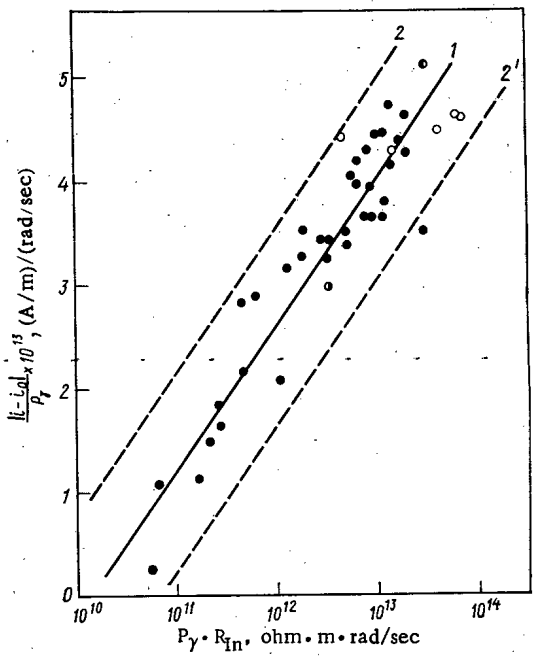

Fig. 3

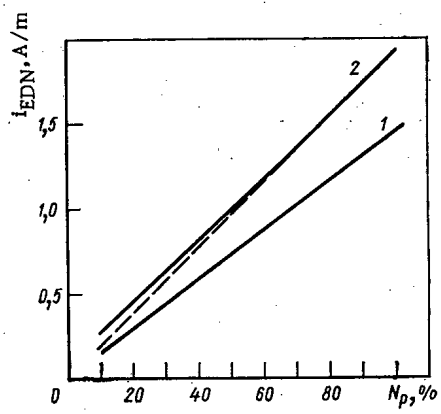

Fig. 4

Fig. 3. Dependence of cable background current, referred to unit γ-radiation dose intensity, on $P_\gamma R_{In}$: 1) Curve corresponding to formula (10); 2, 2') confidence limits, with confidence coefficient 0.99; ●) tests with independent change of radiation intensity and temperature; ◑, ◐, ○) tests of nine cables with different positions in the reactor.

Fig. 4. Calculated dependence of EDN current on reactor capacity: 1, 2) coolant temperature 50 and 280°C respectively.

where i_{EDN} is the EDN current, referred to 1 m length of detector, A/m; ϕ_T is the average thermal neutral flux along the length of the sensitive part of the detector, $n/cm^2 \cdot sec$; R_{In} is the resistance of the detector insulation, referred to 1 m of its length, ohm·m. Figure 2 shows the curve corresponding to formula (5), and the confidence limits for a unidirectional confidence coefficient of 0.99.

Relations (2) and (5) are responsible for a γ-irradiation dose intensity of $2 \cdot 10^3$–$1.5 \cdot 10^5$ rad/sec, with values of the first neutron flux, of energy greater than 1 MeV, within the limits $6 \cdot 10^{10}$–$6 \cdot 10^{12}$ $n/cm^2 \cdot sec$ and with values of the thermal neutron flux of $1 \cdot 10^{12}$–$1 \cdot 10^{14}$ $n/cm^2 \cdot sec$. The low temperature limit of applicability of the formulas (for the series of measurements given) is equal to $(4 \cdot 10^{-3} P_\gamma)$°C, where P_γ is expressed in rad/sec and the upper temperature limit is 720–750°C.

The tendency to flattening out of the curve shown in Fig. 2 for large values of the factor $\phi_T R_{In}$ permits the conclusion to be drawn that EDN having a high insulation resistance at working temperatures and a relatively high intensity of β-particle generation in the emitter, should have the greatest stability with respect to sensitivity.

TABLE 1. Insulation Resistance and Cable Background Current for Different Radiation Intensities and Integrated Doses*

γ-radiation dose intensity, rad/sec	Temperature, °C	Integrated fast neutron flux, n/cm²											
		3,0·10¹⁷		1,6·10²⁰		2,0·10²⁰		2,8·10²⁰		4,6·10²⁰		8,8·10²⁰	
		R_{In}	i	R_{In}	i	R_{In}	i	R_{In}	i	R_{In}	i	R_{In}	i
1,8·10⁴	160	—	—	2,1·10⁹	7,9·10⁻⁹	5,8·10⁸	1,2·10⁻⁸	1,4·10⁸	2,1·10⁻⁸	2,2·10⁹	1,6·10⁻⁸	—	1,1·10⁻⁸
3,6·10⁴	220	1,9·10⁹	1,7·10⁻⁸	9,6·10⁸	1,6·10⁻⁸	4,3·10⁸	1,9·10⁻⁸	—	—	1,2·10⁹	2,6·10⁻⁸	—	1,6·10⁻⁸
7,2·10⁴	320	5,8·10⁸	3,3·10⁻⁸	4,2·10⁸	2,7·10⁻⁸	2,8·10⁸	2,8·10⁻⁸	—	—	5,3·10⁸	4,2·10⁻⁸	—	3,2·10⁻⁸
1,1·10⁵	440	1,4·10⁸	4,8·10⁻⁸	1,4·10⁸	3,7·10⁻⁸	1,6·10⁸	3,7·10⁻⁸	—	—	2,7·10⁸	5,4·10⁻⁸	3,2·10⁸	4,3·10⁻⁸
1,4·10⁵	520	3,2·10⁷	6,6·10⁻⁸	6,3·10⁷	4,6·10⁻⁸	—	—	2,7·10⁷	6,7·10⁻⁸	1,3·10⁸	6,6·10⁻⁸	1,8·10⁸	5,7·10⁻⁸
1,8·10⁵	590	9,3·10⁶	9,4·10⁻⁸	2,6·10⁷	5,7·10⁻⁸	—	—	1,4·10⁷	8,1·10⁻⁸	—	—	—	—

*Insulation resistance R_{In} in ohm·m, and background current i in A/m.

The nature of the sensitivity dependence of EDN on the height of the potential barrier has not been explained, however in future when considering this effect it should be taken into account that, with fast electrons "shooting through" thin films of magnesium oxide [10], a large number of secondary emission electrons are formed, with energies of the order of several electron-volts, and that these electrons are moving mainly from the emitter to the collector. At the same time, according to estimates made, the height of the potential barrier for the conditions of radiation and temperature corresponding to the experimental results shown in Fig. 2, is varying over the limits 0.003 to 30 V. The change of sensitivity of the EDN can be caused by a change of distribution of the electric potential in the dielectric as a function of the level of reactor radiation and temperature, and the effect of this changing distribution on the passage of the secondary emission electrons.

Data on the resistance of the cable insulation were processed just as in the case of the EDN. Empirical relations were obtained between R_{In} and the temperature and radiation intensity: for 150-500°C

$$R_{rad} = 3.3 \cdot 10^{15} T^{-3/2} P_\gamma^{-0.81}, \quad (6)$$

$$R_t = \exp(10400/T + 6.6); \quad (7)$$

and for temperature of 500-720°C

$$R_{rad} = 4100 T^{-3/2} P_\gamma^{-0.81} \exp(18.8 + 8300/T), \quad (8)$$

$$R_t = \exp(18200/T - 3.3). \quad (9)$$

The resistance of the cable insulation R_{In} in the reactor can be determined from formula (1) by means of Eqs. (6)-(9); for this calculation, the confidence limits for unidirectional confidence coefficient of 0.99 correspond to a change of R_{In} from 0.2 to $5R_{In}$.

The resistance of the cable insulation is higher by one or two orders than the resistance of the EDN insulation at the same temperature and radiation intensity. The difference between the values of the insulation resistance outside the reactor and in the reactor, at the same temperature, is considerably less for the cable than for the EDN. With values of the γ-radiation dose intensity of $2.8 \cdot 10^3$-$1.4 \cdot 10^5$ rad/sec, the resistance of the cable insulation depends weakly on the radiation intensity in comparison with the temperature dependence; however, it is stronger by far than in the case of the EDN.

The cable background current is proportional to the radiation intensity at low temperatures and has a polarity which corresponds to a "minus" sign in the core of the cable [6]. In contrast to the EDN current, the main contribution to the generation of the cable background current is carried by the reactor γ-radiation [6]. When processing the experimental data on the cable background current, just as for the EDN, the potential barrier representation was used. Analysis of the data showed that for a constant value of the product $R_\gamma R_{In}$ (γ-radiation dose intensity and insulation resistance) the cable current, referred to unit dose of γ-radiation, depends weakly on the temperature and intensity of the γ-radiation dose. Data on the cable current are represented in Fig. 3 as a function only of the product $P_\gamma R_{In}$. As a result of processing the points of this relation, an empirical relation was obtained between the cable current and the γ-radiation dose intensity, and the factor $P_\gamma R_{In}$:

$$|i_k| = i_0 + 3.6 \cdot 10^{-14} P_\gamma [3.9 \lg(P_\gamma R_{In}) - 40], \quad (10)$$

where $|i_k|$ is the absolute value of the cable current, referred to unit length of cable, A/m; i_0 is the component of the background current, which is independent of the radiation intensity and the temperature, A/m; R_{In} is the resistance of the cable insulation, referred to unit length of cable, ohm·m and P_γ is the γ-radiation dose intensity, rad/sec.

For a cable functioning in the active zone for a long time (up to an integrated neutron flux of order $3 \cdot 10^{17}$ n/cm^2), the value of i_0 is equal to $(1\text{-}2) \cdot 10^{-9}$ A/m, i.e., it amounts to a very small fraction of the total current. The curve obtained from formula (10) is plotted in Fig. 3 and also the confidence limits for the quantity $|i_k - i_0|/P_\gamma$ for a unidirectional confidence coefficient of 0.99. The limits of applicability of formulas (6) and (8) with respect to radiation intensity and temperature coincide with the corresponding limits for formula (2).

In addition to the tests of four cables in the experimental device mentioned above, nine samples of cable were also tested at three other cable positions in the active zone at other values of radiation fluxes [6]. Plotted in Fig. 2 are the experimental results which correspond to the results of these tests and which, as seen from the figure, agree very well with the results of the tests on the four samples. Such good agreement was obtained also in the comparison of the data on the insulation resistance. As a result of the measurements carried out on the nine cable samples, the dependence was obtained of the insulation resistance and cable background current on the level of the reactor radiations for different values of the integrated radiation dose (see Table). The temperature of the samples varied within the limits 160-590°C, on account of radiation heating, depending on the radiation intensity.

By processing the values of R_{In} given in the table, the dependence of R_{In} on the integrated fast neutron flux was obtained:

$$R_{In} \doteq R_0 \exp(3.6 - 2300/T + 0.12\phi\delta t \cdot 10^{-20}), \quad (11)$$

where R_0 is the insulation resistance, calculated by formulas (1) and (6)-(9) and with a corresponding integrated fast neutron flux of order 10^{17} n/cm^2, expressed in ohm·m; T is the absolute temperature, °K and $\phi\delta t$ is the integrated fast neutron flux, n/cm^2.

Formula (11) is obtained on the assumption that R_{In} depends on the radiation intensity considerably more weakly than on the temperature, and is suitable for a rough estimate of R_{In} with an integrated fast neutron flux of up to $9 \cdot 10^{20}$ n/cm^2. With increase of the integrated flux, the value of R_{In} increases or remains approximately constant (depending on the temperature), and therefore in order to estimate R_{In} below, formulas (1) and (6)-(9) can be used.

For an estimate from above of the value of the background current for specified temperature, radiation intensity and integrated fast neutron flux (up to $9 \cdot 10^{20}$ n/cm^2), formula (10) can be used. Significant deviations up to 35% on the lower side of the values obtained by this formula are observed only at $(1.6\text{-}2) \cdot 10^{20}$ n/cm^2. The component of the background current i_0, independently of the radiation intensity, is determined by the operating conditions of the reactor during buildup of the integrated radiation doses. In this experiment, it varied within the limits of $(1\text{-}16) \cdot 10^{-9}$ A/m, but did not exceed 20% of the total current for a dose intensity of $1.8 \cdot 10^5$ rad/sec.

We shall consider the error in measuring the energy release distribution by means of EDN, due to temperature effects. The difference in temperature of detectors positioned at different places in the active zone of the reactor should be reduced, as far as possible, to a minimum. In reactors where the coolant temperature (for example, in a steam—water mixture) is constant with sufficient accuracy, the main reason for the temperature differences of the detectors is the indeterminancy of positioning the detector in a dry channel, causing considerable differences in the magnitude of the temperature drops due to radiation heating. In a calculation, carried out by using relations (1)-(5) for an EDN monitoring system, of the energy release distribution of a large power reactor of the channel type, the spread of the EDN current variations due to temperature effects amounted to ±5%. The calculated dependence of the EDN current of a power reactor on the capacity of the reactor is shown in Fig. 4.

The dependence of the EDN sensitivity on the neutron flux defines the range of operation of the EDN for a specified nominal flux value. In practice, a reduction of the neutron flux usually is associated with a reduction of temperature of the detectors and, consequently, also with an increase of the resistance of the insulation, which promotes stabilization of the factor $\phi_T R_{In}$, i.e., also of the sensitivity of the detector.

The results obtained in this present paper confirm the validity of the assumption concerning the important role of electric fields in EDN insulation for the process of current generation in the detector [11].

LITERATURE CITED

1. I. Ya. Emel'yanov et al., Atomnaya Énergiya, Vol. 30, p. 375 (1971).
2. C. Joslin, Nucl. Eng. Intern., Vol. 17 (1972), p. 399.
3. I. Ya. Emel'yanov et al., Atomnaya Énergiya, Vol. 27 (1969), p. 230.
4. V. F. Suchkov et al., Élektrotekhnicheskaya Promyshlennost'. Kabel'naya Tekhnika, No. 72 (1971), p. 30.
5. V. F. Suchkov et al., Élektrotekhnicheskaya Promyshlennost'. Kabel'naya Tekhnika, No. 95 (1973). p. 3.
6. V. F. Suchkov et al., Corrosion Resistant Cables with Magnesial Insulation [in Russian], Énergiya, Moscow (1969).
7. G. Dau and M. Davis, Nucl. Sci. and Engng, Vol. 25 (1966), p. 223.
8. A. Weinberg and E. Wigner, Physical Theory of Nuclear Reactors [Russian translation], Foreign Literature Publishing House, Moscow (1961), p. 2.
9. H. Warren, Nucl. Sci. and Engng., Vol. 48, p. 331 (1972).
10. Secondary-emission and Structural Properties of Solids [in Russian], Fan, Tashkent, (1970), p. 89.
11. K. Mochizuki et al., Symposium on Nuclear Power Plants Control and Instrumentation, Prague, 22-26 January 1973, IAEA/SM-168/G-6.

THE PROBLEM OF CALCULATING A POLYCELL IN P_3-APPROXIMATION

A. D. Galanin, V. V. Smelov and B. Z. Torlin

UDC 621.039.512.25

For the one-velocity calculations of complex cells in P_3-approximation in [1, 2], certain differences are suggested between the procedure itself. In [1], the neutron field both inside the slug and outside of it, down to a certain arbitrary limit, and differing from the field of the adjoining slugs, is described by a series which takes into account certain azimuthal harmonics of the field. The field of the adjacent slugs is approximately (on average) "matched" to this arbitrary limit.

It is assumed in [2] that the "inherent" field of every slug possesses cylindrical symmetry. The neutron field outside of the slugs is equal to the sum of the intrinsic field of all slugs of the lattice, and therefore they depend on the azimuthal angle. As the basic assumptions made in these papers are different, then it will be interesting to compare them by some example.

For this purpose, a series of calculations was carried out on several variants of a double hexagonal lattice with a 1 : 3 ratio of the number of slugs of first and second type. Both slugs are circular, with external and internal radii of the ring 2.5 and 2 cm respectively. The moderator inside and outside of the ring was assumed to be nonabsorbing with a scattering length of 2.5 cm. The scattering length of the material of the ring-shaped slugs was assumed equal to 10 cm.

In such a cell, the dependence of the "inherent field" on the azimuthal angle φ should be, for a slug of the first type (see Fig. 1):

$$a = b\cos 6\varphi_1, \tag{1}$$

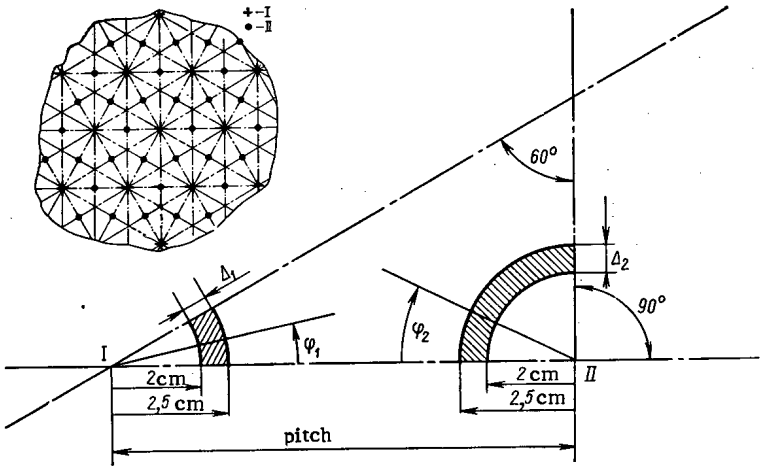

Fig. 1. Arrangement of slugs in the lattice being considered (the chained lines show the axis of symmetry). I) Slug of first type; II) slug of second type.

Translated from Atomnaya Énergiya, Vol. 37, No. 1, pp. 76-77, July, 1974. Original letter submitted August 13, 1973.

TABLE 1. Comparison of Values of Mutual Slug Effect, Calculated by Means of the Procedure from [1, 2]

Lattice pitch, cm	$\Delta_1\Sigma_{a1}$	$\Delta\Sigma_{a2}$	$\bar{\Phi}_2/\bar{\Phi}_1$		δ, * %
			[1]	[2]	
7,5	0,05	0,20	0,7394	0,7410	0,2
10			0,6919	0,6921	0,03
15			0,6402	0,6401	0,016
7,5	0,10	0,50	0,5212	0,5242	0,24
10			0,4724	0,4730	0,12
15			0,4263	0,4264	0,025
7,5	0,20	1,00	0,3784	0,3817	0,9
10			0,3438	0,3448	0,3
15			0,3148	0,3152	0,13

*Divergences between results, obtained by means of the procedures from [1, 2].

and for a slug of the second type:

$$c + d\cos 2\varphi_2. \qquad (2)$$

Neglect of this effect in [2] would be expressed in the accuracy of the results.

The values of the mutual slug effect (ratio of the average fluxes in ring-shaped slugs of second and first type $\bar{\Phi}_2/\bar{\Phi}_1$), calculated by means of the procedures taken from [1, 2], are shown in Table 1 for a number of values of the product of thickness Δ and the microscopic absorption cross-section Σ_a of the ring-shaped slugs of first and second type ($\Delta\Sigma_{a1}$ and $\Delta\Sigma_{a2}$ respectively). It can be seen that the divergence in the values of the mutual slug effect are almost insignificant, but for more closely packed lattices and with greater absorption, these divergences are somewhat larger. But even for lattices with such strong absorption as in the last three variants, neglect of the azimuthal dependence of the "intrinsic field" of the slug in the method from [2] did not lead to significant errors.

LITERATURE CITED

1. V. V. Smelov, Atomnaya Énergiya, Vol. 33, No. 5, 915 (1972).
2. A. D. Galanin and B. Z. Torlin, Atomnaya Énergiya, Vol. 35, No. 2, 125 (1974).

MEASUREMENT OF CERTAIN CHARACTERISTICS OF ^{249}Bk

V. M. Glazov, R. I. Borisova, and A. I. Shafiev

UDC 539.16

In the series of isotopes of berkelium with mass numbers 243-250, the isotope ^{249}Bk is of practical interest. The possibility of accumulation of this isotope in amounts of several milligrams permits its use in a more profound study of the physical and chemical properties of compounds. The wide use of this isotope necessitates a knowledge of certain nuclear characteristics of ^{249}Bk. The purpose of this work was to determine the maximum energy of the β particles of ^{249}Bk and its half-life.

In the work we used a preparation of ^{249}Bk isolated and purified of trivalent elements by repeated sorption of its tetravalent ions on zirconium phosphate from a solution of 1 N nitric acid, freed of cerium on an anion exchange resin [1]. The purity of the preparation of ^{249}Bk was verified by measuring the boundary energy of β radiation, as well as by $\gamma-\alpha$-spectrometry.

In this work the maximum β radiation energy of ^{249}Bk was determined by two methods: on the basis of the Curie graph and by the method of absorption.

The β spectrum of ^{249}Bk was measured with a stilbene crystal detector with a FÉU-13. To construct the Curie graph (Fig. 1) we calibrated the spectrometer according to conversion electrons on the basis of the isotope ^{144m}In, ^{113}Sn, and ^{137}Cs. As can be seen from Fig. 1, in the region of low energies a deviation of the Curie graph from linearity is observed, which is associated with the influence of the finite thickness of the source. The maximum energy of the β particles of ^{249}Bk, determined on the basis of the Curie graph, considering the error, was 123 ± 3 keV.

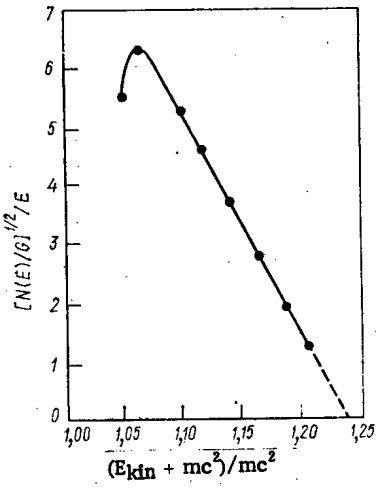

Fig. 1. Curie graph for the β particles of ^{249}Bk.

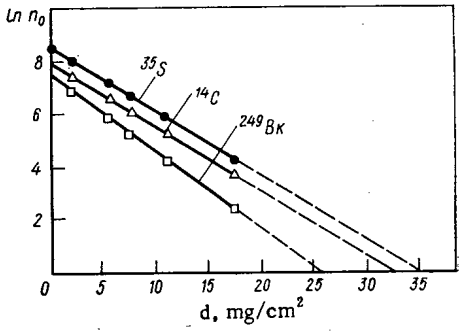

Fig. 2. Curves of the absorption of β particles in aluminum.

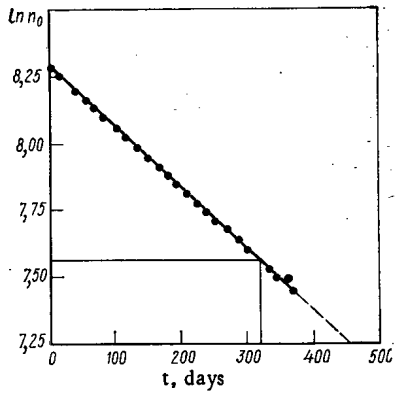

Fig. 3. Determination of the half-life of ^{249}Bk.

Translated from Atomnaya Énergiya, Vol. 37, No. 1, pp. 78-79, July, 1974. Original letter submitted November 4, 1973, revision submitted November 27, 1973.

The method of absorption is based on a comparison of the maximum β particle energies of the isotopes, the energies of which have been sufficiently well determined, with the energy of the unknown isotope. In this work, the absorption curves were taken on a T-25-BFL counter with thickness of mica 1 mg/cm^2 for isotopes with β radiation energy (^{14}C with E = 155 keV; ^{35}S with E = 167 keV) and for ^{249}Bk, the energy of which had to be determined (Fig. 2). The experimental value of the maximum energy of the β particles of ^{249}Bk, determined by this method, proved equal to 124 ± 3 keV. According to the published data, the boundary energy of the spectrum of β particles is 80 ± 20 [2], 100 ± 20 [3], 114 ± 15 [4], and 125 ± 2 keV [5]. Thus, the results of this work are in good agreement with the data of [5].

The half-life of ^{249}Bk was determined by a radiometric method. The activity was measured for one year with a T-25-BFL end-window counter with an accuracy of 0.5%. The stability of the setup was verified according to a preparation of ^{14}C. During the entire period of measurements, the apparatus errors did not exceed the set statistical error, equal to 0.5%, at the 95% confidence level.

The results of the experiment are shown in Fig. 3. The value found for the half-life of ^{249}Bk was 325 ± 7 days. According to the published data, the half-life of ^{249}Bk is equal to 290 ± 20 [2] and 314 ± 8 days [4]. It is evident that the results of this work are in good agreement with the data obtained by other authors [4].

LITERATURE CITED

1. F. Moore, Analyt. Chem., 43, 138 (1968).
2. L. Magnusson et al., Phys. Rev., 96, 1576 (1954).
3. H. Diamond et al., Phys. Rev., 94, 1083 (1954).
4. J. Eastwood et al., Phys. Rev., 107, 1635 (1957).
5. R. Vandenbosch et al., Phys. Rev., 115, 115 (1959).

USE OF RADIATIVE CAPTURE OF THERMAL NEUTRONS TO DETERMINE THE ASH CONTENT OF COAL

L. P. Starchik and Yu. N. Pak

UDC 621.039.89

Various methods have been suggested for monitoring the ash content of coal and its concentration products on the basis of the absorption and scattering of x-rays and gamma rays [1]. Many of these methods are used to analyze concentrated coal. The possibility of determining the ash content of run-of-mine coal by the absorption of hard gamma radiation was demonstrated by Klempner et al. [2]. However, the action of such disturbing factors as variations in grain-size composition and moisture content distort the results of the ash content measurements.

Analysis of the neutron physics of coal reveals that the ash content can be determined by means of the gamma radiation emitted by radiative capture of thermal neutrons.

The coal is made up mainly of carbon and the ash-forming elements. About 95% of the ash is made of aluminum, silicon, sulfur, calcium, and iron. The cross section of the carbon nucleus for the radiative capture of thermal neutrons is so small (about 3 mb) that the gamma radiation arising in this reaction can be neglected. For the ash-forming elements, the capture cross section is about two orders of magnitude higher. The most intense gamma lines due to capture of thermal neutrons by the nuclei of ash-forming elements lie in the region from 4.93 MeV (Si) to 7.73 MeV (Al) [3].

The measurement geometry is shown in Fig. 1. The coal sample is placed in a paraffin reflector between a Po–Be neutron source with a power of about 10^7 neutrons/sec and an NaI(Tl) scintillation detector 80 × 80 mm in size. As a protection against activation and to reduce the background radiation, the detector is surrounded by a screen containing boron, with a density of 3.6 g/cm^2, and is protected from the direct radiation of the source by a lead cone 10 cm long.

Increase in the cell diameter above 50 cm gives practically no increase in the rate of capture of gamma radiation with energies from 5.0 to 7.8 MeV. The optimum thickness of the coal layer was determined from the condition of maximum independence of the measurement results from disturbing factors, in particular the moisture content of the coal. In estimating the ash content of coal from a borehole by means of the (nγ) reaction, Yakubson et al. [4] obtained independence from the moisture content by registering the ratio of the gamma-ray intensities in two energy ranges, E_1 = 1.5–2.5 MeV and E_2 = 3.0–10.0 MeV.

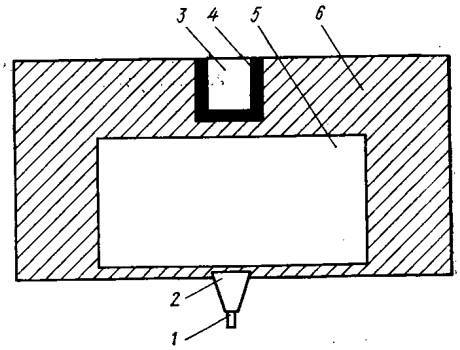

Fig. 1. Measurement geometry. 1) Po–Be neutron source; 2) lead cone; 3) NaI(Tl) scintillation detector; 4) boron screen; 5) coal sample; 6) paraffin reflector.

Translated from Atomnaya Énergiya, Vol. 37, No. 1, pp. 79-80, July, 1974. Original letter submitted January 14, 1974.

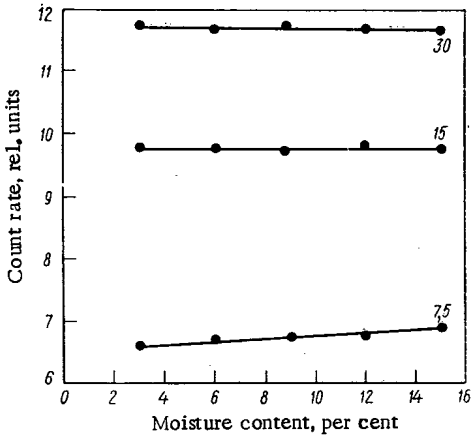

Fig. 2. Count rate of gamma radiation with E_γ = 5.0-7.8 MeV vs. moisture content of coil. Numbers on curves represent thicknesses of coal layers in centimeters.

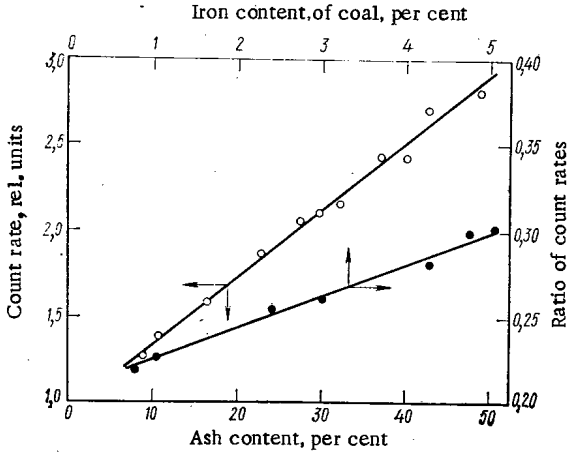

Fig. 3. Calibration curves for determining ash content and iron content of steel.

The Monte Carlo method was used to calculate the distribution of slow neutrons in a hydrogen-containing substance [5]; it was found that at certain distances from the source, the density of the flux of slow neutrons is independent of the moisture content. This was used in choosing the thickness of the test sample of coal. For thicknesses from 15 to 30 cm, the moisture content has practically no effect; for smaller thicknesses (7.5 cm) an increase in moisture content leads to a rise in the gamma quantum count rate at 5.0-7.8 MeV (Fig. 2).

If the layer thickness is between 15 and 30 cm, the bulk density of the coal has a slight influence on the results of an ash content determination (a 15% increase in density leads to a 1.8% increase in count rate).

On the basis of the experimental results we chose a nearly optimal measurement geometry: the cell diameter was 50 cm and its thickness 22 cm.

The count rate most closely and sensitively correlated with the ash content is that between 5.0 and 7.8 MeV (Fig. 3). The error in the analysis of the ash content was 5 rel. % for ash contents up to 50% and a measurement time of 30 min. The fragment size of the coal was 0-25 mm. The weight of the sample was about 50 kg. The background equivalent to the ash content was 4.7%.

The accuracy of determination of the ash content by means of the rate of capture gamma radiation can be influenced by variation in the elementary composition of the ash, mainly by the iron content, because the macroscopic cross section for capture of thermal neutrons by an iron nucleus is several times greater than those for the other ash-forming elements [3]. Therefore the results of analysis of the ash content must be corrected for the iron content of the coal.

The iron content can be monitored independently of the ash content by measuring the ratio of the count rates in the regions 6.6-7.8 MeV and 4.0-5.0 MeV (see Fig. 3).

In the chosen measurement geometry, as well as the (nγ) reaction there may be inelastic scattering of fast neutrons. The (n, n', γ) reaction on carbon leads to the formation of 4.43 MeV gamma rays, which lie below the chosen energy range. The contribution made by 6.1 MeV gamma rays due to inelastic scattering by oxygen nuclei does not interfere with the ash content analysis, because oxygen in the coal is mainly combined with ash-forming elements.

By using the radiative capture of thermal neutrons we can determine the ash content of coal, and by using semiconductive detectors with large sensitive volumes we can analyze the elements contained in the ash.

LITERATURE CITED

1. A. A. Radanovskii, Radioactive Isotopes in Mining and Mineral Processing [in Russian], Atomizdat, Moscow (1965).
2. K. S. Klempner et al., Zavod. Lab., 36, No. 10, 1213 (1970).
3. L. V. Groshev et al., Atlas of Gamma Ray Spectra from Radiative Capture of Thermal Neutrons [in Russian], Atomizdat, Moscow (1958).
4. K. I. Yakubson et al., Radioisotope Devices in Industry and Geophysics [in Russian], Vol. 2, MAGATE, Vienna (1966).
5. V. N. Starikov and F. Kh. Enikeeva, At. Énerg., 27, No. 3, 219 (1969).

INFORMATION

BLACK HOLES ARE REAL

N. A. Vlasov

The astrophysical riddle of "black holes" is assuredly one of the most interesting and basic problems of modern physics. Its study touches upon the most fundamental concepts of space-time and of the evolution of the universe.

The name of "black holes" has been given to celestial bodies whose radius is smaller than the so-called gravitational radius $R_2 = 2GM/c^2$ (where G denotes the gravitational constant). The principal possibility of the existence of black holes is unquestionable and follows from the fact that the gravitational potential, reciprocal to the radius of the body, is unlimited and, if the radius of a body is less than its gravitational radius, no known forces can prevent collapse. As long ago as in the 18th century Laplace noted that one can imagine a body from which it is impossible to escape even at a velocity of light, and gave the correct radius which has been later called the gravitational radius. In fact, neither photons nor neutrons can escape from under the gravitational radius, not to mention particles with a finite rest mass. The sense of the name "black hole" is thus quite clear.

Although the theoretical aspects of black holes have never been questioned, it is not clear whether conditions of their formation are realizable.

The notion that black holes can actually exist grew up in the first half of the present century in connection with the analysis of stellar evolution. With all the immense multitude of processes participating in stellar evolution one can note one common trend: the growth of the density of matter in the interior of stars. The condensation of matter is caused by gravitational contraction. In Sun type stars this condensation is opposed by the kinetic pressure of matter heated by nuclear reactions. When the fuel ends, further contraction and condensation of matter is inevitable. Ultimately, the star can evolve into a white dwarf, a neutron star, or black hole. In white dwarfs and in neutron stars, gravitational contraction is opposed by degenerate electron and neutron gas respectively, whereas in a black hole contraction overcomes any internal pressure.

The particular course of evolution depends on the mass of the star. A star with a mass equal or less than that of the Sun becomes a white dwarf, stars with a mass of one and one half to three solar masses turn into neutron stars, while those with masses more than three times the solar mass should become black holes. The limiting mass separating neutron stars from black holes is not very well known as it depends on still obscure properties of matter of a higher density than nuclei. Nevertheless, three solar masses are considered to be the upper limit of neutron stars. Any star which at the end of its evolution has a mass of more than three solar masses should become a black hole.

The masses of known stars range from tenths to several tens (~60) of solar masses. Still heavier stars are unstable. The probability of formation of stars with different masses is not very well distinguished. If in the course of their evolution stars were to lose no mass, most stars would turn into black holes. However, there is no proof that some mechanism may not exist by means of which a star loses its mass so that the formation of black holes is prevented. Many such mechanisms are now known in astrophysics: from eruptions on cold planets to giant supernova explosions. Thus, notwithstanding its obvious inevitability, the formation of black holes was a hypothesis in need of a conclusive proof.

The discovery of pulsars, which are generally thought to be rotating neutron stars, heightened the belief in the reality of black holes, and stipulated a vigorous discussion and search for such stars. The existence of at least one such black hole has been, apparently, quite conclusively proved [1-3].

Translated from Atomnaya Énergiya, Vol. 37, No. 1, pp. 81-82, July, 1974.

Near the center of the cross in Cygnus,' well visible in our sky, there is a recently discovered x-ray source of variable intensity (Cygnus XI). It has been found that the source coincides with a double star of which only one component is visible. By various estimates, the mass of this invisible component is six times the solar mass. With such a large mass, the invisible body should be a black hole as can be inferred from various conclusions. X-ray radiation is emitted by matter falling onto the black hole. From the large visible star matter flows to the invisible dense star. This matter forms around the black hole a disk similar to the rings of saturn. The smaller the radius of the disk the faster it rotates. Friction between the disk layers causes heating and radiation. The radiation comes not from the black hole proper but from matter still rotating in its gravitational field. An analysis of many observations of the quite characteristic variability of x-ray and visible radiations of the source in Cygnus provides convincing evidence that one of the double-star components is actually becoming a black hole. For an external observer, the transition process is infinitely long, but in the coordinates of the star time flows much faster and the gravitational radius is crossed in a finite and quite short time. That which takes place for an internal observer after the gravitational radius is crossed constitutes an unattainable future for an external observer. Such are the inevitable conclusions of the relativistic lack of clock coordination. Thus, strictly speaking, an external observer can see only the process of contraction until matter crosses the gravitation radius and can never witness the instant of closure.

If the mass of the invisible component of the double star in Cygnus is actually six times the mass of the Sun, its radius must be at least 18 km as the gravitational radius of the Sun is nearly 3 km. Thus, the dimensions of black holes as observed from the outside are very close to the dimensions of nuclear stars whose radii are of the order of 10 km. Consequently, the differences between a neutron star and a collapsing black hole are not especially great for an external observer.

Other possible black holes have also been mentioned but with much less convincing evidence. For example, I. S. Shklovskii [4] suggested that the x-ray source in Scorpius is a black hole. However, in subsequent publications the source "paled" until it has been declared to be a white dwarf. Of particular interest was also a quite long list of double stars among which an invisible component of large enough mass has been looked for, however, only for one of them we have sufficiently convincing evidence for assuming it to be a black hole.

Several different mechanisms of black hole formation are theoretically possible. For example, in very dense matter, such as the expanding Universe is supposed to have been in the distant past, black holes of any, including very small masses could have formed as a result of local condensations. However, all these hypotheses and their modifications such as the suggested fall of black holes to the Earth and their explosions, etc., are not nearly as realistic as the formation of black holes in the process of stellar evolution. The former hypotheses may be difficult to disprove, but are still harder to confirm and all the more to prove.

Black holes are also interesting as marginal objects in the relativistic theory of gravitation. In the course of their formation and evolution, up to 30% of their rest energy can be emitted as electromagnetic, neutron, and gravitational radiation. The rest is forever hidden from our world: all that remains is a gravitational field in the form of a bottomless sinkhole in curved space-time. It has been proved that the mass of a black hole cannot be diminished by any means so that no energy can ever be taken out of it [5]. Modern physics has still not fully mastered such storage objects in the neighborhood of which elementary mechanical processes are irreversible and the familiar law of conservation of the baryon charge becomes meaningless, i.e., ceases to be a law. Several ways out of this difficulty have been suggested. Pati and Salam [6] suggested, for example, that the baryon charge is in general not conserved in weak interaction processes but no free proton decay is observed because such a decay must take place through virtual quarks so that its probability is exceedingly low. This, however, can be considered as an example of a revision of the most fundamental physical concepts caused by speculations about the process of gravitational collapse and the formation of black holes. The future promises not less interesting results of further explorations and deliberations.

LITERATURE CITED

1. M. Ruderman, Ann. Rev. Astr. Aph., 10, 427 (1972).
2. B. Margon et al., Aph. J. Lett., 185, 113 (1973).
3. J. Bregman et al., Aph. J. Lett., 185, 117 (1973).
4. I. S. Shklovskii, Astron. Zh., 50, 233 (1973).

5. J. Bekenstein, Phys. Rev., D7, 949 (1973).
6. J. Pati and A. Salam, Phys. Rev. Lett., 31, 661 (1973).

35TH SESSION OF THE ACADEMIC COUNCIL OF THE JOINT INSTITUTE OF NUCLEAR RESEARCH

V. A. Biryukov

The 35th Session of the Academic Council of the Joint Institute of Nuclear Research (JINR) took place on January 15-18, 1974. The Session was attended by leading scientists of ten Socialist member-countries. The Session summarized the achievements of the Institute in 1973 and approved the research activities planned for 1974.

The Institute's Director N. N. Bogolyubov reported on the fulfillment of the resolutions of the Academic Council. He stressed the importance of the new five-year plan for the future growth of the Institute. In the name of the Board of Directors and of the Academic Council, N. N. Bogolyubov congratulated the staff of the oldest laboratory of the Institute, the Laboratory of Nuclear Problems, on the occasion of the 25th Anniversary of its organization. Scientists of this laboratory heavily contributed to progress in physics of elementary particles and atomic nuclei, in reactor physics and engineering, and to the development of original methods of investigations. The laboratory enjoys well-earned world-wide recognition in all nuclear centers.

Summary reports have been presented by the Directors of the JINR laboratories.

D. I. Blokhintsev told about the new work of the scientists of the Laboratory of Theoretical Physics. Much work has been done last year on the study of self-similar asymptotics within the scope of the general principles of the quantum theory of fields. They were discussed both as a purely theoretical topic and in application to experimental analysis. Conditions have been determined for spectral functions under which the electromagnetic differences in proton and neutron masses is finite. New results have been obtained in studies of the self-similar behavior of interaction processes of high-energy particles.

An asymptotic analysis has been carried out for several quantum-field models based on the composite Young–Mills field which are free from "null-charge" difficulties.

Progress has been achieved in the quasi-potential theory of high-energy particle scattering. Predictions have been made for planning future experiments in the high energy range including experiments in the Batavia and CERN accelerators.

Experimental data on Π-p and Π-n interactions with a 40 GeV/sec momentum, obtained in the Serpukhov accelerator with the aid of a two-meter propane chamber, have been described in cooperation with the scientists of the Laboratory of High Energies on the basis of a coherent state model.

Nonlinear and nonlocal field theories have been advanced including some important calculations in the domain of high and low energies (the pion form factor $F_\pi(t)$).

The nuclear level densities at moderate and high excitation energies have been calculated on the basis of the semimicroscopic approach. The results were found to be in good agreement with experimental data obtained at neutron binding energies. Calculations indicate that large density fluctuations take place in nearly magic and intermediate spherical nuclei even at neutron binding energies and that large differences should be observed in the number of levels with positive and negative parity.

Translated from Atomnaya Énergiya, Vol. 37, No. 1, pp. 82-85, July, 1974.

It has been shown that interactions of ions with nuclei at energies close to the Coulomb barrier give rise to an interference effect involving nuclear forces. This causes drastic changes in cross sections as a function of energy and scattering angles as observed experimentally.

A. M. Baldin reviewed the activity of the Laboratory of High Energies. The 70-GeV accelerator of the Institute of High-Energy Physics (Serpukhov) has been used to study the asymptotic behavior of scattering amplitudes of neutral kaons. A magnetic spectrometer with an on-line computer gave the following results: the $K_L^0 \rightarrow K_S^0$ regeneration amplitude modulus in deuterium has been found to decrease with the incident kaon momentum and the phase of this amplitude, to be independent of the kaon energy (the phase is $-135 \pm 4°$). This agrees with the predictions of the model of complex angular momenta for the case of omega-pole exchange. The energy dependence of the regeneration amplitude modulus in neutrons has been obtained, and the kaon regeneration amplitude in carbon and the phase of this amplitude have been measured. The experimental material has been analyzed at the JINR as well as at the Central Institute of Physical Research (Budapest), the Physics Institute of the Czechoslovak Academy of Sciences (Prague), and at the Institute of High-Energy Physics (Berlin). The analysis of data on the dependence of the vector and scalar form factors of a neutral kaon on the imparted momentum has been completed. It has been shown that assuming $\mu - e$ universality, it is possible to obtain a single solution for the linear parametrization constants of the form factors. Experimental data on elastic small-angle pd scattering, obtained on the same accelerator, have been used to find the nuclear form factor of deuterons. Physicists of the JINR, the Institute of High-Energy Physics (Serpukhov), and the University of California (USA) using the magnetic spark spectromenter analyzed the elastic small-angle scattering of negative pions by protons at 50 GeV. The ratio of the real fraction of the amplitude to the imaginary fraction for elastic forward scattering has been found to be -0.07 ± 0.05.

The Π-p, Π-n, and Π-K interactions at 40 GeV have been studied with the aid of a two-meter propane chamber jointly by 16 laboratories of the member-countries. Preliminary results have been obtained in verifying the inferences of the generalized optical theorem and the Regge-poles model for nuclei.

The interaction of ~3-GeV deuterons has been studied in the Dubna proton synchrotron using a one-meter hydrogen chamber exposed to a separated deuteron beam. The process cross sections for silver, bromine, and oxygen nuclei have been determined in an investigation of the interaction of relativistic α particles (17 GeV momentum) with photoemulsions.

In methodical developments one should especially mention the start-up of a facility equipped with an SKM-200 two-meter streamer chamber. A set of proportional chambers with dimensions 15×15, 20×20, and 90×30 cm has been built. Eight proportional chambers and 40 1×1 m spark chambers have been prepared for the "Foton" facility under construction.

The proton synchrotron has been used to accelerate α particles to an energy up to 20 GeV. Two new secondary-particle channels leading from internal targets and four channels for the extracted beam have been assembled.

A plan has been proposed in cooperation with the Radio Engineering Institute of the Academy of Sciences of the USSR for the construction of a hard-focusing "Nuklotron" accelerator of relativistic particles. The work of the Laboratory of Nuclear Problems has been discussed by V. P. Dzhelepov. A step forward has been taken in the study of antimatter: antitritium has been discovered in a joint experiment of the JINR and the Institute of High-Energy Physics using a 76 GeV accelerator. The exceedingly complex problem of the discovery has been solved by multiple, independent, and simultaneous measurements of particle velocities at very high accuracy. The generation cross section of antitritium nuclei with a momentum of 25 GeV/sec at a zero angle to the proton beam incident on the target is $d^2\sigma/dp\,d\Omega = (1.0 \pm 0.6) \cdot 10^{-35}$ $cm^2 \cdot sec/GeV \cdot sr$ per one aluminum nucleus in the target. The polarization parameters P and R in Π-p and K-p elastic scattering at 40 GeV/sec have been measured in a joint experiment of the Institute of High-Energy Physics, the JINR, Saclay, and the Institute of Theoretical and Experimental Physics.

The accelerator of the Erevan Physics Institute has been used in studies of elastic electron–deuteron scattering at 4 GeV. The work was directed by scientists of the JINR in cooperation with the Erevan Physics Institute and the Bucharest Institute of Atomic Physics. The obtained differential cross sections make it possible without models to receive information about the electromagnetic form factor of deuterons in the region of small impaired moments. The mean-square radius of a deuteron has been found as 2.01 $\pm$ 0.09 F.

Scientists of the JINR, the Bucharest Institute of Atomic Physics, and the Turino University studied ^3H and ^4H scattering of pions on the Dubna synchrocyclotron using a magnetic spectrometer and a helium streamer chamber. New data on this process have been found in the resonance region (3/2, 3/2). The mechanism of nuclear capture of μ mesons by light (C, N, O) and heavy (Ag, Br) nuclei of photographic emulsions has been studied. Radiochemical and nuclear spectroscopic methods have been used to study double charge-reversal of pions on heavy particles with the purpose of explaining the effect of nuclear structure on the probability of this process. The fusion reaction $d\mu + d \rightarrow {}^3He + n + \mu$ in gaseous deuterium has been investigated in order to find the mechansim of production of $(dd\mu)^+$ mesomolecules.

In accordance with the YaSNAPP program, a wide range of isotopes created in nuclear reactions under the action of 670-MeV protons has been studied using nuclear spectroscopic and radiochemical techniques.

A five-meter magnetic spark spectrometer has been put into operation and the first 14,000 photographs have now been collected using the pion beam of the Serpukhov accelerator. The feasibility of new track instrumentation, such as a streamer chamber with holographic track recording and an ultrasonic liquid-hydrogen chamber, has been proved experimentally. Instrumentation systems for measuring the profiles of charged particles have been developed on the basis of ionization and proportional chambers.

The electromagnet windings and pole pieces of the synchrocyclotron now undergoing reconstruction have been manufactured. A frequency-variator prototype has been designed and is now tested on the operating accelerator. The development of various systems for the future accelerator has been continued. The workers of the Laboratory proposed the construction of a 800-MeV high-current proton accelerator of the ring cyclotron type with hard focusing and a 100-mA beam current.

G. N. Flerov reported on experiments on the synthesis of superheavy particles in the Laboratory of Nuclear Reactions. Extensive studies with $^{74,76}Ge$ ion beams provided estimates of the upper limit of spontaneously fissile isotopes of elements with $Z \geqslant 110$ at the level $\sigma \leqslant 10^{-34}$ cm^2 for nuclei with half-lifes 10^{-3} to 10^5 sec. Experiments have been carried out for the investigations of the interaction mechanism of xenon, krypton, and germanium ions with nuclei. The search for superheavy elements in nature has been continued.

A new technique of gaseous chemistry has been developed for chemical investigations of transactinide elements with the purpose of studying bromine compounds and for experiments on the chemistry of the 105th element. A highly efficient method of gas thermochromatography has been devised for chemical separation and identification of elements with $Z \geq 105$.

The construction of the BÉSM-2 mass operator for the cyclotron beam has been completed and studies of proton-rich cesium and barium isotopes have been started. New proton emitters have been discovered. Studies of neutron-rich isotopes revealed the heaviest carbon isotopes ^{19}C and ^{20}C, the latter being observed for the first time. The decay characteristics of the new neutron-rich isotope ^{41}Cl have been investigated.

New techniques have been devised for measuring the lifetimes of composite nuclei based on the "shadow effect" in which a single-crystal target is cooled to liquid-nitrogen temperature. The Doppler shift effect in recoil nuclei has been used to measure the lifetimes of the various levels of neutron-deficient nuclei. The effect of ionization of internal atomic shells in collisions of heavy germanium and xenon ions with the target atoms as well as the production of quasi molecules have been studied.

The U-300 cyclotron has been used as a hot-cathode plasma source of germanium and metallic ions, the material being supplied by cathode sputtering. A microtron with 17 orbits has been put into operation and provided a 10-MeV electron beam of up to 20 μA. Heavy-ion beams have been used to produce molecular and viral filters with pores of a regular geometric form and very low dispersion ($\sim$1%). The filters have been successfully tested in industrial conditions.

The completion of the overhauling and start-up of the IBR-30 reactor of the Laboratory of Neutron Physics has been reported by I. M. Frank. Several units of the reactor have been reconstructed in order to improve the reliability of the machine and of the protection system. In 1973 the reactor provided more than 3000 h of experiment time. A second experiment has been carried out on measuring the magnetic moments of compound states of disprosium nuclei using the new method of neutron resonance shifts as a result of superfine magnetic interaction in nuclei oriented at extremely low temperatures. The range of neutron energies has been significantly extended and the energy resolution has been improved. Experiments have been continued on the containment of ultracold neutrons in copper, glass, quartz, beryllium-glass, and carbon-glass vessels in order to find the reasons for the discrepancy between the experimental

and theoretical neutron absorption factors. The studies have been conducted in cooperation of the I. M. Kurchatov Atomic Energy Institute on the IRT-M reactor.

The α decay of neutron resonances of deformed nuclei has been studied using the IBR 30 reactor and an electron accelerator. The total α widths have been found for several resonances and their analysis indicates the absence of any significant factors that forbid α decay. A study of nuclear levels of ^{148}Sm of radiation capture reactions of resonance neutrons has been completed. Primary γ radiation spectra of 23 neutron resonances and of the averaged neutron spectrum have been investigated. The spins of many resonances have been accurately determined.

Nuclear reactions involving charged particles, including the energy and angular dependence of the spin reversal probability in inelastic proton scattering by ^{24}Mg have been investigated. It has been shown that unlike polarization, the probability of spin reversal is not zero in the region of isolated resonances.

Two peaks corresponding to one- and two-phonon scattering have been detected in neutron scattering in liquid helium using the DIN-1 spectrometer. Neutron experiments confirmed the existence of Bose condensate in superfluid helium.

The design of a measuring and computing center for the IBR-2 reactor has been worked out together with the Laboratory of Computing Techniques and Automation and the Central Institute of Physics Research (Budapest).

The activities of the Laboratory of Computing Techniques and Automation have been described by M. G. Meshcheryakov. The stack processing mode added to the BÉSM-6 machine of the JINR more than doubled the throughput of the computer. The BÉSM-6 and three BÉSM-4 computers have been fitted with standard ES-5012 magnetic-tape storage systems manufactured in Bulgaria. The fast-access memory of the BÉSM-4 computer has been expanded to 12 k.

The NPD and AÉLT-1 automatic systems are used to mass process chamber photographs. Perfection of the NDP system has been continued. Experimental processing of photographs taken in the one-meter hydrogen bubble chamber has been started with the automatic scanner (spiral meter). The link between the semiautomatic system of PUOS instruments and the BÉSM-4 computer has been expanded, and two measuring SAMET stands (produced in Czechoslovakia) have been connected to the system.

The development of optical links with the computer has been continued. A library of display subroutines has been completed for an M-6000 computer for the SIGDA graphic display and the OSK-2 dot display. The development of instrumentation and the first group of systematic mathematical software for the M-6000 based display terminal for processing graphic information with the BÉSM-6 computer has been completed. A graphic display terminal using a TEKTRONIX storage tube has been put into operation and is now being experimentally tested.

A sectionalized system of programs has been developed for processing photographs taken with the "Lyudmila" chamber. Basic systematic GIDRA subroutines are being developed in cooperation with the Institute of High-Energy Physics (GDR) and the Institute of Experimental Physics (Czechoslovakia). A set of programs has been prepared for mathematical processing of experimental data obtained with filmless spark chambers on the JINR and the Institute of High-Energy Physics (Serpukhov) accelerators.

New applied mathematical methods have been developed for calculating the shape of electron storage rings for a collective accelerator. Programs have been compiled for mathematical simulation of the behavior of a charged layer by the method of enlarged particles using a display terminal. The periodic trajectories of charged particles in the JINR proton synchrotron have been analyzed taking into account geometric distortions.

V. P. Sarantsev told about the work of the Department of New Acceleration Methods on the design of the basic units of a collective heavy-ion accelerator. Theoretical problems associated with generation of pulsed magnetic fields in a thin-walled metallic adhesation chamber and the calculation of fields within the chamber have been considered. Parameters of the extraction system and of the accelerator solenoid have been calculated.

A working model of a thin-walled vacuum adhesation chamber made of 5-mm stainless steel has been designed and built on the basis of theoretical calculations and experimental measurement of the magnetic, thermal, and mechanical properties of materials. The chamber is capable of operating in pulsed magnetic fields at pressures of 10^{-8} torr.

A system for generating the constant magnetic field and three-stage supply system for the pulsed accelerating field have been designed and built. The latter problem involved the design of commutators capable of switching 5-kA currents at 30 kV.

Generation of the adhesator magnetic fields required the design of an efficient measuring system including Hall magnetometers for measuring pulsed magnetic fields with an accuracy of 10^{-3} and constant magnetic fields within 10^{-4} (at field intensities exceeding 2 kG). Two magnetometers based on nuclear magnetic resonance are used to calibrate the various magnetometers. The fields are analyzed by connecting the measuring equipment directly to the M-6000 computer.

A high-energy proton accelerator system based on a superconducting cyclotron section has been investigated.

The Deputy Director of the Institute K. Lanius reported on international activities and ties of the JINR. In 1973 the Institute's Laboratories conducted more than 250 scientific and methodological research projects in cooperation with other member countries. During one year the Dubna Institute has been visited by more than 840 specialists of many countries, and nearly 560 JINR scientists participated in various conferences and visited foreign research centers. Seventeen scholarship students of different countries worked in the Institute. The Institute organized five scientific conferences, two schools, and eight working meetings. They include the 3rd International Symposium on High-Energy and Elementary Particle Physics (Romania), the 7th International Symposium on Nuclear Electronics (Hungary), and the 3rd International Seminar on Nonlocal Quantum Theory (USSR).

In 1974 the JINR will hold the 4th International Symposium on High-Energy and Elementary Particle Physics (Varna), an International Symposium on Interactions between Composite Nuclei (Dubna), the 2nd School on Neutron Physics (Alushta), the 3rd School on Computer Applications in Physical Experiments (Tashkent), and others.

During the Session of the Academic Council, winners of the JINR competition for best scientific works have been presented with diplomas. The first prize was awarded to two groups of authors for the papers "Self-Similarity in High-Energy Physics" and "Slow Extraction of Accelerated Beam from the JINR Proton Synchrotron:" the second prize was awarded to the papers "Regeneration of Neutral Kaons in Hydrogen," "Nuclear Spectroscopic Analysis of Short-Lived Isotopes in Accordance with the YaSNAPP Program," "Analysis of New Particle Detection Methods and Design of a Crystalline Filament Counter," and "Development and Improvement in Efficiency of the BÉSM-6 Computer."

CONFERENCE OF THE IAEA GROUP ON THE DESIGN OF FUSION REACTORS

G. N. Popkov

The conference took place at the Calem Laboratory (Great Britain) on January 29 to February 15, 1974. The Conference was attended by representatives of the USA, German Federal Republic, the USSR, Great Britain, Japan, France, Italy, the Netherlands, Sweden, and also of the Euratom and IAEA.

Information provided by the various countries was used to analyze problems arising in connection with the design of controlled thermonuclear reactors of various types, ways of overcoming the many difficulties have been indicated, and the principal problems which must be solved before thermonuclear power plants become a reality have been noted.

During the first week the participants reported on various thermonuclear reactor projects and on individual engineering problems associated with their design. On the basis of these reports the Conference was divided into eight groups dealing with specific subjects: impurities, protection of first wall, reactor firing, radiation damage and materials; assembly, diassembly, and accessibility; tritium, fusion–fission reactors, environmental protection. All these problems have been discussed during the two weeks of the Conference and concluding reports were prepared.

Such a schedule has definite advantages over the traditional ways of conducting scientific conferences. Thus, the participants had ample opportunity to discuss in detail every report, to examine together with the author unclear or debatable questions, to organize meetings on problems arising in the course of the Conference, and to determine the scope of questions on which there is a general agreement.

The Conference proved that outside the Soviet Union the design of the thermonuclear reactors has already passed the stage of preliminary tests and timid trials and has now become a field of vigorous scientific and engineering activity going on at many laboratories and in design groups numbering 20-30 people each. A new field of science and engineering has been born with its specific problems, interests, approaches, and solutions. The conference heard about more than ten projects of future power reactors which are now at the proposal stage, six of them being of the Tokamak type. One of the most thoroughly worked out project is the Tokamak reactor of the Wisconsin Laboratory. Japanese designers suggested the use of Li_2O as blanket material. In the Princeton Laboratory project much attention has been devoted to the description of a poloidal diverter.

The most burning question was the problem of impurities in Tokamak type reactors. The problem has been discussed in three sessions. Tokamak experiments in the USSR indicate that in agreement with theory, impurities diffuse into the plasma filament at a much higher rate than the plasma diffusion rate. Several suggestions have been discussed for preventing plasma contamination by impurities (diverters, gas blankets, plasma rotation, resonance acceleration of impurity ions, selection of wall materials). Since none of the suggestions offers a radical solution to the problems of impurity, it has been proposed to design a Tokamak reactor operating in a pulsed mode. Preliminary estimates indicate that the difficulties associated with pulse operation can be overcome if the pulse duration is 100 sec or more.

Projects of other reactor types are at a less advanced stage. For example, reactors of the toroidal Theta-pinch type require considerable further advances in energy storage devices for supplying the adiabatic-compression coils, in materials insulating the first wall, in the problem of preventing wall impurities from contaminating the plasma during adiabatic compression, in providing pinch stability, and in the feasibility of a modular version.

Translated from Atomnaya Énergiya, Vol. 37, No. 1, pp. 85-86, July, 1974.

Two reports on reactors with laser triggering discussed the design of the chamber elements and touched upon subjects common to all thermonuclear reactors: the first-wall load, the blanket, and energy conversion. The laser system proper, radiation injection into the interaction chamber, and the protection of the final optical elements have not been discussed from a practical point of view. The absence of the principal element, a laser with suitable parameters, and the lack of corresponding plasma experiments, makes the entire project rather abstract.

Problems associated with the use of tritium, with material properties, and with the assembly and diassembly of reactors have been discussed in specific cases. The discussions resulted in a formulation of the basic requirements of a practical system due to the presence of tritium. Thus, the escape of tritium from the reactor in 24 hours should not exceed 10^{-7} of its total content (according to the norms accepted in most countries).

A discussion of prospective materials indicates that the specific features of thermonuclear reactors necessitate accurate data on the strength, corrosion and radiation resistance, resistance to fragility, swelling, sputtering caused by neutrons and ions, and blistering of a wide range of construction materials. A discussion of the problems associated with reactor assembly, disassembly, and maintenance indicate that probably as a result of the effects of plasma radiation, it is impossible to manufacture reactor components (especially the blanket) with a sufficiently long service life so that the reactor design must foresee easy diassembly and assembly of the reactor core exposed to strong neutron radiation and containing tritium.

In conclusion, one should note the rapid pace and wide range of design work on thermonuclear power reactors in the West, particularly in the USA. An ever growing number of engineers and specialists in adjacent fields participate in these works.

SEMINARS AND EXHIBITIONS OF THE ALL-UNION "IZOTOP" CORPORATION

A Scientific-engineering exhibition "Atoms at Work" has been held in January 1974 in Tallin. The following sections have been represented in the exhibition: atomic power, scientific research, nuclear physics instrumentation, and radiation engineering. Models of the VVÉR-440 and BN-350 power reactors, of the Tokamak-3 and PR-6 thermonuclear plants, as well as a thermometer reactor of the future have been exhibited.

The section "Nuclear Physics Instrumentation and Radiation Engineering" displayed various radioisotope devices and radiation tools manufactured by the "Izotop" corporation for the national economy.

A seminar on "Applications, Nomenclature, and Quality of Radiation Protection Technology," organized by the Leningrad division of the "Izotop" corporation and the Leningrad science popularization society "Znanie," has been held in January, 1974. In the seminar participated representatives of the Leningrad Sanitary-Epidemological Station, the Kol'sk Branch of the Academy of Sciences of the USSR, the V. G. Khlopin Radium Institute, and the S. M. Kirov Academy of Military Medicine. Lectures were heard and recommendations have been worked out on the quality and nomenclature of the manufactured products. The participants visited an exhibition of radiation safety devices.

A seminar on "Application of Radioisotopes in the Food Industry" has been organized by the Tashkent division of the "Izotop" corporation in cooperation with the Ministry of the Food Industry of the Kazakh SSR in Alma-Ata in February 1974. The participants of the seminar accepted recommendations on the wider use of radiation technology in the country's food industry and on the establishment of a special section at the Academic Council of the Ministry of Food Industry of the USSR on the application of radiation technology.

An exhibition and seminar on "Past Experience and Future Prospects of the Application of Radiation Technology in the Chemical Industry" has been held by the Sverdlovsk regional division of the "Izotop" corporation of the bichromate plant in Pervoural'sk in March 1974. The seminar was attended by 85 representatives from 35 industrial and research organizations of 14 Ural' cities. The participants accepted recommendations on expanding the application of radiation technology in the chemical industry.

An exhibition and seminar on "Application of Isotopic Techniques and Radioisotopic Instruments in the Chemical Industry" has been organized by the Moscow regional division of the "Izotop" corporation in March 1974. The seminar was attended by representatives from 28 industrial and research organizations. The participants visited the Voskresensk chemical combine which successfully employs nearly 150 radioisotopic instruments.

A seminar on "the Application and Safety of Radioisotopic Instruments in the Light Industry" has been conducted by the Kiev republican division of the "Izotop" corporation in cooperation with the Ministry of Light Industry of the Ukrainian SSR in March, 1974. Reports were read and special motion picture films were shown. According to the recommendations worked out by the participants, the survey of the Enterprises of the Ministry of Light Industry of the Ukrainian SSR will continue in 1974. It has been recommended to include lectures on the application and use of radioisotopic instruments in the curricula of Higher Course on Improving the Qualifications of Leading and Technical Workers. The seminar's recommendations will be published and distributed.

A seminar on "Application of Isotopes and Radiation Instruments in the National Economy" took place in Berdyansk in March, 1974. The purpose of the seminar was to expand the applications of radioisotope technology in the regional and city industrial enterprises. The participants familiarized themselves with the operation of more than fifty radioisotopic instruments successfully used in various technological processes of petroleum plants.

Translated from Atomnaya Énergiya, Vol. 37, No. 1, pp. 86-87, July, 1974.

KTN-2 TANTALUM AND NIOBIUM CONCENTRATION METER

B. E. Kolesnikov, E. D. Kokhov,
Yu. D. Lavrent'ev, and A. P. Khukhyanskii

The All-Union Scientific-Research Institute of Radiation Engineering developed an automatic x-ray radiometric instrument for measuring the concentration of tantalum and niobium in powdered products. The instrument has the following technical specifications:

Range of measured concentrations, %	
tantalum	0.05-6.0
niobium	0.05-70.0
Sensitivity threshold, %	
tantalum	0.03
niobium	0.03-0.05 depending on the sample composition;
Relative measuring error	less than 3%
Time of three measurements	10-30 min

The output information is displayed in digital form in the form of a number proportional to the content of the determined element.

The instrument uses a ^{170}Tm radioisotopic source (TU-3 MRTU 10-108-68) with an activity of 0.5 g·eq Ra. A special intermediate target and differential filters are used for the analysis of each element. The weight of the analyzed sample is 60 g. The radiation detector is a 1-mm thick Na I (Tl) scintillation counter. The instrument operation is based on measuring the radiation of a standard background [1-3].

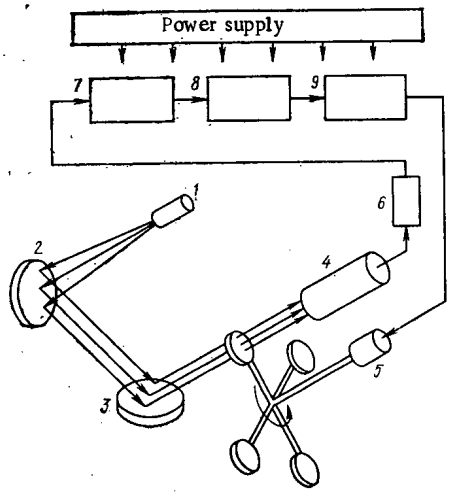

Fig. 1. Block diagram of KTN-2 concentration meter.

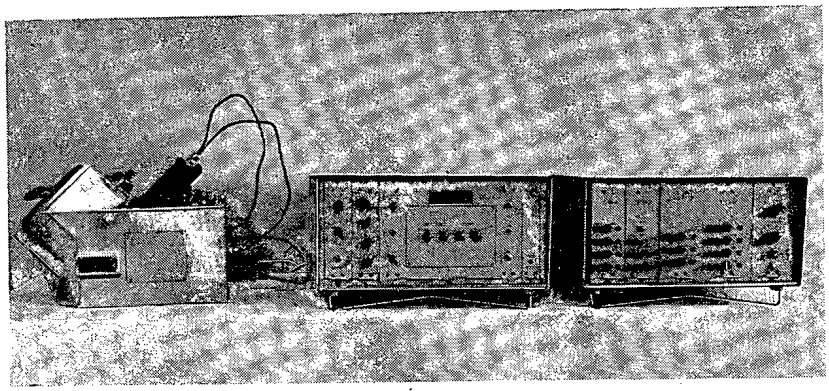

Fig. 2. External view of the KTN-2 instrument.

Translated from Atomnaya Énergiya, Vol. 37, No. 1, pp. 87-88, July, 1974.

The K-series emissions of the analyzed element and the standard are separated by means of two pairs of differential filters [4].

The instrument block diagram is shown in Fig. 1. The transducer includes the ionizing radiation source 1, intermediate target 2, the analyzed sample 3, radiation detector 4, the filter changing mechanism 5, and preamplifier 6. The electronic measuring unit includes discriminator amplifiers 7, counter 8, and filter control unit 9.

The instrument operates as follows. The four differential filters are inserted in turn into the sample radiation flux. The corresponding four pulse trains are amplified, amplitude selected in the discriminator, and applied to the counter. The count rate difference obtained with the first pair of filters is proportional to the characteristic radiation flux of the analyzed element, and that obtained with the second pair of filters, to radiation flux of the standard.

The counter automatically computes the ratio of the above count rates, i.e., the ratio of the characteristic radiation flux and the flux provided by the standard. The external view of the instrument is shown in Fig. 2.

The instrument has been tested in industrial conditions in the determination of tantalum and niobium content in powdered products. The analyzed samples contained tantalum pentoxide, niobium pentoxide, phosphorus, sulfur, elements of the iron group, and traces of rare earths. The content of these elements varied within very wide ranges.

The content of tantalum has been determined with the aid of a calibration curve plotted from data obtained with standard samples consisting of actual process products certified by chemical analysis. Since the accuracy of chemical analysis does not exceed 10%, the calibration curve was plotted by the method of least squares from the results of measurements on 20 standard samples. All in all 53 samples have been analyzed.

In the determination of niobium content, the measuring range has been divided into two subranges: 0.05 to 15.0% and 15.0 to 70.0%. The content of niobium in the 15.0 to 70.0% range was determined from a calibration curve similar to that for tantalum. Twenty one samples have been analyzed. The measurements in the 0.05 to 15.0% range are affected by tantalum content, which is considerable in these samples. The variation of tantalum content has been taken account of by introducing a suitable correction found from a plot of the dependence of niobium sensitivity on titanium content.

A check of the compatibility of the results of chemical and x-ray radiometric analyses as described in [5] proved that at the 1% significance level the differences between the results are statistically insignificant.

By suitable selection of intermediate targets and differential filters the instrument can be used to analyze other elements with atomic numbers from 40 to 75.

LITERATURE CITED

1. V. A. Meier and V. S. Nakhabtsev, in: Problems of Ore Geophysics [in Russian], Izd. LGU, No. 6 (1965), p. 34.
2. A. P. Ochkur and A. Yu. Bol'shakov, in: Problems of Ore Geophysics [in Russian], LGU, No. 6, (1965), p. 49.
3. R. I. Plotnikov and G. A. Pshenichnyi, X-Ray Radiometric Fluorescent Analysis [in Russian], Atomizdat, Moscow (1973).
4. B. E. Kolesnikov et al., Radiatsionnaya Tekhnika, No. 9, 259 (1973).
5. V. V. Nalimov, Application of Mathematic Statistics in the Analysis of Materials [in Russian], Fizmatgiz, Moscow (1960).

TRANSPORTATION AND RELOADING CONTAINER FOR REMOTE-CONTROLLED GAMMA THERAPY INSTRUMENTS

V. T. Emel'yanov, V. M. Kondrashov, and M. P. Sinodov

The All-Union Scientific-Research Institute of Radiation Engineering designed a new transportation and reloading container KTP-5. The set consists of the KP-5 container for source storage and for loading and reloading RAD-1, LUCh-1, AGAT-S, and AGAT-R gamma therapy instruments, a trolley, and external packing for shipping the KP-5 container and source to the place of use (Fig. 1).

The KP-5 container consists of a stainless steel casing with a depleted uranium shield. Inside the block is a rotating drum with three holes along its periphery and a fixed insert with the reloading channel. Two holes are used for the source holders while the third contains a rod which passes into the reloading channel of the fixed insert and serves at the same time to protect and clamp the rotating drum during transport. The source holders are loaded into the container from the drum side. On the reloading channel side of the casing is a centering ring by means of which the container makes contact with the radiation head of the instrument for loading or reloading. All uranium blocks are jacketted in stainless steel. The container is provided on both ends with covers with uranium elements mounted on them to serve as an additional protection against γ radiation penetrating the jackets of uranium blocks.

The provision of three sockets enables simultaneous storage in the container of the two holders for the new and replaced sources as necessary for instrument reloading.

The KP-5 container (Fig. 2) is used to load AGAT-S and AGAT-R gamma therapy instruments. The provision of the container with a trolley considerably facilitated the transportation of the source to the desired location and contacting the radiation head of the instrument. The reloading crew received a dose well below the safe level.

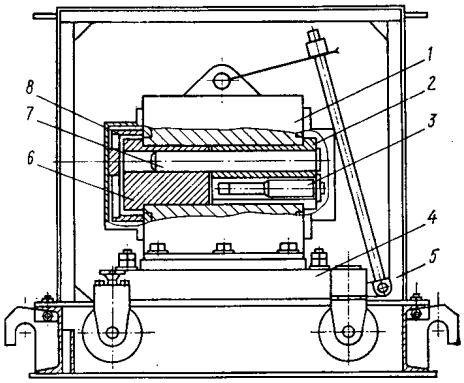

Fig. 1. Transportation and reloading container KTP-5: 1) KP-5 reloading container; 2) drum; 3) source holder; 4) trolley; 5) external packing; 6) insert; 7) rod; 8) centering ring.

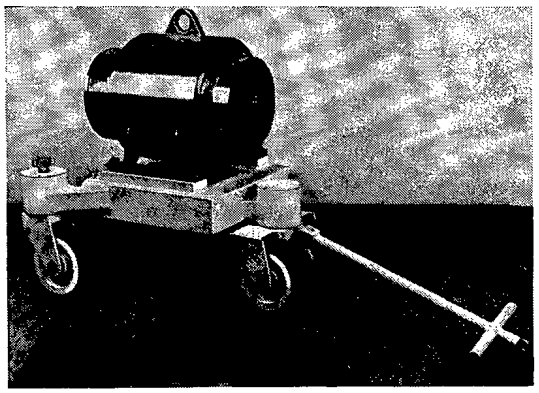

Fig. 2. KP-5 reloading container on trolley.

Translated from Atomnaya Énergiya, Vol. 37, No. 1, p. 89, July, 1974.

A prototype of the KTP-5 container successfully passed all radiation, mechanical, and heat tests as required by the Comecon and the IAEA standards on the safe transportation of radioactive materials.

The shielding properties of the KP-5 container have been tested using a ^{60}Co γ source with an exposure dose rate of 1.14 R/sec at a distance of 1 m. It has been found that the maximum surface dose rate of the container at a point closest to the source was about 32 mR/h corresponding to the third category of transport packing. In mechanical tests the KTP-5 container was dropped from a height of 9 cm on a concrete base with a 30 mm thick steel blade and from a height of 1 m on a pin. Heat tests were conducted in a firebox (oven dimensions 2800 × 2800 × 1700 mm). The container was heated in the firebox for 25 min to 800°C and remained at this temperature for the next 30 min.

To check its radiation safety the container, after passing the mechanical and heat test, was once again subjected to radiation tests which proved that its safety remained as before even if the Comecon and IAEA standards allow a fivefold increase of the exposure dose rate at some points of a container.

The tests proved that the KTP-5 container meets all Comecon and IAEA requirements on safe transportation of radioactive materials and facilitates the loading and reloading of remote-controlled gamma therapy instruments. The new transportation and reloading container has been accepted for mass production in 1973.

NEW GAMMA FLAW DETECTORS FOR TESTING THE WELDING OF MAIN PIPELINES

V. N. Khoroshev, A. I. Murashov,
V. N. Polosatov, and N. I. Neustruev

The highly reliable welded joints necessary in large-diameter pipes require, in addition to improvements in welding techniques, also large-scale and high-grade nondestructive testing.

To improve testing efficiency thus allowing large-scale testing of the quality of welded joints of pipes, the All-Union Scientific-Research Institute of Radiation Engineering has designed at the request of the Institute of Construction of Main Pipelines two γ flaw detectors, Magistral' and Magistral'-1, employing γ sources of high activity. The characteristics of the γ sources used with the flaw detectors are listed in Table 1.

Although the purpose and the setup of the Magistral' and Magistral'-1 flaw detectors are different, both instruments use standardized units as their basis. The Magistral' flaw detector (Fig. 1) is intended for testing the quality of welded joints of 1020-1620-mm main pipes with walls up to 35 mm thick both by panoramic irradiation at pipe welding stations, and by a frontal beam in the pipe thread. The γ flaw detectors include the radiation head, drive, control panel, manual drive, container, cables, the radiation head holder, stand, and spare instruments and devices.

The radiation head mounted on the stand is manually introduced into the pipe thread. The radiation beam is remotely controlled by means of manual or electromechanical drives. The beam is shaped by exchangeable collimators mounted on the radiation head. The electromechanical drive and the control panel are supplied with 24 V dc. The panel has pilot lights which indicate the position of the radiation source. If the current is cut off, the source is automatically returned to the "storage" position. In manual drive, the position of the source is indicated by the state of the manual-drive handle.

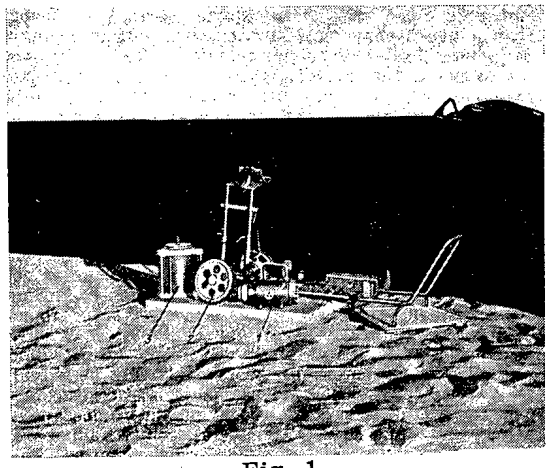

Fig. 1

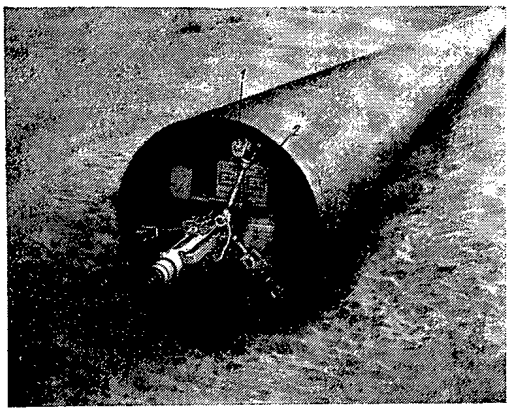

Fig. 2

Translated from Atomnaya Énergiya, Vol. 37, No. 1, pp. 90-91, July, 1974.

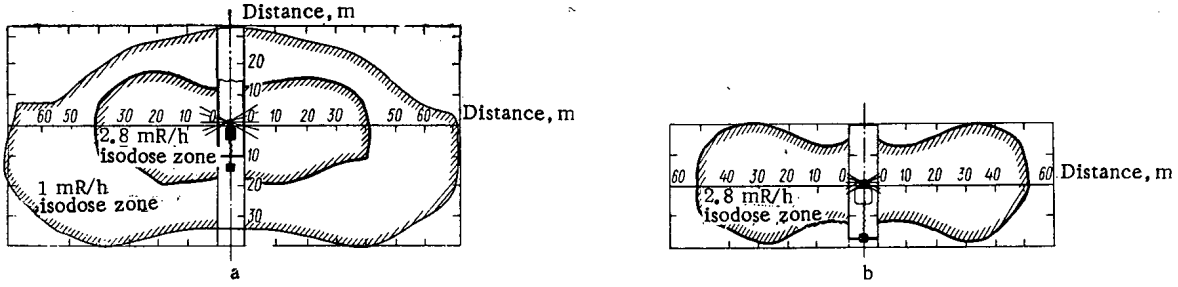

Fig. 3. Isodoses in panoraming x-raying of 1420 × 17.5 pipes using ^{192}Ir (exposure dose rate 2.85 mR/sec) (a) and ^{137}Cs (exposure dose rate 5 mR/sec) (b) radiation sources.

TABLE 1. Characteristics of γ Radiation Sources

GOST	Type of source	Exposure dose rate of γ radiation at a distance of 1m, R/sec		Size of active portion, mm		External dimensions of source (vial), mm			
						diameter		height	
		nominal	maximum deviation	diameter	height	nominal	maximum deviation	nominal	maximum deviation
16002—70	^{137}Cs GID-Ts-4	$5{,}0\cdot10^{-3}$	$\pm1{,}2\cdot10^{-3}$	no more 10	no more 11	14	0,36	19	—1
16003—70	^{192}Ir GID-I-7	$2{,}5\cdot10^{-2}$	$\pm0{,}6\cdot10^{-2}$	6,0	6,0	8	0,30	9	—0,9

By using the uranium shields, the weight of the radiation head has been reduced to 25 kg in spite of considerable radiation source activities (see Table 1). With the source in the "storage" position, the exposure dose rate at a distance of 1 m does not exceed 2.8 mR/h .

The Magistral'-1 gamma flaw detector is used for panoramic inspection of welded joints of 1020 to 1620 mm main pipes along the thread, and is used in conjunction with the AKP-141 automatic set (Fig. 2) which automatically positions and operates the flaw detector while it travels inside the pipe for distances up to 1.5 km.

The AKP-141 set has been jointly designed by the Kiev "Gazstroimashina" Design Bureau (the running section and power supplies) and the "Gazpriboravtomatika" Design Bureau (automatic control circuits). The Magistral'-1 flaw detector consists of a radiation head, drive, container, radiation head holder (the same as in the Magistral' set), cables, two collimators, two radioisotopic servo systems, and a reference container. The radiation head, drive, servo systems (electronic circuits and detectors), and collimators are mounted on the running part of the AKP-141 set and are connected through cables with the automatic control circuits and power supplies.

As proved in many tests, the positioning of the AKP-141 set and execution of control commands by the servo system using scintillation detectors is very reliable. The accuracy of positioning the AKP-141 set against a tested joint in a pipe 1420 × 17.5 mm in diameter was ±10 mm amounting to 0.7% of the pipe diameter as compared with 2% desired by the customer. Parallel tests of a similar positioning and command system based on magnetic induction gave negative results as its positioning accuracy was about 10% of the pipe diameter. Using a GID-I-7 (^{192}Ir) source, the time necessary for panoramic and frontal x-raying of 1420 × 17 mm pipes was 0.2 and 1.5 min respectively, and with a GID-Ts-4 (^{137}Cs), 0.3 and 3 min respectively.

The sensitivity of roentgenograms has been estimated with the aid of GOST 7512-69 No. 3 grooved sensitivity standards as better than 2-3% for unshielded films and 4-6% with shielded film.

The extent of radiation danger zones at a distance of 1 m for panoramic x-raying using the ^{192}Ir source (exposure dose rate 2.85 mR/sec) and ^{137}Cs source (exposure dose rate 5 mR/sec) are shown in Fig. 3. The measurements were made using an RUP-1-1 meter with an accuracy of ±20%. The use of higher source activities extended the danger zones. This circumstance must be considered in organizing the inspection.

The Magistral' and Magistral'-1 gamma flaw detectors passed all industrial tests and have been recommended for quantity production in 1975.

The expected economical gain provided by one Magistral' gamma flaw detector is estimated as about 10,000 rubles annually.

Yu. M. Dymkov

THE NATURE OF PITCHBLENDE*

Reviewed by V. L. Barsukov

Pitchblende is one of the most important sources of uranium and radium. At the same time, pitchblende is one of the most complex natural objects and the difficulties encountered in its analysis gave rise to various, frequently conflicting, views on its nature and origin.

Till now, for example, there is no agreement if pitchblende should be considered as an independent mineral (of a single solid phase) or as an aggregate of several minerals (several solid phases). Some researchers believe that nasturan and pitchblende are synonymous while others insist that they denote different objects; some mineralogists consider nasturan (the basic component of pitchblende) as a variety of UO_2 uraninite, while others regard it as compound of a composition different from UO_2.

The peculiar, kidney-shaped form of pitchblende deposits was at one time responsible for the view it is of colloidal origin. These views still find their way into geological literature in spite of the many recent proofs of crystallization growth of kidney-shaped nasturan individual or aggregates.

The lack of clear notions about the origin of pitchblende, the mechanism of its crystallization, its phase transformations during the deposition process, and the subsequent transformation of its composition and morphology, makes it very difficult to form a theory of its origin, to refine our knowledge about the conditions of formation of uranium deposites, and to find criteria of prospecting for and evaluating the latter.

The book of Yu. M. Dymkov fills in many blanks in the genetic mineralogy of uranium. The book summarizes and analyzes extensive information about natural and synthetic uranium compounds, and describes the results of the author's precision investigations which provide unambiguous answers to many problems.

The author cites new evidence that natural pitchblende is actually always an aggregate of several mineral phases: nasturan (having a spherocrystalline or spherulitic structure), uranite (possessing morphological symptoms of a cubic system), coffinite (uranium silicate), and many products of their variations. One cannot but agree with the statement that the terms "pitchblende," "nasturan," and "uraninite" should not be used as synonyms so as not to aid the confusion already existing in mineralogy.

The book cites new evidence that even the uranium oxides, nasturan and uraninite, are multiphasic. It is shown that this multiphasic nature is regular and is explained by the complex processes (changes in the degree of uranium oxidation, substitutions between nasturan and coffinite, metamictization of uranium, etc.), which take place during the deposition (crystallization) of uranium oxides and continue after their formation.

The crystallization mechanism of the formation of kidney-shaped nasturan deposits is now generally accepted, in a large measure owing to the work of Yu. M. Dymkov. The main part of the reviewed book is devoted to the proof that nasturan is a spherocrystalline variety of natural uranium oxides, primordially of a cubic system, that formed as a result of breakup of cubic and other forms of nucleating uraninite crystals. These uraninite nuclei of nasturan spherulites have been first detected by Yu. M. Dymkov in an electron microscopic study of pitchblende and are described in the book. The breakup of nucleating uraninite crystals, established by Yu. M. Dymkov, is an important discovery, as it has been assumed until now that nuclei of spherical crystals form only in the breakup of noncubic minerals.

*Atomizdat, Moscow, 1973.

Translated from Atomnaya Énergiya, Vol. 37, No. 1, p. 93, July, 1974.

The book considers in detail and successively all basic stages in the ontogenesis of nasturan and coffinite: the origin and growth, changes in the course of growth and thereafter, the conditions of combined growth of spherical crystals and their relation to other minerals are analyzed.

More disputable are the concepts of Yu. M. Dymkov about the filogenesis of nasturan, i.e., about the history of its origin as an individual chemical compound, which are the topic of the book's last chapter. However, even here the author presents several interesting problems which merit the attention of all mineralogists.

The book is undoubtedly an important milestone in the study of uranium minerals. Its conclusions and the systematic analysis of natural material will have a marked effect on subsequent studies of not only uranium but also other ore deposits. One must stress the fine arrangement of the book, the high quality of microphotographs and figures, the convenient headings, and the thoughtful presentation of actual reference material.

B. I. Spitsyn and B. B. Gromov

PHYSICOCHEMICAL PROPERTIES OF RADIOACTIVE SOLIDS*

Reviewed by E. V. Sobotovich

The authors of this monograph make an attempt to generalize the basic experimental data in the field of solid state radiochemistry, a new field of science which takes its origins in the synthesis of some branches of sciences such as radiochemistry, radiation chemistry, and physical chemistry of heterogeneous processes. This synthesis has been stimulated by practical needs of the national economy and by the growth of atomic engineering.

Special emphasis is placed on the effect of self-irradiation as distinguished from external radiation. On this basis the authors stress the fertility of the comparative study of external and internal irradiation in the analysis of radiation changes in solid samples. The available literature deals mainly with individual problems of solid radiochemistry (dosimetry, defects in crystalline structure, annealing of radiation damages). Thus, to generalize the most important directions, the authors put primary emphasis on such traditional physicochemical processes as the solution kinetics, heterogeneous isotopic exchange, surface structure and absorptive properties, electrochemical effects on the radioactive metal—solution interface, and radiolysis of radioactive salts. However, the consideration of most problems is limited to a discussion of specific relationships and contains no extensive generalizations. This can be explained in part by the fact that solid state radiochemistry is in its incipient stage, and also by the lack of a general theory of chemical reactions, by the state of the theory of radiolysis in solid crystals, of the solid state theory, etc. Nevertheless, the discussion of a wide range of phenomena associated with self-irradiation sufficiently fully characterizes the present state of solid state radiochemistry.

*Atomizdat, Moscow (1973).

Translated from Atomnaya Énergiya, Vol. 37, No. 1, pp. 93-94, July, 1974.

A. Thomas and F. Abbey*

CALCULATION METHODS FOR INTERACTING ARRAYS OF FISSILE MATERIALS†

Reviewed by I. A. Stenbok

Engineering methods of the calculation of fissile material systems are discussed. With the aid of these methods it is possible simply and without resorting to computer techniques to estimate optimum sizes and configurations of assemblies of interacting elements or products of fissile materials.

A general formulation of the problem is stated and an expression is derived for the multiplication factor of a system of interacting elements. Since an exact solution becomes very tedious if the number of elements exceeds four, and manual calculations are impracticable, simple methods are employed in practical work. The authors describe three such methods. The first (the Oak Ridge method) is based on an experimental measurement of the critical parameters of an assembly of elements having a simple geometry (cylinders, plates, spheres in a regular lattice). Two variables are used: the multiplication factor of a single element and the solid angle at which the central element of the system is seen from the point of location of the neighboring element. Tables and graphs are given from which it is possible quickly and simply to estimate the critical parameters of regular systems. The second method has been developed by the authors and is called by them the "interaction parameter method." It consists in principle in the determination of interaction parameters defined as the number of neutrons emitted by the fissile body as a result of interaction with neutrons of an isolated source. This parameter can be measured experimentally or obtained by exact computation. Measuring methods and results are cited, and working formulas and parameters calculated for different assemblies are given. The results obtained by the interaction-parameter and Oak Ridge methods are compared. An advantage of the first method is its possible application in irregular systems of inhomogeneous elements (of course, with some limitations).

The third method, the so-called PQR method, has been developed for storage and transportation systems for fissile materials. In addition to the simplified methods, the direct Monte Carlo method is also discussed.

The book will be very valuable to engineers interested in nuclear safety problems, and to students of nuclear power engineering.

*Pergamon Press (1973).
† International Series of Monographs in Nuclear Energy.

Translated from Atomnaya Energiya, Vol. 37, No. 1, p. 94, July, 1974.

breaking the language barrier

WITH COVER-TO-COVER ENGLISH TRANSLATIONS OF SOVIET JOURNALS

in physics

Title	# of Issues	Subscription Price
Astrophysics *Astrofizika*	4	$120.00
Fluid Dynamics *Izvestiya Akademii Nauk SSSR mekhanika zhidkosti i gaza*	6	$180.00
High-Energy Chemistry *Khimiya vysokikh énergii*	6	$155.00
High Temperature *Teplofizika vysokikh temperatur*	6	$150.00
Journal of Applied Mechanics and Technical Physics *Zhurnal prikladnoi mekhaniki i tekhnicheskoi fiziki*	6	$175.00
Journal of Engineering Physics *Inzhenerno-fizicheskii zhurnal*	12 (2 vols./yr. 6 issues ea.)	$175.00 ($87.50/vol.)
Magnetohydrodynamics *Magnitnaya gidrodinamika*	4	$125.00
Mathematical Notes *Matematicheskie zametki*	12 (2 vols./yr. 6 issues ea.)	$185.00
Polymer Mechanics *Mekhanika polimerov*	6	$140.00
Radiophysics and Quantum Electronics (Formerly Soviet Radiophysics) *Izvestiya VUZ. radiofizika*	12	$180.00
Solar System Research *Astronomicheskii vestnik*	4	$ 95.00
Soviet Applied Mechanics *Prikladnaya mekhanika*	12	$175.00
Soviet Atomic Energy *Atomnaya énergiya*	12 (2 vols./yr. 6 issues ea.)	$175.00 ($87.50/vol.)
Soviet Physics Journal *Izvestiya VUZ. fizika*	12	$180.00
Soviet Radiochemistry *Radiokhimiya*	6	$165.00
Theoretical and Mathematical Physics *Teoreticheskaya i matematicheskaya fizika*	12 (4 vols./yr. 3 issues ea.)	$160.00

Back volumes are available. For further information, please contact the Publishers.

SEND FOR YOUR FREE EXAMINATION COPIES

PLENUM PUBLISHING CORPORATION
227 WEST 17th STREET
NEW YORK, N. Y. 10011
Plenum Press • Consultants Bureau
• IFI/Plenum Data Corporation

In United Kingdom: 4a Lower John Street, London W1R 3PD, England

The Plenum/China Program.

An event of singular importance for international science and technology.

Following closely upon the appearance of the first scientific periodicals in China since the Cultural Revolution, Plenum proudly announces the publication of authoritative, cover-to-cover translations of the major, primary journals from China, under the Plenum/China Program imprint.

These authoritative journals contain papers prepared by China's leading scholars and present original research from prestigious Chinese institutes and universities.

In addition to the biomedical and geoscience journals listed for 1974, the Plenum/China Program will publish cover-to-cover translations of periodicals in physics, chemistry, computer science, automation, mathematics and the engineering disciplines. The translations will be prepared by a large team of experts selected especially for the program, and each journal will be under the direct supervision of an outstanding authority in the field.

The first issue of each of the translation journals will be published in early 1974, and, as with our Russian periodicals under the Consultants Bureau imprint, the translations of the Chinese journals will be available within six months following the appearance of the original Chinese edition.

Subscriptions are now being accepted. Examination copies will be available in early 1974.

available in 1974

	Subscription Rates*
Acta Botanica Sinica (2 issues)	$ 75
Acta Entomologica Sinica (2 issues)	$ 55
Acta Geologica Sinica (2 issues)	$ 75
Acta Geophysica Sinica (1 issue)	$ 27.50
Acta Microbiologica Sinica (2 issues)	$ 55
Acta Phytotaxonomica Sinica (4 issues)	$125
Acta Zoologica Sinica (4 issues)	$125
Chinese Medical Journal (12 issues)	$195
Geochimica (4 issues)	$110
Kexue Tongbao—Scientia (6 issues)	$ 90
Scientia Geologica Sinica (4 issues)	$125
Vertebrata PalAsiatica (2 issues)	$ 60

forthcoming

Acta Astronomica Sinica (2 issues)

Acta Biochimica et Biophysica Sinica (2 issues)

Acta Mathematica Sinica (4 issues)

Genetics Bulletin (4 issues)

Huaxue Tongbao—Chemical Bulletin (6 issues)

*These prices are for the 1973 Chinese volumes which will be published in translation during 1974. Prices somewhat higher outside the U.S.

plenum
PLENUM PUBLISHING CORPORATION
227 West 17 Street, New York, N.Y. 10011
In United Kingdom 8 Scrubs Lane, Harlesden, London, NW10 6SE, England